Optimisation of proteomics techniques for archival tumour blocks of a South African cohort of colorectal cancer

Sophia Catherine Rossouw

A thesis submitted in fulfilment of the requirements for the degree of Doctor Philosophiae in Bioinformatics at the South African National Bioinformatics Institute, University of the Western Cape.

2020

Supervisor: Prof Alan Christoffels
Co-supervisor: Dr Jonathan Rigby

Optimisation of proteomics techniques for archival tumour blocks of a South African cohort of colorectal cancer.

by S.C. Rossouw

Keywords

Formalin-fixed paraffin-embedded (FFPE) proteomics

Colorectal cancer (CRC)

FFPE archival tissue

Protein extraction protocol

Protein purification methods

Acetone precipitation and formic acid resolubilisation (APFAR)

Detergent removal plates (DRP)

In-solution digestion

SP3/HILIC-on-bead-digestion

Bottom-up/shotgun mass spectrometry

Abstract

Optimisation of proteomics techniques for archival tumour blocks of a South African cohort of colorectal cancer.

by S.C. Rossouw (PhD Thesis, South African National Bioinformatics Institute, University of the Western Cape).

Introduction: Tumour-specific protein markers are usually present at elevated concentrations in patient biopsy tissue; therefore tumour tissue is an ideal biological material for studying cancer proteomics and biomarker discovery studies. To understand and elucidate cancer pathogenesis and its mechanisms at the molecular level, the collection and characterisation of a large number of individual patient tissue cohorts are required. Since most pathology institutes routinely preserve biopsy tissues by standardised methods of formalin fixation and paraffin embedment, these archived, FFPE tissues are important collections of pathology material, often accompanied by important metadata, such as patient medical history and treatments. FFPE tissue blocks are conveniently stored under ambient conditions for decades, while retaining cellular morphology due to the modifications induced by formalin. However, the effect of long-term storage, at resource-limited institutions in developing countries, on extractable protein quantity and quality is not yet clear. In addition, the optimal sample preparation techniques required for accurate, reproducible results from label-free LC-MS/MS analysis across block ages remains unclear.

Methods: FFPE human colorectal carcinoma resection samples were used to determine the optimal protein extraction parameters (tissue/starting material volumes as well as protein extraction buffer composition and volume) required for accurate label-free, unfractionated, LC-MS/MS analysis. In addition, three different protein purification workflows were compared, namely detergent removal columns (DRC) or plates (DRP), the acetone precipitation and formic acid resolubilisation (APFAR) method, as well as Single-Pot Solid-Phase-enhanced Sample Preparation (SP3) using hydrophilic interaction liquid chromatography (HILIC) and magnetic resin. The effect of archival time (after approximately 1, 5 and 10 years of storage) was also assessed, as well as the performance of the different sample preparation methods

across different sample ages. Data were evaluated in terms of amount of protein extracted, peptide/protein identifications, method reproducibility and efficiency, and peptide/protein distribution according to biological processes, cellular components, and physicochemical properties.

Results: The addition of 0.5% (w/v) PEG 20,000 to the protein extraction buffer resulted in overall lower peptide and protein identifications (6828 ± 560 for validated peptides and 1927 ± 125 for validated proteins), compared to buffer without the addition of PEG (7068 ± 624 for validated peptides and 1952 ± 183 for validated proteins identified). Furthermore, the total protein yield is significantly ($p < 0.0001$) dependent on block age, with older blocks (5 and 10-year-old) yielding less protein (at 2.46 ± 0.03 mg/ml and 1.65 ± 0.04 mg/ml, respectively) than approximately 1-year-old blocks (3.82 ± 0.03 mg/ml) (with experiment power = 0.7 and $\alpha = 0.05$ for $n = 17$ per group). Block age differences were also observed in tissue proteome composition, with greater proteome composition correlation detected between the 5 and 10-year-old blocks processed via the APFAR and DRP methods (r^2 values of 0.823 and 0.835, respectively), whereas the HILIC method yielded comparable relative protein abundances for all block ages. Moreover, the different protein purification methods generated different results regarding the number of peptides and proteins identified (with the DRP method having the highest overall peptide and protein identifications, and the APFAR method having the lowest), and the different methods also introduces an observable bias with regard to proteome composition (this bias is also more pronounced for 1-year-old blocks, compared to older blocks). Differences in PCA variance were also shown, with the DRP method having the lowest variance (10.73%) between block ages, followed by the HILIC method (13.68%), and the APFAR method, which has the highest variance at 14.57%. The APFAR method had the highest overall digestion efficiency (with ≥85% of all peptides having no missed cleavages), and the HILIC method had the lowest overall digestion efficiency, with ≥80% of all peptides having no missed cleavages. Regarding the optimal protein purification technique required for archived tissues, the DRP and SP3/HILIC methods performed the best, with the SP3/HILIC method performing consistently across all block ages and requiring less protein (and therefore less starting material) than the other methods, therefore making it the most sensitive and efficient protein purification method.

Conclusions: The results confirm findings of previous studies, in which higher protein yields (>10 µg) (of FFPE animal tissues and human cells) where found to compromise the function of PEG 20,000. Therefore, it is demonstrated here that this effect is also observed in FFPE human colon tissue. Overall, the results indicate that long-term storage of FFPE tissues (at a resource-limited hospital) does not significantly interfere with retrospective proteomic analysis. In addition, variations in pre-analytical factors (spanning a decade), such as tissue harvesting, handling, the fixation protocol used as well as storage conditions, does not affect protein extraction and shotgun proteomic analysis to a significant extent.

April 2020

Declaration

I declare that *Optimisation of proteomics techniques for archival tumour blocks of a South African cohort of colorectal cancer* is my own work (except where acknowledgements indicate otherwise), that it has not been submitted for any degree or examination in any other university, and that all the sources I have used or quoted have been indicated and acknowledged by complete references.

Full name: Sophia Catherine Rossouw April 2020

Signed: .....  .....

Acknowledgements

I would like to particularly thank my mom and Dan for their overall support and help, and especially thank Dan for his additional help with my project, programming tutorials and advice. Also, a special thank you to Prof Alan Christoffels for his support and guidance during this project. I am also very grateful to Dr Hocine Bendou for his help and input in the data analysis components, Prof Renette Blignaut for her help with the statistics, and Dr Jonathan Rigby for his co-supervision role and support. I would also like to thank Mr Charles Gelderbloem, Mr Yunus Kippie, Ms Audrey Ramplin and the Pharmacy department for technical assistance and support during the project, as well as Prof Gerhard Walzl and Mrs Andrea Gutschmidt of the Immunology department at Stellenbosch University for their help and kindness in offering the use of their lab. Thank you to everyone at SANBI for your help and input over the years. I am grateful for all the kindness, support and help.

This research project was supervised by Prof Alan Christoffels of the South African National Bioinformatics Institute (SANBI) at the University of the Western Cape, and co-supervised by Dr Jonathan Rigby of the Department of Anatomical Pathology in Tygerberg Hospital at the University of Stellenbosch. This work was financially supported by the South African Research Chairs Initiative of the Department of Science and Technology and National Research Foundation of South Africa.

List of abbreviations

% (v/v)	Percentage volume solute per 100 ml
% (w/v)	Percentage gram(s) solute per 100 ml
% (w/w)	Percentage gram(s) solute per 100 grams
µg	Microgram
µl	Microlitre
µm	Micron
°C	Degrees Celsius
ACN	Acetonitrile
AmBic	Ammonium bicarbonate
ANOVA	Analysis of variance
APFAR	Acetone precipitation and formic acid resolubilisation
BCA	Bicinchoninic acid
CRC	Colorectal cancer
D	Kolmogorov-Smirnov test statistic
Da	Dalton
DRC	Detergent removal columns
DRP	Detergent removal plates
ERLIC	Electrostatic repulsion hydrophilic interaction chromatography
ESI	electrospray ionisation
F	F-ratio (test statistic used in ANOVA)
FA	Formic Acid
FDR	False discovery rate
FFPE	Formalin-fixed paraffin-embedded
Fig(s).	Figure(s)

FNR(s)	False negative rate(s)
g	Gravity
GO	Gene ontology
H	Kruskal–Wallis test statistic
H_2O	water
H&E	Haematoxylin and Eosin
HIAR	Heat-induced antigen retrieval
HILIC	Hydrophilic interaction liquid chromatography
hr(s)	hour(s)
HUPO	Human Proteome Organisation
IHC	Immunohistochemistry
pI	Isoelectric point
kDa	kilo Dalton
L	Litre
LC	Liquid chromatography
LC-MS/MS	Liquid chromatography coupled to tandem mass spectrometry
LFQ	Label-free quantitative/quantitation
MIAPE	Minimal information about a proteomics experiment
mg	milligram
ml	millilitre
mm	millimetre
mm^2	square millimetre
mm^3	cubic millimetre
mM	milli-Molar
min(s)	minute(s)
MMTS	Methyl methanethiosulphonate
MS	Mass spectrometry
MS-grade H_2O	Mass spectrometry-grade water

MW	Molecular weight
NSAF	Normalised Spectrum Abundance Factor
PCA	Principal component analysis
PCC	Pearson's correlation coefficient
PEG 20,000	Polyethylene glycol 20,000
pH	Hydrogen ion concentration
PSI	Proteomics Standards Initiative
PSM(s)	Peptide spectrum match(es)
PTM(s)	Post-translational modification(s)
r^2	Pearson correlation coefficient
RPM	Revolutions per minute
s	Second(s)
SDS	Sodium dodecyl sulphate
SP3	Single-Pot Solid-Phase-enhanced Sample Preparation
TCEP	Tris(2-carboxyethyl)phosphine
TEAB	Triethylammonium bicarbonate
TFA	Trifluoroacetic acid
UniProtKB	Universal Protein Resource Knowledge Database
W	Shapiro–Wilk test statistic
WCPL(s)	Whole cell protein lysate(s)

List of figures

List of tables

Table of contents

Publications from this thesis:

1. Rossouw, S.C., Bendou, H., Blignaut, R.J., Bell, L., Rigby, J., Christoffels, A.G. (2021). Evaluation of protein purification techniques and effects of storage duration on LC-MS/MS analysis of archived FFPE human CRC tissues. Pathol. Oncol. Res. Accepted for publication in 2021.

2. Rossouw, S.C., Bendou, H., Blignaut, R.J., Bell, L., Rigby, J., Christoffels, A.G. (Approved for peer review). The effect of polyethylene glycol 20,000 on protein extraction efficiency of FFPE tissues. AJLM. Approved for peer review – awaiting feedback.

Chapter 1: Introduction to thesis and research statement

1.1 Brief summary of the literature

Formalin-fixed, paraffin-embedded (FFPE) patient biopsy tissue archives are important collections of pathology material and ideal subject material for proteomic studies that investigate the molecular features of diseases (Craven *et al*., 2013; Avaritt *et al*., 2014; Bronsert *et al*., 2014; Gustafsson *et al*., 2015). This is due to the fact that these archives are accompanied by patient records and metadata that contain patients' medical history, disease progression and treatment response, often over decades. FFPE tissue archives also contain all the disease subtypes and variations among demographic groups and often contain sufficiently large patient sample cohorts for statistical significant biomarker studies. For these reasons they are a precious and important resource for clinical and translational research, retrospective proteomic studies and biomarker discovery. Over the past two decades, the field of FFPE tissue proteomics has grown and developed immensely due to the existence and availability of these vast, untapped archives of FFPE tissue blocks. This has allowed for extensive development and standardisation in the mass spectrometry-based proteomic field regarding methods for the analysis of FFPE tissue (Avaritt *et al*., 2014; Bronsert *et al*., 2014; Wiśniewski *et al*., 2013; Gustafsson *et al*., 2015). There are, however, pre-analytical challenges to overcome with FFPE tissue analyses, including the pre-analysis treatment of the tissue after the biopsy is taken (keeping the tissue "fresh" before fixation so that necrosis does not occur), variations in fixation time (causing incomplete/partial fixation or over-fixation of the tissue), and inaccessibility or degradation of proteins due to inappropriate preservation and/or long-term storage (Sprung *et al*., 2009; Wolff *et al*., 2011; Tanca *et al*., 2011; Craven *et al*., 2013; Gustafsson *et al*., 2015). The analytical challenges mainly include optimal conditions for protein extraction as well as optimal analysis conditions during mass spectrometry (MS) analysis (Magdeldin & Yamamoto, 2012; Avaritt *et al*., 2014; Wiśniewski *et al*., 2013). The optimal conditions and procedures for efficient and reproducible protein processing from FFPE tissues have not yet been standardised and new sensitive techniques are continually being developed and improved upon. It is therefore of great interest to establish an efficient protein processing method, across

various block ages, and also to determine the impact of block age on FFPE blocks stored at a low-resource government hospital in a developing country (such as South Africa) with regard to obtainable protein yield and proteomic-level features.

1.2 Research statement – research rationale

Proteins are the products of active genes and influence the molecular pathways in cells directly, whereas all genes are not active or translated into functional proteins (Mishra & Verma, 2010). Proteins therefore provide better information about disease pathology, and proteomics allows for the study and profiling of protein signatures in tissues, which assists in the process of biomarker discovery. Tumour-specific protein markers are usually present at elevated concentrations in patient biopsy tissue (Gustafsson *et al*., 2015). Therefore, tumour tissue is a desirable biological material for cancer proteomics investigations, as well as the discovery phases of biomarker studies. For this purpose, large numbers of individual patient tissue cohorts are required. Such large volumes of fresh, cryopreserved tissue are often not feasible with regard to ethics, costs, logistics, and standardised sample collection and cryopreservation methods. However, most pathology institutes have vast archives of FFPE tissue samples that are stored at room temperature, thereby removing much of the cost and difficulty of obtaining fresh cryopreserved tissue.

MS analysis allows for the elucidation and generation of peptide/protein profile signatures from FFPE patient biopsy tissues as well as protein expression changes between healthy and disease tissue, and identification of unique protein markers associated with a disease (Findeisen & Neumaier, 2009; Wiśniewski *et al*., 2013; Gustafsson *et al*., 2015; Wiśniewski *et al*., 2015). It also offers greater advantages over traditional antibody–based clinical assays. These advantages include the ability to identify thousands of peptides from heterogeneous tissues, greater assay specificity, cost–effectiveness, and time–effectiveness (Findeisen & Neumaier, 2009). Therefore it has become increasingly necessary to develop and standardise protocols for the proteomic analysis of FFPE tissues. However, the effect of long-term storage, at resource-limited institutions in developing countries, on extractable protein quantity/quality has not yet been investigated. In addition, the optimal sample preparation techniques required for accurate, reproducible results from label-free LC-

MS/MS analysis across block ages remains unclear. This study aims to improve FFPE sample preparation methods for label-free, LC-MS/MS analysis and possible future identification of biomarkers for CRC in South African populations.

1.3 Aims and objectives of thesis research project

The aims of the project were to determine:
(1) The optimal protein extraction protocol (including the optimal protein extraction buffer – either with or without addition of PEG 20,000) and purification method(s) across all block ages, as well as
(2) The proteomic-level effects of long-term storage on patient FFPE colorectal carcinoma resection tissues using label-free mass spectrometry analysis. The project adopted a phased approach:

1. In the first part of the study, a pilot experiment was performed using 3 patient cases. The objectives of this pilot study were to establish:
1.1 The volume of tissue and protein extraction buffer required to generate an adequate protein yield for subsequent unfractionated, label-free LC-MS/MS analysis
1.2 An efficient protein extraction protocol for FFPE tissues – by comparing the protein extraction efficiency of buffer either with or without the addition of PEG 20,000
1.3 The optimal search engine settings and protein sequence database (for peptide spectrum matching via a database search) required for data analysis

2. In the second part of the study, 17 patient cases were selected (per experimental condition) to give a sample size with 70% confidence level ($\alpha = 0.05$) based on the previous study's results. The objectives were to determine:
2.1 The most efficient and reproducible sample preparation/protein purification method required at different block ages, for 1, 5 and 10-year-old FFPE tissue samples
2.2 The proteomic-level effects of long-term storage of FFPE tissue blocks at a resource-limited pathology archive

1.4 Thesis overview

Chapter 2: Literature review.

A literature review of FFPE tissue fixation dynamics, challenges and advantages with regards to proteomic analysis.

Chapter 3: The effect of polyethylene glycol 20,000 on protein extraction efficiency of formalin-fixed, paraffin-embedded tissues.

This study established the optimal tissue and protein extraction buffer volumes required for accurate label-free LC-MS/MS analysis and demonstrated that the absence of PEG 20,000 increases the number of peptides and proteins identified by unfractionated LC-MS/MS analysis.

Chapter 4: Evaluation of protein purification techniques and effects of storage duration on LC-MS/MS analysis of archived FFPE human CRC tissues.

This study evaluated the protein extraction efficiency of 1, 5 and 10-year old human colorectal carcinoma resection tissues and assessed three different gel-free sample preparation/protein purification methods for label-free LC-MS/MS analysis. The results found that the protein yield (mg/ml) is significantly dependent on block age, with older blocks yielding less protein than newer blocks. Block age also impacted on tissue proteome composition. Additionally, the different protein purification methods generated different results regarding the number of peptides and proteins identified, sample proteome composition, differences in reproducibility in terms of peptide identification overlap, PCA variance, as well as protocol digestion efficiency. Overall, it was found that the DRP and HILIC methods performed the best.

Chapter 5: Conclusions and future prospects.

Chapter 2: Literature review

This study had access to human colorectal carcinoma resection samples, and since tumour-specific protein markers are present at elevated concentrations in patient tissues, this makes it a desirable biological material for cancer proteomics studies. Since FFPE tissue samples can be stored at room temperature, it removes most of the cost and difficulty of obtaining fresh cryopreserved tissue. However, formalin-fixation poses some challenges with regard to tissue proteome analysis. The advantages and challenges of FFPE tissue proteomics are discussed, as well as FFPE sample preparation methods for label-free, LC-MS/MS analysis, with a brief introduction to MS data analysis and colorectal cancer (CRC).

2.1 Formalin-fixed, paraffin-embedded (FFPE) tissue proteomics

2.1.1 The formalin-fixation process

Tissues from biopsies, resections and/or surgery are routinely taken from patients as a treatment option and/or to facilitate more accurate diagnosis. The current universal tissue preservation method of choice is formalin-fixation and paraffin-embedment, to avoid tissue auto-proteolysis and putrefaction, and to allow tissue specimens to be analysed and examined at a later stage (Stanta, 2011; Avaritt *et al*., 2014; Bronsert *et al*., 2014; Gustafsson *et al*., 2015). Formalin-fixation is also considered to be a superior preservative, since formaldehyde quickly and easily penetrates and fixes tissues because of its small molecular size, it causes minimal tissue shrinkage and distortion, and produces exceptional staining results in histopathology (Klockenbusch *et al*., 2012; Magdeldin & Yamamoto, 2012; Gustafsson *et al*., 2015). The FFPE method of tissue preservation also allows for the indefinite room temperature storage of FFPE blocks, thereby removing much of the cost and difficulty associated with fresh-cryopreserved tissue storage. The technique involves the immersion and incubation of tissues in formaldehyde solution, which is then replaced with alcohol (ethanol) in a dehydration step. Dehydration of the sample is achieved by removing all the water from the sample via ethanol incubation and subsequent alcohol clearing with xylene incubation. The xylene is then replaced by molten paraffin, which

infiltrates the sample. The final step involves paraffin-embedding and hardening of the sample, which involves embedment of the specimen into liquid embedding material such as wax. Samples are then stored and archived for future use (Daniele *et al*., 2011; Bronsert *et al*., 2014; Gustafsson *et al*., 2015).

During the formalin-fixation process, the formaldehyde solution penetrates the tissue and reacts by cross-linking cellular molecules such as nucleic acids, polysaccharides, and amino acids including lysine, arginine, histidine and cysteine. Several aspects of the formaldehyde-protein interactions have still not been resolved (Klockenbusch *et al*., 2012; Magdeldin & Yamamoto, 2012; Maes *et al*., 2013; Gustafsson *et al*., 2015). Currently accepted/most probable formaldehyde-induced cross-linking reactions in biological tissues involve the formation of reactive methylol adducts (mass shift of +30 Da), unsaturated Schiff base "azomethine" adducts (mass shift of +12 Da) and the formation of acetals (Magdeldin & Yamamoto, 2012; Gustafsson *et al*., 2015) (Fig. 1).

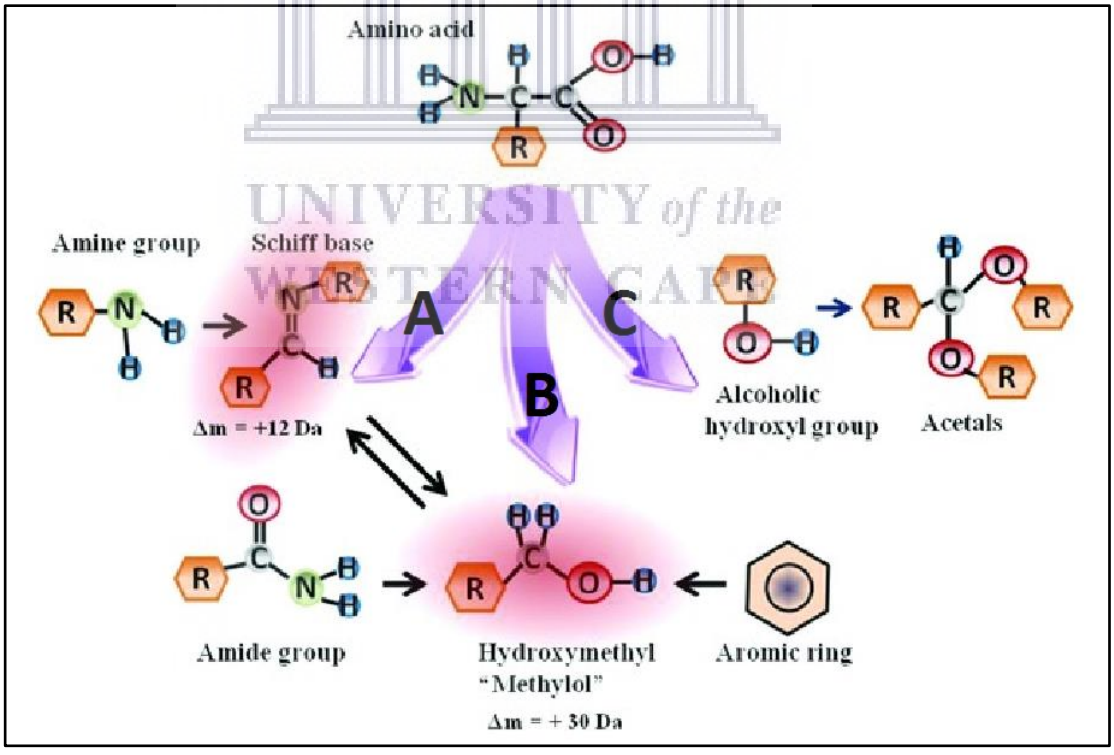

Figure 1. Schematic representation of the most probable formaldehyde-induced protein modifications in FFPE tissues. (A) Condensation of amine groups with aldehydes results in the formation of unsaturated Schiff base "azomethine" adducts with a mass shift of +12 Da (Δm = 12 Da), which is a reversible reaction with the methylol adduct. (B) The interaction between formaldehyde and basic amino acid residues, amide groups or aromatic rings results in the formation of reactive methylol adducts (Δm = 30 Da). (C) Another modification involves the formation of acetals. (Image modified from Magdeldin & Yamamoto, 2012)

Formaldehyde cross-linking of proteins may be initiated through the creation of a hydroxymethyl-methylol adduct when the aldehyde group in formaldehyde reacts with primary amines (nucleophilic groups) in proteins, followed by water elimination to form a Schiff base (Fig. 1). A subsequent nucleophilic substitution reaction, between the methylene carbon of the Schiff base and a nucleophile in the amino acid residue, forms a methylene bridge. The resulting methylene bridge links two peptide sequences and therefore also adds to the total molecular weight of the modified protein (Klockenbusch *et al*., 2012; Magdeldin & Yamamoto, 2012; Maes *et al*., 2013; Gustafsson *et al*., 2015). In addition to these reactions, primary amines can react with hydroxyl groups to create acetals or alternatively with aromatic rings, creating hydroxymethyl groups, which are further involved in cross-linking reactions. The same or different peptides can also react through an amide moiety to form stable methylene diamide bridges in a secondary consolidation process. However, even though studies involved in elucidating formalin-fixation reactions with proteins have made significant progress, the detailed chemical modifications that occur in FFPE tissue still requires extensive experimental research. And since FFPE tissue blocks are molecularly more complex than the chemical models studied so far, additional work is required to explain the extent of formaldehyde cross-linking in these blocks (Magdeldin & Yamamoto, 2012; Fowler *et al*., 2013; Avaritt *et al*., 2014; Gustafsson *et al*., 2015).

Studies have found that formaldehyde also induces protein modifications on different levels in FFPE tissues (Magdeldin & Yamamoto, 2012; Fowler *et al*., 2013; Avaritt *et al*., 2014). These modifications occur at the primary, secondary, tertiary as well as quaternary protein structure (Fig. 2). Therefore, in addition to changing protein molecular weight (MW), formaldehyde-induced modifications may also affect protein physicochemical properties such as the isoelectric point (pI) and/or hydropathicity. However, more research is required to explain the extent of formaldehyde cross-linking and its effects on FFPE tissue blocks. Successful proteomic analyses of FFPE tissues is highly dependent upon the efficient cleavage of the formaldehyde-induced cross-links and complete reversal of these formaldehyde-induced protein modifications (Klockenbusch *et al*., 2012; Magdeldin & Yamamoto, 2012; Maes *et al*., 2013; Gustafsson *et al*., 2015). However, since the full extent of formaldehyde-

induced crosslinking chemistry and its kinetics within FFPE tissues are not yet well understood, complete reversal is never achieved.

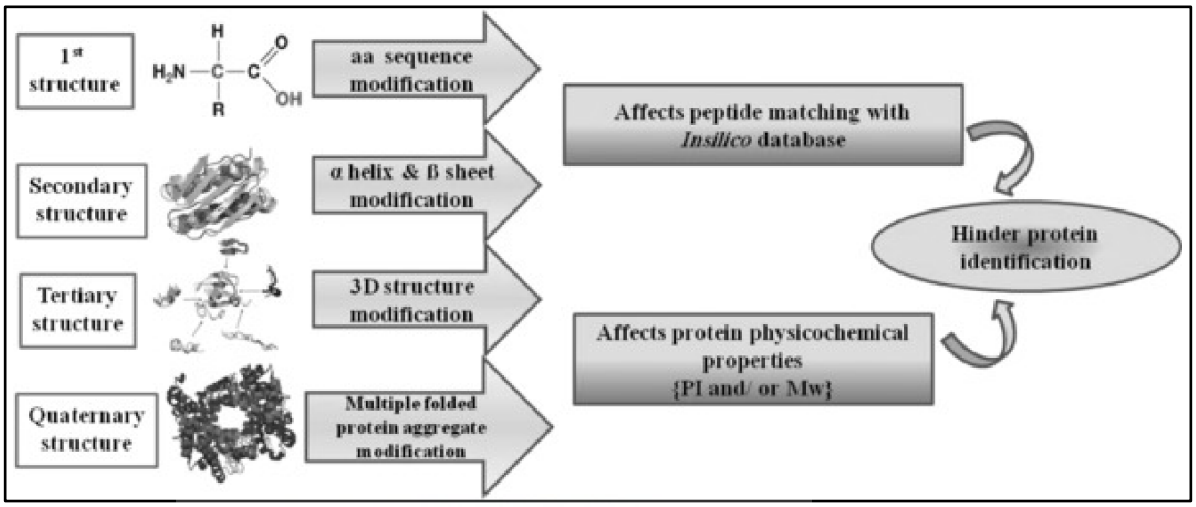

Figure 2. The effect of formaldehyde fixation on protein structure and physicochemical properties. Formaldehyde induces protein modifications on different levels of protein structure in FFPE tissues. These probable changes that proteins undergo include: amino acid (aa) sequence modifications at the primary structure level, α-helix and β-sheet modifications at the secondary structure level, 3-D structural modifications at the tertiary level, and/or multiple protein aggregates at the quaternary level due to formaldehyde cross-linking between molecules. These modifications may, in turn, affect protein physicochemical properties, such as isoelectric point (pI) and/or molecular weight (MW), as well as peptide matching to *in sillico* databases during data analysis of mass spectra obtained. Formaldehyde fixation therefore has the ability to hinder accurate protein identification of FFPE samples analysed via mass spectrometry. (Image taken from Magdeldin & Yamamoto, 2012)

2.1.2 The advantages and challenges of FFPE tissue analysis – an overview of pre-analytical and analytical factors

Since patient tissues are routinely taken and preserved, there are currently millions of FFPE tissue blocks in hospital and/or pathology archives across the world and millions of new blocks, from new patient cases, are added every year (Stanta, 2011). These FFPE tissue archives have often accumulated patient samples for decades, and contain all the disease subtypes and variations among demographic groups and often comprise large cohorts and sufficient sample numbers for statistical significant biomarker studies (Fowler *et al*., 2013; Avaritt *et al*., 2014; Bronsert *et al*., 2014; Gustafsson *et al*., 2015). In addition, the samples are complemented with accompanying clinical records and patient metadata that also provide insight into disease prognosis and treatment response. For these reasons FFPE tissue archives are

a precious and important resource for clinical and translational research, retrospective proteomic studies and biomarker discovery.

Tumour tissue represents the ideal biological material for cancer proteomics studies and biomarker discovery, since tumour-specific protein markers are typically present at elevated concentrations in patient biopsy tissue (Maes *et al*., 2013; Gustafsson *et al*., 2015). However, freshly-frozen cryopreserved tissue poses challenges with regard to required resources, standardised sample collection, cryopreservation and logistical constraints that significantly increase research costs. In contrast, FFPE samples are easily stored and obtainable, therefore requiring fewer resources to maintain FFPE sample archives.

Moreover, Fu *et al*. (2013) found that formalin-fixation was a better long-term storage option for tissue compared to cryopreservation. They investigated the effects of applying different heating and pressure settings on the quality of proteins extracted, using dounce homogenisation of tissues in 100 mM Tris–HCl (pH 8.0) and 100 mM DTT buffer with subsequent addition of SDS (to a final SDS concentration of 4%). They found that the quality of proteins extracted from cryopreserved tissue (snap frozen and stored at -80 ºC, either for 3 months or 2 years) were inferior to that of FFPE blocks (stored for either 3 months or 15 years) with regards to protein recovery and protein identifications. Therefore, combined with the problems associated with fresh/cryopreserved tissue storage and handling, FFPE tissue is considered a good alternative to fresh/cryopreserved tissue. For these reasons, techniques (such as mass spectrometry (MS)-based proteomics) required to access proteomic information from FFPE tissues and determine changes (or similarities) in the proteome composition of tumour vs. healthy tissues have been extensively developed and standardised in the last decade (Fowler *et al*., 2013; Avaritt *et al*., 2014; Bronsert *et al*., 2014; Wiśniewski *et al*., 2013; Gustafsson *et al*., 2015). Even with all the advantages that FFPE tissues possess, FFPE tissue analyses presents many challenges, including pre-analytical as well as analytical factors that influence downstream results (Maes *et al*., 2013; Thompson *et al*., 2013; Piehowski *et al*., 2018).

2.1.2.1 The impact of pre-analytical factors on FFPE tissue proteomics results

The pre-analysis handling and treatment of the tissue, includes minimising ischaemic time and keeping the tissue "fresh" after surgery/biopsy and before fixation, so that necrosis/putrefaction does not occur. Other pre-analytical factors include proper fixation and storage of the tissue (minimising significant temperature fluctuations and light exposure during storage) as well as storage duration (Daniele *et al*., 2011; Thompson *et al*., 2013; Maes *et al*., 2013; Bass *et al*., 2014). Proper fixation of the tissue, such as ensuring that the tissue specimen size is right (not too large for proper formalin penetration) and keeping the fixation time optimal, significantly impacts on downstream protein analysis. Variations in fixation time may cause incomplete or partial fixation of the tissue (leading to degradation of proteins during storage) and extended periods of fixation leads to over-fixation, which increases the extent of formalin-induced molecule cross-linking and protein modification, making it increasingly difficult to access proteins in their original biological form (Sprung *et al*., 2009; Tanca *et al*., 2011; Wolff *et al*., 2011). The impact of storage time on the number of proteins identified via label-free LC-MS/MS from FFPE colon adenoma tissue samples was evaluated by Sprung *et al.* (2009) and they found no significant difference even from tissues that had been stored for up to 10 years. Similarly, Craven *et al*. (2011) found no significant difference in protein identifications from FFPE kidney tissue (normal and tumour) samples that were stored up to 10 years. During the completion of this thesis, Piehowski *et al*. (2018) published their work in which they used tandem mass tag labelling and high pH fractionation to evaluate the impact of storage time on FFPE ovarian adenocarcinoma specimens (as old as 32 years) and found an overall decline in identifiable peptides and phosphopeptides due to the formalin fixation process but no further decline/degradation due to storage duration. Even though the aforementioned studies focused on storage duration/block age, to our knowledge there is no evidence to demonstrate the outcome of different protein purification techniques on older samples. There remains a need to provide empirical evidence for the impact of storage duration and conditions within the context of a resource-limited environment, such as the Anatomical Pathology department at Tygerberg Hospital (Western Cape, South Africa).

2.1.2.2 The impact of analytical factors on FFPE tissue proteomics results

The main analytical factors that determine the successful outcome of a FFPE tissue shotgun MS proteomics experiment can be divided into factors that are required for robust and efficient protein extraction and factors required for effective protein purification, protein digestion and sample clean-up for LC-MS/MS analysis.

Requirements for efficient protein extraction from FFPE tissues

One of the major analytical challenges in FFPE tissue proteomics is the efficient extraction of proteins from these samples (Magdeldin & Yamamoto, 2012; Fowler *et al*., 2013; Avaritt *et al*., 2014; Wiśniewski *et al*., 2013). Strategies that have been employed to facilitate efficient protein extraction include the use of strong detergents, hydrophilic synthetic polymers (such as PEG 20,000 – discussed in more detail in chapter 3) as well as heat-induced antigen retrieval (HIAR).

Shi *et al*. (1991) developed HIAR, which is a superior IHC staining technique, and involves the incubation of FFPE tissue sections in a suitable buffer (the constituents of which depends on the experimental aims to be achieved, in their case an IHC study) (after deparaffinisation and rehydration steps) at a high temperature (90 – 120°C) for up to several hours. The high temperature incubation denatures the proteins in the FFPE tissue, causing them to unfold and lose their conformations and, in so doing, also breaks the formaldehyde-induced cross-links. The HIAR process is stabilised by selecting an appropriate buffer and pH, which is optimal for most biological reactions (pH 6 to 8), water-soluble and able to stabilise proteins (by keeping the pH of the buffer solution within 1.0 pH unit of the proteins' isoelectric point). HIAR is usually followed by additional sample preparation methods to allow for efficient tryptic digestion to generate peptides that are analysed via MS. The HIAR technique has been successfully and extensively employed in FFPE tissue proteomics, with many research groups also aiming to improve upon it or adapting variations of it (Magdeldin & Yamamoto, 2012; Fowler *et al*., 2013; Avaritt *et al*., 2014; Gustafsson *et al*., 2015).

The detergent of choice for total tissue solubilisation and protein extraction is sodium dodecyl sulphate (SDS) (Wiśniewski *et al*., 2009; Botelho *et al*., 2010; Pellerin *et al*., 2015). Shi *et al*. (2006) found that 2% SDS is a critical chemical component for the successful extraction of protein from FFPE tissue sections, as well as heating or boiling (HIAR method) the samples in extraction buffer (at not more than 100˚C). Other studies found similar results; with Speers & Wu (2007) recommending the use of a buffer with greater than 1% SDS, while Wiśniewski *et al*. (2009) recommends a concentration of 4% SDS for maximal protein extraction (Kachuk *et al*., 2015). SDS is a powerful anionic detergent that disrupts cell membranes, disaggregates protein complexes, and denatures and solubilises proteins. It does this by binding to amino acids via hydrophobic and ionic interactions, thereby altering the protein's spatial conformational structure. This inhibits proteases from accessing protein cleavage sites (which have become distorted through SDS binding) and also inhibits protease activity by changing enzyme conformational structure (through SDS binding) (Wiśniewski *et al*., 2009; Botelho *et al*., 2010; Pellerin *et al*., 2015). Unfortunately, SDS usage has many analytical disadvantages that have to be addressed while preparing a sample for MS analysis. Due to its interactions with proteins, SDS strongly inhibits trypsin (enzyme) activity, even at very low concentrations, thereby limiting protein identification. In addition, SDS alters the chromatographic separation of peptides and also interferes with electrospray ionisation (ESI) mass spectrometry by dominating mass spectra and significantly suppressing analyte ion signals (due to SDS being readily ionisabile and being present in greater abundances than individual peptide ions). For these reasons, SDS must be completely depleted from a sample before enzymatic digestion and LC-ESI MS/MS analysis (Wiśniewski *et al*., 2009; Botelho *et al*., 2010; Kachuk *et al*., 2015; Pellerin *et al*., 2015).

Protein purification, digestion and sample preparation for LC-MS/MS analysis

Shotgun MS analysis requires a relatively simplified, purified and homogenous peptide sample for generation of spectra (Aguilar, 2004). Therefore, the upstream sample processing of biological samples requires a combination of techniques to ensure that a purified homogenous peptide sample is produced (Aguilar, 2004). For this purpose, various sample preparation methods are used to remove detergents and contaminants that are not compatible with protein digestion and MS analysis.

FFPE samples taken from patients for diagnosis are usually very small, and therefore there is a limited amount of starting material available for analysis. SDS removal with minimal sample loss is a challenging task and several gel-free approaches have been proposed over the years. Of interest to this current study are sample purification approaches that include the use of detergent removal resin (ThermoFisher Scientific, 2017), or protein precipitation with organic solvents, such as the acetone precipitation and formic acid resolubilisation (APFAR) method (Botelho *et al*., 2010; Doucette *et al*., 2014; Kachuk *et al*., 2015), and/or methods using hydrophilic interaction liquid chromatography (HILIC) and magnetic resin (such as the Single-Pot Solid-Phase-enhanced Sample Preparation (SP3) method) (Hughes *et al*., 2014; Hughes *et al*., 2019) in the sample processing workflow prior to LC-MS/MS.

The detergent removal columns/plates contain a proprietary detergent removal resin, which facilitates the removal of commonly used detergents, such as SDS, from a protein sample with minimal sample loss (ThermoFisher Scientific, 2017) (Fig. 3).

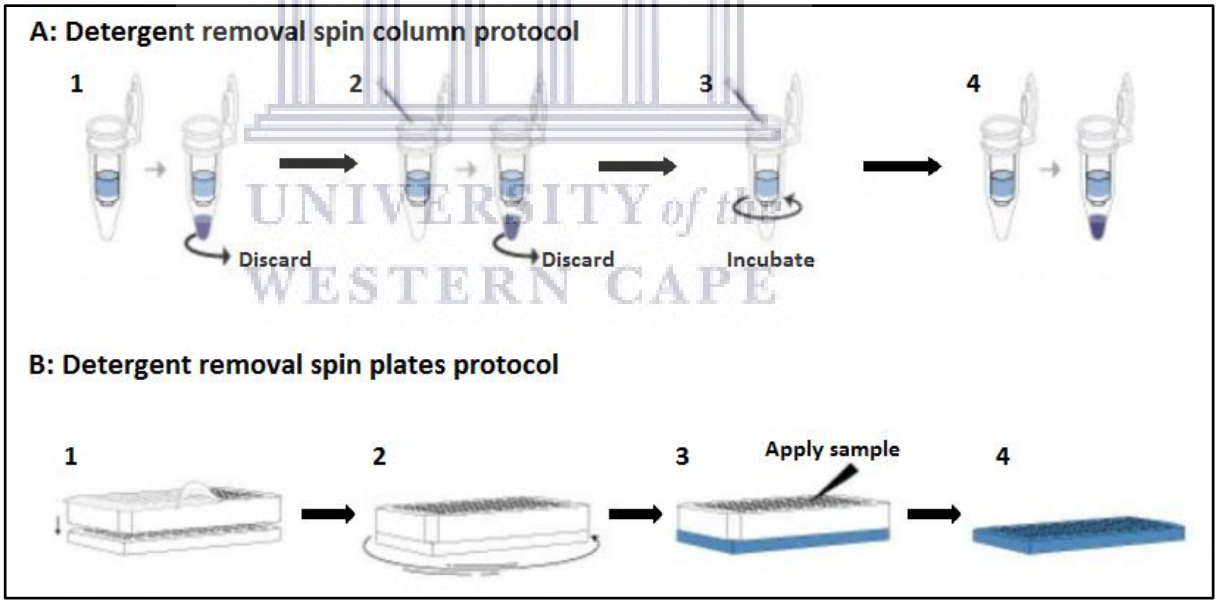

Fig. 3. The detergent removal procedure using ThermoScientific Pierce® Detergent Removal Resin in spin columns and plates. (A) The steps involved in the DRC protocol are (1) storage buffer removal by centrifugation, (2) column washes with equilibration buffer, (3) addition of sample and incubation, (4) centrifugation and elution of detergent-free protein sample for further use in downstream analyses. (B) The steps involved in the DRP protocol are (1) plate equilibration to room temperature, followed by packaging removal and wash plate assembly, (2) the plate assembly is centrifuged to remove the storage buffer, and wells are washed with equilibration buffer three times, (3) the detergent removal plate is then placed on top of a sample collection plate (blue) and the samples are applied to each well, the plate is then incubated at room temperature after which the plate assembly is centrifuged to (4) elute the detergent-free samples in the sample collection plate. The eluted samples are depleted of detergent and can be used for tryptic digestion and LC-MS/MS analysis. (Image modified from ThermoFisher Scientific, 2017)

Figure 3 shows the different steps involved in removing commonly used detergents and surfactants from a sample, using either detergent removal columns (DRC) or 96-well detergent removal filter plates (DRP). The DRC protocol (Fig. 3 A) involves centrifugation of the column to remove the storage buffer, which is then discarded. This is followed by column washes with equilibration buffer. The sample containing the detergent to be removed is then added to the column and incubated, after which the column is centrifuged to elute the detergent-free protein sample. The sample is now ready for further use in downstream sample processing for LC-MS/MS. The ThermoScientific Pierce® Detergent Removal Spin Plate (DRP) protocol allows for multiple samples to be processed, using the same high-performance resin of the DRC protocol. The DRP protocol (Fig. 3 B) involves equilibration of the spin plate to room temperature, followed by removal of the sealing material from the bottom of the plate. The plate is then placed on top of a wash plate and the sealing material from the top of the detergent removal plate is removed. The plate assembly is then centrifuged to remove the storage buffer, and the flow-through discarded. This is followed by washing the plate's wells with equilibration buffer three times. The detergent removal plate is then placed on top of a sample collection plate (blue) by aligning the alphanumeric indices on the plate. The samples (25-100µL per well) are added to the centre of the resin beds in each well, and the plate is incubated at room temperature. The plate assembly is then centrifuged and the detergent-free samples are collected in the sample collection plate. After detergent removal, the eluted samples are depleted of detergent and can be used for tryptic digestion and LC-MS/MS analysis (ThermoFisher Scientific, 2017). For both protocols, the high-performance column resin can remove detergents that are at concentrations between 1-5%, with greater than 95% efficiency. In addition, the detergent removal columns and plates provide high protein/peptide recovery for samples.

Another effective strategy to deplete SDS in a protein sample (prior to tryptic digestion and/or LC-MS/MS analysis) is the precipitation of proteins in the sample by addition of an organic solvent (Botelho *et al*., 2010; Doucette *et al*., 2014; Kachuk *et al*., 2015). The latest advancement in this technique, made by Doucette *et al*. (2014), involves protein precipitation in acetone followed by resolubilisation of the precipitated proteins with ice cold (-20°C) formic acid and dilution in water for storage (-20°C) before further processing and LC-MS/MS analysis (Fig. 4). By using

this technique, they found significant recovery of membrane proteins, which exceeded that of protein recovery from a cytosolic fraction, although the technique recovers both membrane and water-soluble proteins. In addition, the resolubilised proteins remained soluble and stable at room temperature without modification (such as formylation, which is typical of proteins suspended in formic acid at room temperature) when analysed by LC-MS/MS.

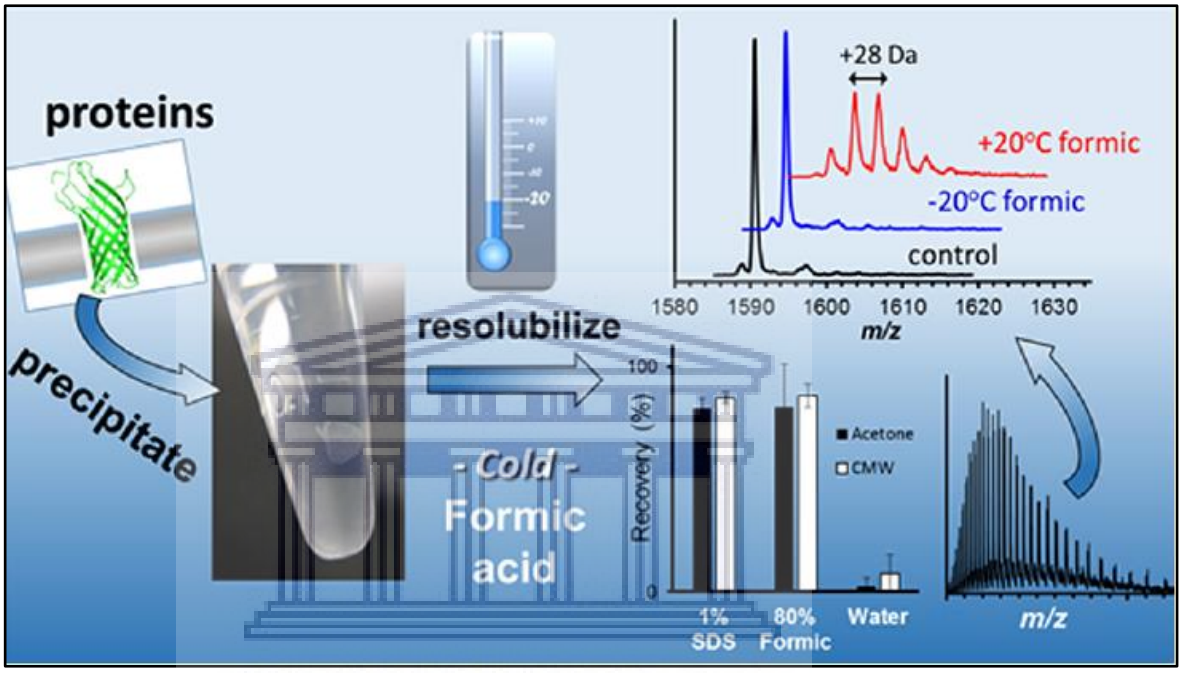

Fig. 4. The acetone precipitation and formic acid resolubilisation (APFAR) method. Proteins in a sample are precipitated by the addition of ice cold acetone, followed by overnight incubation at -20˚C. Samples are centrifuged to collect the precipitated protein, which is washed with ice cold acetone. This precipitation process is repeated for approximately three pelleting steps, which is followed by pellet/protein precipitate solubilisation with formic acid and resuspension in solution before quantitation and subsequent downstream processing and analysis via LC-MS/MS. (Image modified from Image taken from Doucette *et al*., 2014)

The Single-Pot Solid-Phase-enhanced Sample Preparation (SP3) method (Hughes *et al*., 2014; Hughes *et al*., 2019) is fast, uncomplicated, and addresses sample preparation challenges such as quantity-limited biological samples and downstream detergent interference. Carboxylate-coated paramagnetic beads (which are immobilised on the surface of a microcentrifuge tube via placement on a magnetic rack) are used, onto which proteins and peptides are immobilised, after addition of an organic solvent, such as acetonitrile (Fig. 5).

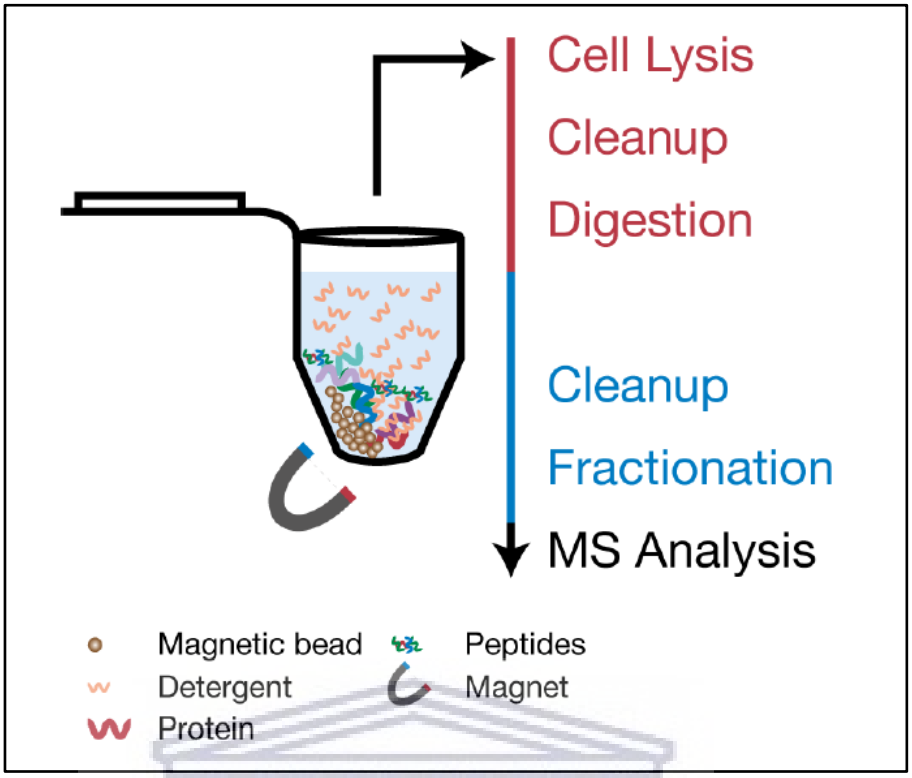

Fig. 5. The SP3 method workflow. The entire SP3 method can be performed in a single tube. Carboxylate-coated paramagnetic beads are immobilised on a magnetic rack. The detergent-containing protein extract is added to the tube and upon the addition of acetonitrile, the proteins are immobilised onto the paramagnetic beads. This immobilization on the bead surface permits washing and removal of detergents and contaminating substances before tryptic digestion and/or further downstream sample processing and LC-MS/MS analysis. Protein/peptide elution is achieved by adjusting the solution's pH. (Image modified from Hughes *et al.*, 2014)

This mechanism is similar to hydrophilic interaction chromatography (HILIC) or electrostatic repulsion hydrophilic interaction chromatography (ERLIC) whereby solutes in an ion-exchange column can be retained through hydrophilic interaction when the column is eluted with an organic mobile phase, even if they have the same charge as the stationary phase. During HILIC the mobile phase forms a solvation layer on the surface of the stationary phase, thereby creating a liquid-liquid analyte extraction system. Analyte elution is achieved as the mobile phase's polarity is altered – resulting in analytes eluting in order of increasing polarity (Alpert, 1990; Alpert, 2008). Similarly, the carboxylate-coated paramagnetic beads (of the SP3 method) act as the column's stationary phase would and allows for the trapping of proteins and peptides in a solvation layer, which forms on the hydrophilic surface of the beads after addition of an organic solvent. By controlling the pH of the solution, the interaction between the proteins/peptides and paramagnetic beads can be adjusted; keeping the solution acidic promotes HILIC-style binding to proteins/peptides, which

allows for detergent removal, whereas increasing the pH of the solution makes it basic and causes ERLIC-style repulsion between the proteins/peptides and the negatively charged carboxylate groups on the beads' surface resulting in elution of the proteins/peptides from the beads. Therefore, the entire SP3 process can be performed in a single tube (as shown in figure 5), providing a rapid and efficient means of proteomic sample preparation (Hughes *et al*., 2014; Hughes *et al*., 2019).

2.2 MS analysis in clinical proteomics

Since the proteome is the cellular workforce of an organism, its complete characterisation is important to understand the underlying biological phenomena and processes within an organism (Aebersold & Mann, 2003; Nahnsen *et al*., 2013; Zhang *et al*., 2013; Kumar *et al*., 2017). MS analysis has developed over the last two decades into the analytical method of choice for most proteomics studies. MS analysis allows for the elucidation and generation of peptide/protein profile signatures from FFPE patient biopsy tissues as well as protein expression changes between healthy and disease tissue. It also enables identification of unique protein markers associated with a disease (Findeisen & Neumaier, 2009; Wiśniewski *et al*., 2013; Gustafsson *et al*., 2015; Wiśniewski *et al*., 2015).

The clinical proteomics approach can be defined as the use of proteomics techniques, together with bioinformatics tools, to investigate disease-associated changes in peptide and protein profile patterns for diagnostic purposes (Findeisen & Neumaier, 2009). Since the vast improvements made in MS instrumentation over the last few decades, the proteomics field has also significantly progressed together with the development of biomarker discovery approaches using MS-based techniques. These advances can be grouped into three main approaches, namely protein or peptide profiling methods, non-gel-based methods, and gel-based or two-dimensional gel electrophoresis methods. However, only protein or peptide profiling and non-gel-based methods are applicable for clinical proteomics approaches, since these methods offer the greatest reproducibility and high-throughput capabilities (Findeisen & Neumaier, 2009). This study will focus on non-gel-based LC-MS/MS approaches for peptide/protein identification, characterisation, and quantification.

2.2.1 Liquid chromatography coupled to tandem MS (LC-MS/MS)–based analysis

Liquid chromatography coupled to tandem mass spectrometry (LC-MS/MS) is a powerful analytical chemistry technique, which combines the capability of liquid chromatography to separate complex analyte mixtures with the highly sensitive and selective mass analysis capabilities of mass spectrometry (Shen & Noon, 2004; Bessant, 2017). The tandem mass spectrometry (MS/MS or MS2) technique involves the coupling of two (or more) mass analysers in an additional reaction step, thereby increasing their complex analyte analysis capabilities. The setup mainly involves two mass filters that are arranged sequentially with a collision cell between them (Fig. 6).

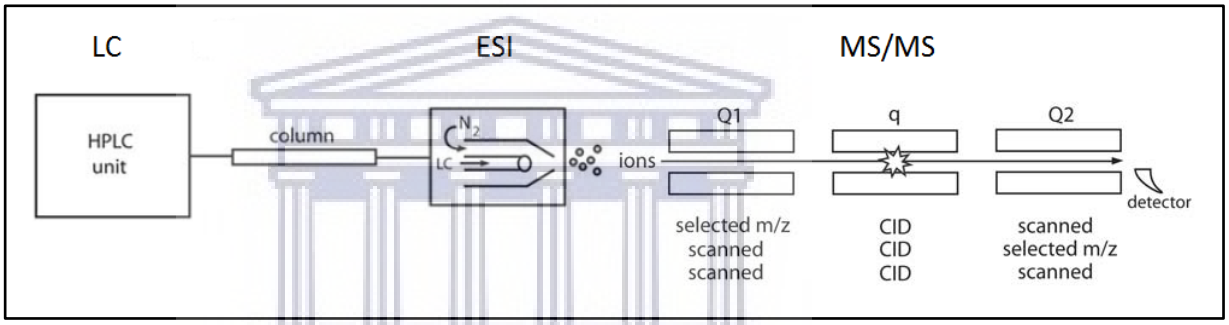

Fig. 6. A simplified schematic representation of a LC-MS/MS analysis setup. The HPLC system is coupled to the ionisation (ESI) source of the mass spectrometer through a chromatography column. The sample to be analysed flows from the HPLC unit, is separated in the column and ionised by ESI before being analysed by the mass spectrometer. In the MS/MS step, the selected precursor ions are isolated and fragmented by CID and resultant product ions are scanned, detected and their spectra recorded. (Image modified from Shen & Noon, 2004)

Due to their chemical structures, the peptides and proteins interact with the chromatographic surface in an orientation-specific manner, which determines their retention time. This principle forms the basis of the selectivity that can be achieved with HPLC techniques (Aguilar, 2004). Mass spectrometry also measures the mass-to-charge ratio (m/z) of a molecule that has been ionised and its fragment ions, thereby generating a mass spectrum, which is an output plot of m/z vs. ion intensity/abundance (Shen & Noon, 2004; Bessant, 2017).

Due to its ability to be online coupled to a liquid chromatography system, ESI is the most extensively applied ionisation technique in proteomics and the method of choice

when analysing large biomolecules and highly complex samples (Lai, 2013; Villar & Cho, 2013). ESI is also a favoured ionisation method because it ionises (addition of a charge) peptide analytes without fragmenting them, therefore making it a "soft ionisation" method (Bessant, 2017). During the ESI process, peptide analytes are encapsulated in solvent droplets and then ionised by applying an ultra-high-voltage to the aqueous sample. This produces a fine spray of droplets, from which solvent continually evaporates to create analyte ions (Lai, 2013; Bessant, 2017; Netzela & Dasari, 2017) (Fig. 7).

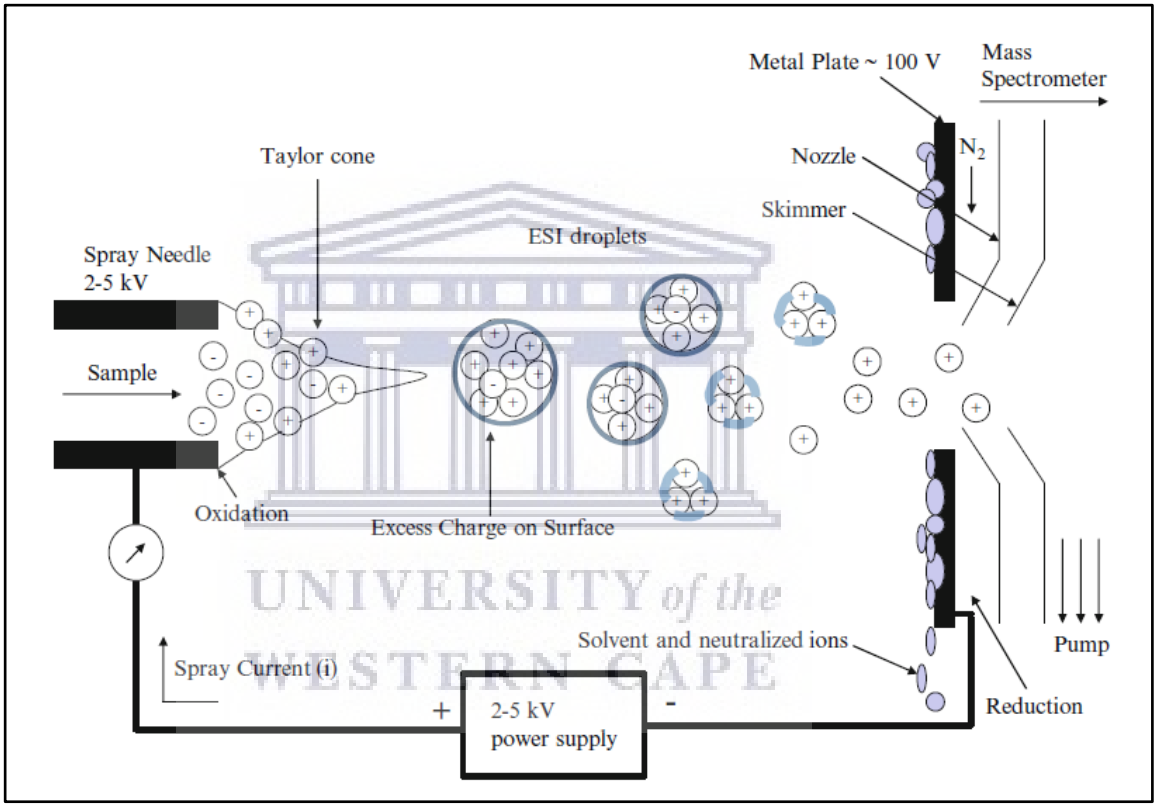

Fig. 7. The ESI process. The analyte solution (containing peptides) is forced through the chromatographic system's capillary column, which has been supplied with a high voltage. This creates a Taylor cone at the tip of the spray needle. As these charged droplets of analyte ions and solvent travel from the Taylor cone toward the mass spectrometer, the solvent continually evaporates creating analyte ions. These analyte ions (charged peptides) move into the mass spectrometer where they are analysed. (Image taken from Villar & Cho, 2013)

During a nano-ESI MS-MS run, analyte ions are produced at the ESI source and captured and focussed for effective ion transmission (Michalski *et al*., 2011). The ions travel through the mass analyser for analysis of molecular mass and measurement of ion intensity and arrive at different parts of the detector according to their mass-to-charge (m/z) ratio (Karas *et al*., 2000). Uncharged, neutral ion species

are filtered-out and only ions of interest are selected for analysis; ionised species that undergo tandem mass spectrometry (MS/MS) analysis are submitted to two stages of mass analysis scans, which are separated by a stage of selection and a stage of fragmentation in a collision cell (Christin *et al*., 2011; Blein-Nicolas & Zivy, 2016). Ions sent into the collision cells undergo collision-induced fragmentation into fragment ions or product ions. In nano-ESI LC–MS/MS experiments, structural data are efficiently generated by peptide fragmentation in the mass spectrometer via electron transfer dissociation (ETD), collision-induced dissociation (CID) and/or higher energy collisional dissociation (HCD) (Shen & Noon, 2004; Pejchinovski *et al*., 2015). Primarily of interest to this study is the CID method, in which peptide fragmentation occurs mainly at amide bonds along the backbone, thereby generating b- and y-type fragment ions, which is used for structural determination (Fig. 8).

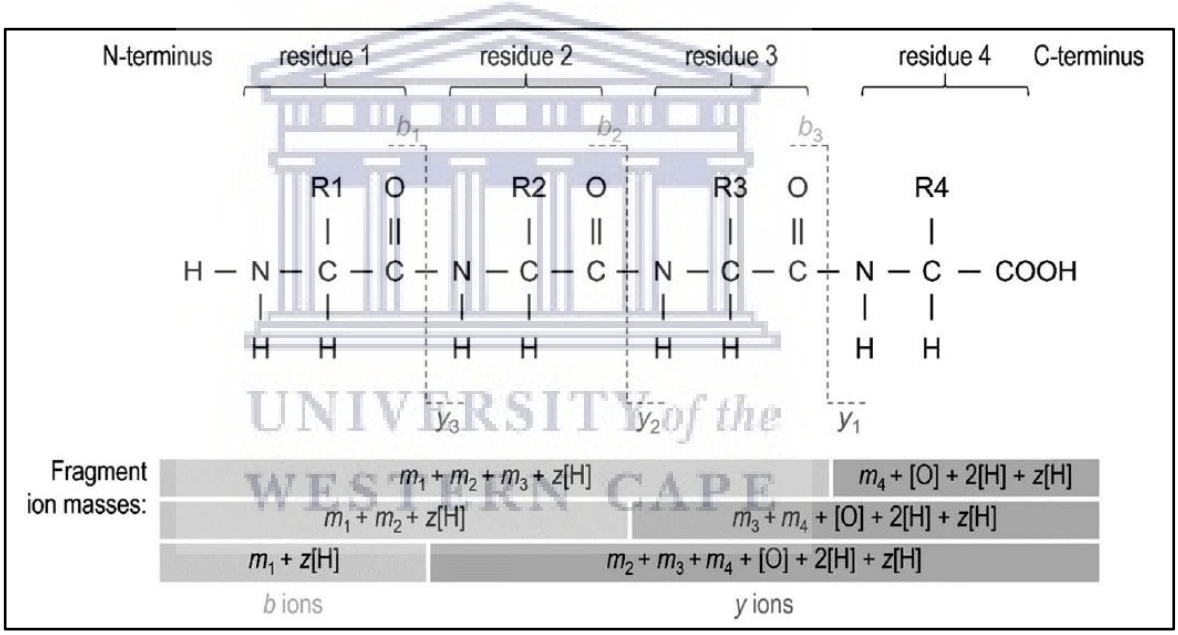

Fig. 8. A generalised product ion series produced by a peptide sequence after fragmentation via the CID method. The chemical structure of a generic four amino acid peptide is shown, with vertical dotted lines indicating typical CID fragmentation points. The corresponding calculations of b- and y-ion masses are shown in the table below. (Image taken from Bessant, 2017)

During the CID process, fragment ions are produced by the collision of isolated precursor ions with noble gases (e.g argon, helium), leading to their kinetic energy being converted into vibrational internal energy. This increase in vibrational internal energy causes peptide bond breakage and generation of fragment ions. Since the fragments generated with CID all originate from the precursor, supplementary information relating to the primary sequence as well as peptide/protein PTMs is

obtained (Fig. 8). However, each fragmentation method has advantages and disadvantages and it remains unclear which one is the most suitable for peptide identification (Shen & Noon, 2004; Pejchinovski *et al*., 2015). After CID, the fragment ions are collected into "packets" and stabilised before being transferred to the detector (orbitrap) (Michalski *et al*., 2011). The ions' m/z ratios and intensities are recorded as a tandem mass spectrum (Netzela & Dasari, 2017). Each tandem mass spectrum contains all the information that is needed to successfully identify the peptide. While this process ends for one set of analytes, another set of analytes (ions) are selected for fragmentation in the collision cell and detection in the orbitrap. This process is repeated for all ions that are to be fragmented and analysed (Michalski *et al*., 2011).

LC-MS/MS is currently one of the fundamental analytical approaches used in proteomics (Christin *et al*., 2011; Lai *et al*., 2013; Blein-Nicolas & Zivy, 2016). A typical LC-MS/MS setup allows for protein identification, characterisation and quantitation from complex, heterogeneous biological samples, such as cancer biopsies. LC-MS/MS-based proteomics consists of three main approaches, namely bottom-up, middle-down, or the top-down approach (Zhang *et al*., 2013; Blein-Nicolas & Zivy, 2016) (Fig. 9).

As shown in figure 9, the top-down approach analyses intact proteins, whereas the bottom-up and middle-down approaches involves the characterisation and analysis of proteins through proteolysis (of a protein mixture from a whole cell or tissue extract) and subsequent peptide generation and analysis (Zhang *et al*., 2013). Of interest to this study is the bottom-up proteomics approach (also referred to as shotgun MS), since it is difficult to obtain and maintain intact proteins during the sample processing stages for the top-down MS technique. In addition, top-down MS has decreased throughput ability due to the limitations and challenges faced with intact protein detection by MS (Duncan *et al*., 2010; Doerr, 2013; Vehus *et al*., 2016). Furthermore, for FFPE tissue proteomics, top-down approaches lead to variability in the protein extraction and fractionation results since the tissue solubilisation and HIAR technique (described in section 2.1.2.2.1) for intact, full-length proteins still requires standardisation (Gustafsson *et al*., 2015). The extraction of full-length proteins from older FFPE blocks is also more difficult due to the extent of formalin-induced

crosslinking, which is a continual process (Lemaire *et al*., 2007). The shotgun MS approach is therefore more suitable for FFPE tissue MS analysis. The main disadvantage of shotgun MS is the loss of some biological information, however, it is still considered a successful technique due to its high-throughput proteome profiling ability, relative ease of sample handling and processing, as well as increased detectability by the instrument (Duncan *et al*., 2010; Doerr, 2013).

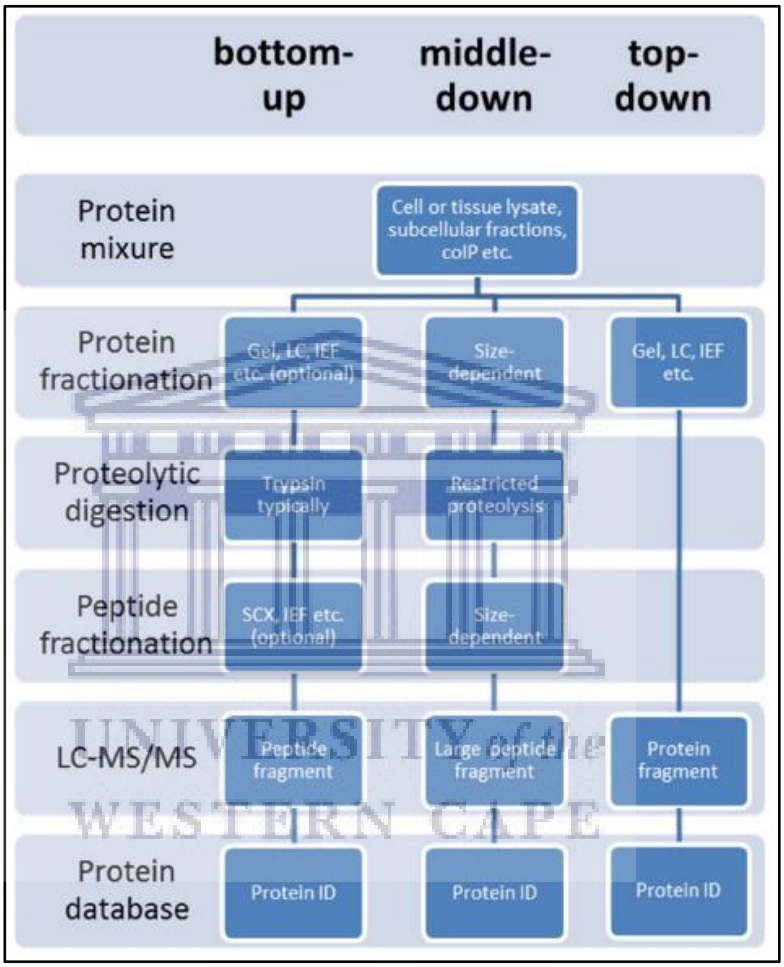

Fig. 9. The three main LC-MS/MS-based proteomics approaches. The bottom-up and middle-down approaches involves proteolytic cleavage of the sample to be analysed, whereas the top-down approach analyses non-digested, intact proteins. (Image taken from Zhang *et al*., 2013)

2.2.2 Shotgun LC-MS/MS data analysis

It is challenging to perform well-considered MS data analysis while also keeping abreast of the latest best practises, standards and publication guidelines for MS-based protein identification, characterisation and quantification methods (Vaudel *et al*., 2014). Shotgun MS is one of the most popular approaches used to profile proteomes

from biological samples in a high-throughput manner. Figure 10 shows a typical bottom-up (shotgun) tandem mass spectrometry workflow. One of the major difficulties of this approach is to reconstruct the proteomic "information" contained within the original sample before it was processed for MS analysis (Blein-Nicolas & Zivy, 2016; Kumar *et al*., 2017).

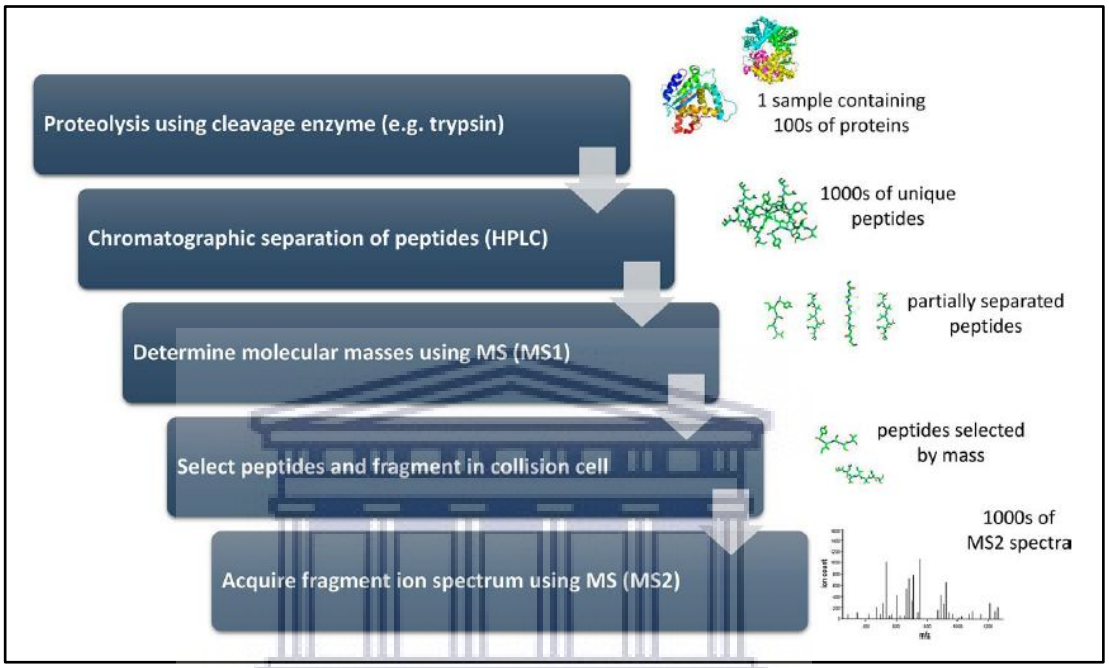

Fig. 10. A typical bottom-up (shotgun) tandem mass spectrometry workflow. A typical shotgun MS sample analysis workflow involves proteolytic cleavage of the sample to be analysed, followed by chromatographic separation of the peptides generated. Partially separated peptides are subjected to a first round of mass spectrometry analysis (MS1) whereby their m/z values are determined, and according to these values, similar groups of peptides are selected (in a data-dependent manner) and fragmented. The second mass spectrometry scan (MS2) produces fragment ion spectra, which are used to identify the peptides and corresponding proteins form a database. (Image taken from Bessant, 2017)

Biological tissues consist of complex mixtures of proteins as well as proteins with PTMs and even through proteolytic cleavage, peptide fractionation and LC-separation, the peptide mixtures generally remain complex. It is therefore necessary to address two main issues when designing a shotgun MS experiment; the first is to ensure that the relevant data is extracted from the sample, and secondly to employ the best methods of data analysis to answer the research question. These two issues relate to MS data acquisition, processing and analysis and are under constant development since there are no gold standard methods in place yet (Blein-Nicolas & Zivy, 2016). The main bioinformatics steps involved in a protein identification, characterisation

and quantification workflow are: (1) raw MS file conversion to community standard formats, (2) peptide spectrum matching (PSM) via database search using multiple search engines, (3) peptide and protein identification and validation using the target-decoy approach, (4) functional and gene ontology (GO) enrichment analysis and/or identification of PTMs, and (5) data storage, sharing and re-use.

2.2.2.1 Raw MS file conversion

The data from a MS experiment consists of raw mass spectra, which are processed and used to identify and characterise peptides and proteins, and quantify the protein abundance of the sample analysed (Martens *et al*., 2011). A mass spectrometer produces raw data files in a binary output file format, which is proprietary/trademarked and varies depending on the instrument's manufacturer (Kessner *et al*., 2008; Deutsch, 2012; Keerthikumar & Mathivanan, 2017). In addition, mass spectrometer instruments require the use of commercial software for FDA approval, therefore most instruments operate on a Microsoft Windows® operating system. This has hindered data analysis and sharing as well as the ability to develop transparent, open source software for downstream analysis. It is therefore necessary to first convert the raw binary files to a community standard format for data analysis. This format conversion step is platform dependent because it requires vendor libraries. Therefore the format conversion step usually takes place on a Windows operating system, using a compatible format converter, such as msConvert, which forms part of the ProteoWizard software package. The community standard format for mass spectra files is mzML, however, data repositories such as PRIDE also accept mzIdentML, mgf (peak list files), and mzXML (Kessner *et al*., 2008; Deutsch, 2012; Martens *et al*., 2011; Keerthikumar & Mathivanan, 2017) format. msConvert reduces the amount of data to interpret by applying a peak-picker, which is a software program that transforms the bell-shaped profile mode peaks into single data points, called a peak list (Deutsch, 2012; Chambers *et al*., 2012; French *et al*., 2015; Keerthikumar & Mathivanan, 2017). The overall mzML file structure contains all the unprocessed spectra, of both MS1 and MS2 scans, including additional spectrum and instrument annotation and associated metadata (such as experimental protocol, instrumentation, and operational parameters, etc.). The mzML format is encoded in XML and is a rich, schema-linked controlled vocabulary, which allows for accurate

and unambiguous annotation of metadata. In addition, mzML comes with a set of semantic validation rules (Kessner *et al*., 2008; Deutsch, 2012; Martens *et al*., 2011; Keerthikumar & Mathivanan, 2017). In the past, some researchers have used Windows emulators to circumvent the use of a Windows operating system, although these may not function in all scenarios as intended. It is therefore advisable to only use a Windows operating system to convert the raw data files to mzML (or any other functional) format and to perform all downstream processing using other operating systems (Vizcaíno *et al*., 2017).

2.2.2.2 Peptide spectrum matching (PSM) via protein sequence database search

One tandem MS run generally produces thousands of spectra, which may be interpreted using either a de novo or protein database search method (Kumar *et al*., 2017). De novo approaches suffers from low resolution, low sensitivity, and partial coverage in peptide detection and therefore these methods are not viable for high-throughput proteomics. Therefore the preferred method of peptide and protein identification (and relative quantification) from the spectra is protein sequence database searching (Kumar *et al*., 2017) (Fig. 11).

The protein sequence database has a major impact on the final list of identified proteins and is one of the major influencing factors in identifying proteins present in the sample, and therefore also in deriving the experiment's biological conclusions (Kumar *et al*., 2017). A shotgun proteomics workflows will only retrieve and identify proteins contained within the database, therefore it is crucial to choose the correct and most appropriate database for the identification procedure. The database should therefore contain all possible protein sequences. On the other hand, if the database is too large, there is more chance for the search engines to introduce false positive identifications. In addition, when different search parameters are applied, it changes the effective search space, thereby making the choice of database an important consideration. It is therefore important to determine which database would be optimal for best protein discovery without increasing false positives (Kumar *et al*., 2017). For these reasons it is best to use a curated protein database that is continuously updated and reviewed, such as UniProt (Apweiler *et al*., 2004).

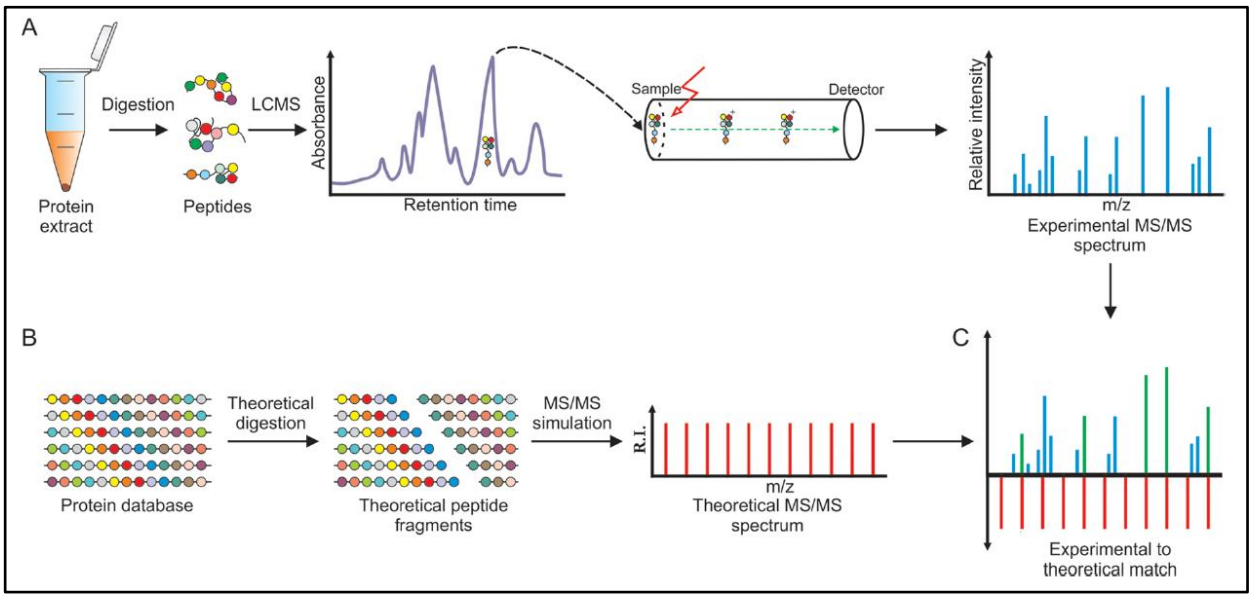

Fig. 11. Peptide spectrum matching (PSM) via protein sequence database search. (A) A shotgun/bottom-up MS sample preparation and LC-MS/MS workflow generates experimental MS/MS spectra. (B) Protein sequences from a database are theoretically cleaved *in sillico* according to the cleavage rules of the specific protease (such as trypsin) used in the experiment. The theoretical peptides also undergo simulated "fragmentation" (according to the specific parameters set for the database search algorithm), which is similar to that of the experimental process. This produces a database of theoretical mass spectra, which display the same fragmentation pattern specific to the experimental process, dissociation method and instrument used in (A). Theoretical and experimental spectra are then compared (C) and match to allow for peptide identification. (Image taken from Chugunova *et al*., 2018)

PSM and subsequent peptide identification is achieved by using a protein sequence database (that represents all biological protein sequences that might be present in the sample), which is theoretically digested *in silico* according to the cleavage rules of the specific protease (such as trypsin) used in the experiment (Hubbard, 2010; Zhang *et al*., 2013; Vaudel *et al*., 2014; Kumar *et al*., 2017) (Fig. 11). In addition, the theoretical peptides undergo simulated "fragmentation" (according to the specific parameters set for the database search algorithm), which is similar to that of the experimental process. This produces a database of theoretical mass spectra, which display the same fragmentation pattern specific to the experimental process, dissociation method and instrument used. To obtain PSMs, the theoretical spectra are compared to each experimental spectrum obtained from the MS analysis of the sample (Fig. 11). All the PSMs, which are the peptides that best explain/match an experimental spectrum, are retained for further analysis (Hubbard, 2010; Vaudel *et al*., 2014; Kumar *et al*., 2017; Wright & Choudhary, 2017). Due to random chance, some fraction of the positive PSMs may be due to false matches (false positives). To

estimate the percentage of possible false matches, multiple hypothesis testing is applied to the whole list of PSMs. The method of target-decoy-database searching, which produces the false discovery rate (FDR) estimation, is now considered best practise (Elias & Gygi, 2010). This method involves searching and comparing experimental spectra against the target database, which contain true representative biological protein sequences, as well as a decoy database that contains decoy or false proteins, which may just be the reversed versions of the true/target sequences. The decoy database can be constructed using tools such as DBToolkit or SearchGUI, which offers an option to automatically add decoy sequences to your target protein sequence database file. The positive hits from the decoy database then allows for construction of PSM scores, which allows for the estimation of the percentage of false positive PSMs assigned from the target database. The FDR corrected list of PSMs is then used to identify the list of peptides and proteins expressed in the sample. Accurate protein identification is crucial for determining and comparing qualitative/quantitative changes between different biological samples and/or biological states (disease vs. healthy). And since MS-based protein quantification is dependent on peptide detection, it is also influenced by factors that affect peptide discovery (Karpievitch *et al*., 2012; Vaudel *et al*., 2014; Kumar *et al*., 2017; Wright & Choudhary, 2017).

For the purpose of PSM processing, multiple search engines have been developed, each with its own advantages and drawbacks (Hubbard, 2010; Vaudel *et al*., 2014; Kumar *et al*., 2017). While it is considered best practise to use only one and the same version of protein sequence database for protein/peptide identification throughout a MS proteomics project, it is advised to combine multiple search engines and their results (Martin *et al*., 2013; Vaudel *et al*., 2014). Of interest to this study are search engines such as X! Tandem, MyriMatch, MS Amanda, MS-GF+, and OMSSA, which can all be simultaneously utilised through SearchGUI (Vaudel *et al*., 2011). SearchGUI is an open-source graphical user interface tool, which allows for the simultaneous running of multiple search engines and storage of their results (upon search completion) in separate files in a previously selected output folder/directory. SearchGUI can be used together with freely available open-source tools such as PeptideShaker (Vaudel *et al*., 2015), which enables visualisation, comparison and further analysis (such as peptide and protein identification) of all the search engines'

results. SearchGUI may be used as a stand-alone tool or it can be added to a data analysis workflow pipeline (Vaudel *et al*., 2011).

2.2.2.3 Peptide and protein identification and validation using the target-decoy approach

PeptideShaker is a freely available, open-source proteomics informatics tool that is used for the analysis and interpretation of primary data, data sharing and dissemination, as well as the re-analysis of publicly available MS-based data (Vaudel *et al*., 2015). PeptideShaker uses the target-decoy search strategy to identify peptides and proteins and it also unifies and collates the PSM lists of different search algorithms, to allow for the use of multiple search engines. It also provides statistical confidence estimates for each peptide and protein by taking into account the protein inference issues; it provides FDRs at the PSM, peptide and protein levels. In addition, it calculates reliable false negative rates (FNRs) to enable filtering of results according to a FDR-versus-FNR cost-benefit rationale, which shows the specificity and sensitivity of the results. PeptideShaker can also be used to provide confident PTM modification site inference using the latest PTM localisation methods (Vaudel *et al*., 2015). In addition, PeptideShaker uses spectrum counting based protein quantification, which relies on the reasoning that highly abundant peptides will have a higher intensity, and are therefore more likely to generate acquisition of MS/MS spectra (Vaudel *et al*., 2011; Vaudel, 2017). Consequently, peptides from abundant proteins are more likely to be identified and possess more spectra. The NSAF method followed involves counting the number of spectra attributed to a protein (Powell *et al*., 2004). This count is then normalised for the length of the protein, the presence of shared peptides, as well as redundant peptides (Vaudel *et al*., 2011; Vaudel, 2017). PeptideShaker also allows for inspection of the GO of a dataset, by conducting a GO enrichment analysis of all validated proteins. This is presented as a list of all GO terms together with their prevalence (percentage frequency of occurrence) within the dataset, and the significance level is calculated using hypergeometric testing. The GOSlim UniProtKB-GOA is used to keep the number of GO terms at a manageable level (www.ebi.ac.uk/GOA).

2.2.2.4 Data storage, sharing, re-use and current MS-based proteomics best practises (MIAPE and HUPO PSI)

To avoid the serious shortcomings of MS-based proteomics experiments, the experimental design should be standardised with respect to pre-analytical, analytical and post-analytical variabilities, thereby allowing comparison of results between different experiments (Findeisen & Neumaier, 2009). The Human Proteome Organisation (HUPO) is a Proteomics Standards Initiative (PSI) that has released recommendations about the Minimal Information About a Proteomics Experiment (MIAPE) as a guideline to researchers to increase independent reproducibility of published data (Taylor *et al*., 2007).

HUPO PSI working groups have highlighted the importance of appropriate education and MS-based proteomics training for proper application of such a complex technology (Bell *et al*., 2009). The HUPO PSI has developed several guidelines for performing proteomics experiments. These include identification and monitoring of any lab-derived contaminations (such as keratins) that may negatively impact on the data obtained. In addition, the use of target-decoy search strategies have been made mandatory, and FDRs should be reported. To address the issue of redundant identifications, which are sequence variants of the same protein, unique peptides and tandem mass spectra need to be monitored to ensure that the minimum list of protein identifications is reported. Furthermore, to eliminate aliases, a gene-centric database could ensure that only a single descriptive name is assigned to each protein sequence. Also, to aid data sharing and the ease of data submission to repositories, tools for transforming data into standardised formats are required (Bell *et al*., 2009). Most journals that report on proteomics and proteomics informatics have adopted the HUPO PSI and MIAPE guidelines as requirements for publication.

Due to the variety of data types and experimental workflows as well as the inherent complexity of MS-based data, its public deposition and storage are still less developed compared to other data-intensive disciplines such as genomics (Martin *et al*., 2013; Vaudel *et al*., 2014; Perez-Riverol *et al*., 2015). Over the years several public repositories for MS-based proteomics experiments have been established, including the Global Proteome Machine Database (GPMDB), PeptideAtlas, and the

PRIDE database. To enable better integration of these public repositories, ProteomeXchange consortium was established. It allows for the coordinated sharing, mining and re-use of public proteomics data (Perez-Riverol *et al*., 2015).

2.3 Colorectal cancer (CRC)

Due to the availability of vast archives of FFPE tissue blocks, the field of FFPE tissue proteomics has grown and developed immensely over the past two decades, leading to extensive development and standardisation in the MS-based proteomic field towards improving methods for analysis of FFPE tissues (Avaritt *et al*., 2014; Bronsert *et al*., 2014; Wiśniewski *et al*., 2013; Gustafsson *et al*., 2015). This has also given rise to the field of clinical FFPE proteomics and progressed towards protein biomarker discovery, since tumour-specific protein markers are present in higher abundance within patient tumour tissue (Gustafsson *et al*., 2015). Of interest to this study is human CRC.

CRC is a complex, heterogenous disease caused by genetic and/or epigenetic changes in the epithelial cells of the large intestine that eventually result in the formation of precancerous lesions (Adeola *et al*., 2014; Balboa *et al*., 2014; Yamagishi *et al*., 2016). These lesions may give rise to adenomatous polyps and/or adenocarcinomas that may develop into cancer (Fig. 12).

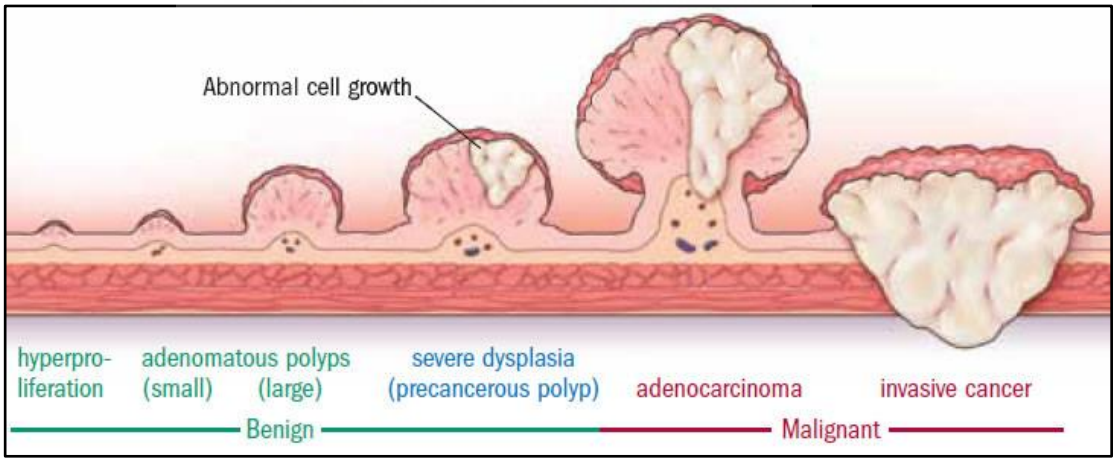

Fig. 12 The stages of adenomatous polyps in the colon/colorectal region. A schematic representation of how adenomatous polyps develop and transform from benign growths into precancerous lesions that lead to the formation of adenocarcinomas and eventually invasive tumours of colon cancer. (Image taken online from www.health.harvard.edu/)

There are two main types of CRC, namely sporadic (nonhereditary) and hereditary (Coetzee & Thomson, 2013; Balboa *et al*., 2014). Of interest to this study is sporadic CRC, which occurs in individuals without a genetic predisposition or family history of CRC (Yamagishi *et al*., 2016). The exact factors that predispose an individual to develop sporadic CRC are still unclear, however, it is widely believed to be attributed to accumulation of genetic alterations (due to environmental carcinogens, age-related factors, lifestyle and diet) as well as chronic infection and inflammatory diseases such as long-standing ulcerative colitis, diverticulosis or colonic Crohn's disease (Ballinger & Patchett, 2003; Balboa *et al*., 2014).

Most sporadic CRC tumours occur on the left side of the large intestine, namely beyond the descending colon region and into the sigmoid colon and rectum areas (Ballinger & Patchett, 2003). Sporadic CRC pathogenesis usually follows the "adenoma-carcinoma" sequence whereby an initial benign adenoma develops into a carcinoma (Ballinger & Patchett, 2003; Adeola *et al*., 2014) (Fig. 12). CRC stages progress from the tumour being confined to the bowel wall, then extending through the bowel wall, followed by further stage of regional lymph node involvement and eventually distant metastases (Fig. 13). CRC treatment often involves surgery with tumour resection and, if possible, end-to-end anastomosis of the remaining "healthy" colon to restore colonic continuity (Ballinger & Patchett, 2003).

Classification and diagnosis of CRC uses all available information to define the disease subtype, including disease location, cellular morphology, immunophenotype, immunohistochemistry (IHC), as well as genetic and clinical features (Ballinger & Patchett, 2003; Jass, 2007). A screening colonoscopy is generally advised for high risk individuals that have a family history of hereditary CRC or a first-degree relative that developed CRC before 50 years of age (Ballinger & Patchett, 2003). Healthy individuals over the age of 50 years are encouraged to be screened for CRC, since it has been shown to significantly reduce CRC mortality. However, due to the cost and invasive procedures, this strategy has not yet been widely adopted by healthy individuals (Ballinger & Patchett, 2003; Quesada-Calvo *et al*., 2017). There is currently still a great need for non-invasive, sensitive, specific, and cost-effective diagnostic screening and biomarkers to determine the presence of pre-neoplastic

lesions and/or early CRC stages to reduce CRC incidence and increase patient survival (Quesada-Calvo *et al*., 2017).

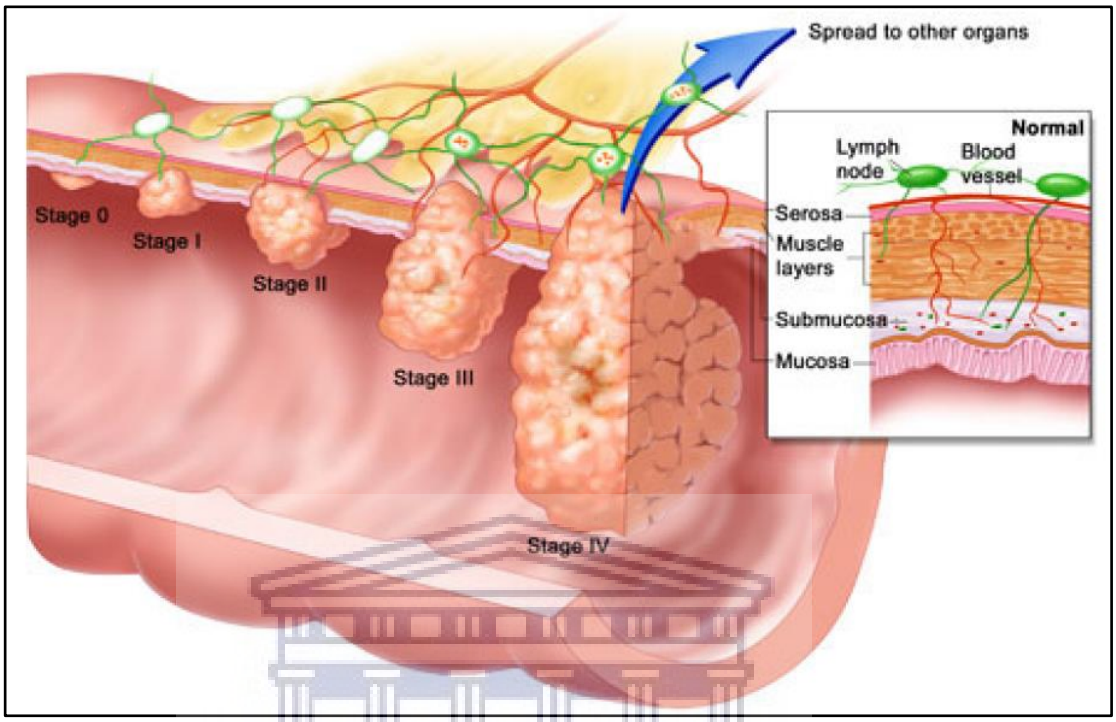

Fig. 13. The stages of CRC development. A schematic representation of the stages (0 to IV) of CRC tumour development and growth within the colon. At stage 0 the tumour has not grown beyond the inner layer of the colon wall. Stage I has the tumour growing into the outer layer of the colon wall. At stage II the tumour is protruding through the wall but has not spread to the lymph nodes yet. Tumour cells start spreading to the lymph nodes at stage III and to distant organs, such as the liver and/or lungs in stage IV. (Image taken online from http://coloncancerpreventionproject.org)

2.3.1 Implications of CRC heterogeneity for biomarker discovery

In addition to the occurrence of different CRC types and subtypes, CRC is also highly heterogeneous and displays intertumoral heterogeneity (cancer variation among different patients with the same CRC type/subtype), intratumoral heterogeneity and molecular heterogeneity (variation within the same tumour with respect to tumour cell morphology, cell type, and distinct genomic profiles separating clonal populations), as well as interbiopsy heterogeneity (different genetic signals existing in different parts of the same biopsy specimen) (Balboa *et al*., 2014; Punt *et al*., 2016). This heterogeneity may be attributed to the diverse scenarios in which CRC develops and each tumour may have a unique signature (Balboa *et al*., 2014). In general, cancer

heterogeneity may be attributed to three main theories, namely due to natural selection, clonal evolution and/or cancer stem cell theory (Adeola *et al*., 2014). The mutational rates in tumours have been found to be, on average, 200 times greater than in normal cells (Bielas *et al*., 2006). This, together with the different genomic and epigenomic conditions that exist within a tumour, contributes to the development of intertumoral heterogeneity (Balboa *et al*., 2014). A tumour's heterogeneous features are unique, for the most part, and improbable to be identical in another organism. The intertumoral heterogeneity that develops during CRC pathogenesis brings about a different mutational spectrum between patients with the same type of CRC. Intertumoral heterogeneity will affect patient prognosis and treatment and explains why different individuals respond differently to treatment. It is therefore becoming progressively important to establish the genetic and protein profiles of patients so as to determine tumourigenesis and tumour progression (Balboa *et al*., 2014).

Protein profiles or a panel of several proteins (biomarker signature) may be more effective than single protein biomarker(s) for development of screening tests, due to the heterogeneous nature of CRC (Quesada-Calvo *et al*., 2017). These "cancer" protein profiles, which may be associated with precancerous or cancer progression, are regulated and expressed by dysplastic and neoplastic tissues. Colon tissue therefore presents a direct source to study these protein changes. In addition, the availability of vast amounts and different patient cases of archived FFPE tissues increases the probability of identifying significant and specific potential CRC biomarker panels (Quesada-Calvo *et al*., 2017).

2.3.2 MS-based proteomics to classify and diagnose CRC

Recent advances in MS-based proteomics have enabled researchers to apply these techniques in the fields of biology, pathology and drug discovery (Chen & Yates, 2007; Nibbe & Chance, 2009; Adeola *et al*., 2014). MS is currently one of the most powerful proteomic tools and is able to produce data with excellent sensitivities and specificities on cancers. MS-based proteomics techniques are able to differentiate protein expression levels between disease states, identify and quantitate expressed proteins as well as generate protein expression profiles for cancer characterisation and subtype classification (Chen & Yates, 2007; Adeola *et al*., 2014). These techniques

also allow for the study and profiling of molecular signatures in tissues as well as monitoring changes in protein post-translational modifications (PTMs), which assist in the process of biomarker discovery. Peptide/protein profiles may be used to generate subtype-specific protein expression signatures as well as indicate tumour grade (Diamandis, 2004; Chen & Yates, 2007; Nibbe & Chance, 2009).

2.4 Conclusions

Over the past two decades, the field of FFPE tissue proteomics has grown and developed immensely due to the existence and availability of vast, untapped archives of FFPE tissue blocks (Avaritt *et al*., 2014; Bronsert *et al*., 2014; Wiśniewski *et al*., 2013; Gustafsson *et al*., 2015). This has also allowed for extensive development and standardisation in the MS-based proteomic field, as well as genomics and immunohistochemical studies that have focussed on improving methods for analysis of FFPE tissue. There are, however, pre-analytical and analytical challenges to overcome to ensure that the true representation of the proteome in FFPE tissues is analysed (Magdeldin & Yamamoto, 2012; Craven *et al*., 2013; Avaritt *et al*., 2014; Wiśniewski *et al*., 2013). In this study we could not control or correct for the pre-analytical factors impacting on the FFPE tissues analysed. Therefore, the main focus was to establish optimal analytical conditions for effective protein extraction, digestion and sample purification for LC-MS/MS analysis, and to evaluate the impact of storage time on extractable protein yield and quality. To our knowledge, there is no general agreement as to the choice of detergent or buffer system required for efficient and reproducible protein extraction from human FFPE tissues. In addition, sample preparation methods may vary considerably and there are no standard protocols in place yet.

Chapter 3: The effect of polyethylene glycol 20,000 on protein extraction efficiency of formalin-fixed, paraffin-embedded tissues

Abstract

Introduction: The optimal conditions and procedures for efficient and reproducible protein extraction of FFPE tissues have not yet been standardised and new sensitive techniques are continually being developed and improved upon. To our knowledge, there is no general agreement as to the choice of detergent or buffer system (and/or addition of PEG 20,000) required for efficient and reproducible protein extraction from human FFPE tissues. Moreover, the effect of PEG 20,000 on protein extraction efficiency has not been evaluated using human FFPE colorectal cancer tissues, only by using human cell lines and rat tissues. This study therefore aims to assess the impact of PEG 20,000 on the protein extraction efficiency, reproducibility, and protein selection bias of the protein extraction buffer used for FFPE colonic resection tissue in label-free LC-MS/MS analysis. The sample pellets were also tested for residual protein, not extracted in the initial extraction.

Method: FFPE human colorectal carcinoma resection samples were used to determine the optimal protein extraction parameters (tissue/starting material volumes as well as protein extraction buffer composition and volume) required for accurate label-free LC-MS/MS analysis. In addition, three different protein purification workflows were compared, namely detergent removal columns (DRC), the acetone precipitation and formic acid resolubilisation (APFAR) method, as well as the Single-Pot Solid-Phase-enhanced Sample Preparation (SP3) method (using hydrophilic interaction liquid chromatography (HILIC) and magnetic resin). Data were evaluated in terms of protein concentration extracted, peptide/protein identifications, method reproducibility and efficiency, and protein/peptide distribution according to biological processes, cellular components, and physicochemical properties. Data are available via ProteomeXchange with identifier PXD014419.

Results: The results show that the absence of PEG 20,000 increases the number of peptides and proteins identified by unfractionated LC-MS/MS analysis, and the method is more reproducible. However, no significant differences were observed with regard to protein selection bias. In addition, by building on from previous studies,

which found that higher protein concentrations (>10 µg) (of FFPE animal tissues and human cells) compromise the function of PEG, that this effect is also observed in FFPE human colon tissue.

Conclusion: We propose that studies generating high protein yields would benefit from the absence of PEG 20,000 in the protein extraction buffer.

3.1 Introduction

Archival FFPE tissue repositories are valuable resources for clinical proteomic studies, which may include retrospective as well as protein biomarker discovery and validation studies (Tanca *et al*., 2014; Gustafsson *et al*., 2015; Shen *et al*., 2015). These repositories contain numerous varieties of patient tissue specimens, including rare malignancies together with metadata such as patient medical records, which contain information about diagnosis, survival, and response to therapy. Due to this and the fact that FFPE samples are easily stored and obtainable, many recent proteomics, genomics and immunohistochemical studies have focussed on improving methods for analysis of FFPE tissue (Tanca *et al*., 2014; Gustafsson *et al*., 2015; Shen *et al*., 2015).

It is of great interest in clinical and translational research to develop and standardise FFPE sample MS-based proteomic methods to determine changes (or similarities) in the proteome composition of tumour vs. healthy tissues (Bronsert *et al*., 2014; Scheerlinck *et al*., 2015). Part of this process involves using an optimal and efficient protein extraction buffer, which generates reproducible results. Studies have found that experimental factors, such as protein extraction buffer, pH, detergents, denaturants, and temperature, play important roles in the final attainable protein yield from FFPE tissues (Shi *et al*., 2006; Shen *et al*., 2015). Other factors to consider include limited availability of precious clinical specimens and therefore a limited amount of starting material (tissue) available for optimising the protein extraction procedure. Therefore, proteomics workflows (including protein extraction, protein sample enrichment, fractionation and digestion) need to be optimised to generate quality peptide/protein samples of suitable quality for high sensitivity tandem LC-MS analysis, using limited starting-sample volumes (Gustafsson *et al*., 2015; Ruderman, 2017).

A great challenge faced with regard to sample processing and protein extraction of FFPE tissues, is the effect of the formaldehyde fixation chemistry on the tissues. Formaldehyde causes chemical modifications to cells and molecules such as proteins, DNA and RNA; of interest to this study is protein fixation due to formation of methylene bridges between amino groups. Therefore, to ensure accurate and efficient protein extraction from FFPE tissues for proteomic analysis, it is very important to overcome the issue of the formaldehyde cross-linking between molecules, since the cleavage of these methylene bridges is required for proper trypsin digestion (Magdeldin & Yamamoto, 2012; Fowler *et al*., 2013; Avaritt *et al*., 2014; Gustafsson *et al*., 2015). For this reason multiple strategies have been employed, including the use of denaturants, detergents, and antigen retrieval. However, several aspects of the formaldehyde-protein interactions have still not been resolved. Recently, Paine *et al*. (2018) were able to identify small (low molecular weight) proteins and neuropeptides, without antigen retrieval and enzymatic digestion steps, via mass spectrometry imaging. They hypothesise that not all proteins, especially small proteins (with short amino acid sequences and low lysine content), react with formaldehyde to the same extent. However, larger proteins (with longer amino acid sequences and greater lysine content) were more challenging to detect via mass spectrometry, and therefore have a greater probability of being more extensively crosslinked by formaldehyde.

Shi *et al*. (1991) developed a superior immunohistochemistry staining technique, which involves heat-induced antigen retrieval (HIAR) of FFPE tissue sections through incubation in a suitable buffer (after deparaffinisation and rehydration steps) at a high temperature (90 – 120°C) for up to several hours (however, the buffers/solutions used for antigen retrieval by Shi *et al*. (1991) did not contain PEG 20,000 or SDS, since it was an IHC study). The HIAR technique has been successfully and extensively employed and modified in FFPE tissue proteomics, with many research groups also aiming to improve upon it or adapting variations of it (Magdeldin & Yamamoto, 2012; Fowler *et al*., 2013; Avaritt *et al*., 2014; Gustafsson *et al*., 2015). To further increase protein extraction efficiency from FFPE tissues, strong detergents such as SDS (for total tissue solubilisation), as well as nondenaturing, hydrophilic synthetic polymers, such as PEG 20,000, have been used to solubilise or precipitate and stabilise proteins for separation, purification, and

storage (Busby & Ingham, 1980; Ogorzalek Loo *et al*., 1994; Speers & Wu, 2007; Zhao & O'Connor, 2007). However, complete SDS removal before enzymatic digestion and LC-MS/MS analysis is crucial, since it inhibits enzyme activity and causes ion signal suppression and interference, even at very low concentrations (Ogorzalek Loo *et al*., 1994; Speers & Wu, 2007; Wiśniewski *et al*., 2009; Botelho *et al*., 2010; Kachuk *et al*., 2015). Since SDS removal, with minimal sample loss, is a challenging task, several gel-free approaches have been proposed over the years. These approaches include incorporating the use of detergent removal columns (DRC) (ThermoFisher Scientific, 2017), protein precipitation with organic solvents, such as the Acetone precipitation and formic acid resolubilisation (APFAR) method (Botelho *et al*., 2010; Doucette *et al*., 2014; Kachuk *et al*., 2015), and/or methods using hydrophilic interaction liquid chromatography (HILIC) and magnetic resin (such as the Single-Pot Solid-Phase-enhanced Sample Preparation (SP3) method) (Hughes *et al*., 2014; Hughes *et al*., 2019) in the sample processing workflow prior to LC-MS/MS.

Other challenges faced in FFPE proteomic studies, which cannot be remedied after the fact, are pre-analytical factors that affect protein extraction efficiency and often produce variable protein yields, including tissue ischemic time, the composition of the fixative, fixation time (duration/range of formalin-fixation times used), as well as block age and storage conditions (Thompson *et al*., 2013; Bronsert *et al*., 2014; Gustafsson *et al*., 2015). These pre-analytical factors could potentially have an adverse effect on any study conducted, since the various pre-analytical processing methods and/or conditions could have an adverse effect on any downstream analysis performed on the tissue.

Of interest to this study are the effects of polyethylene glycol (PEG) on protein extraction efficiency of human FFPE tissues, using LC-MS/MS analysis, as there is no current consensus with regard to PEG usage and advantages for human FFPE tissues. PEG is a high molecular weight carrier substance, which reduces non-specific adsorption of proteins to surfaces, such as experimental plastic-ware (micropipette tips and microcentrifuge tubes), and prevents subsequent protein loss (Wiśniewski *et al*., 2011; Shen *et al*., 2015). PEG can vary in polymer size, and for this study PEG 20,000 was chosen because it is the most extensively used form in FFPE tissue

proteomics, subsequently all references to PEG in this study are to the 20,000 form. PEG can, however, cause interference and ion signal suppression in downstream LC-MS/MS analysis, if it is not completely removed from the sample analysed (Wiśniewski *et al*., 2011; Scheerlinck *et al*., 2015). Removal of high concentrations of PEGs is challenging and PEG carry-over into sample fractions and LC columns are a huge problem (Busby & Ingham, 1980; Zhao & O'Connor, 2007). In addition, sample purification steps often lead to sample loss and low throughput. PEGs also precipitate proteins through a steric exclusion mechanism, whereby they occupy most of the space in solution, thus concentrating the proteins until they exceed solubility and precipitate (Juckes, 1971; Foster *et al*., 1973; Busby & Ingham, 1980; Feist & Hummon, 2015). Therefore subsequent centrifugation may pellet the precipitated proteins (Feist & Hummon, 2015). Any precipitated proteins in the sample pellets will therefore be lost after clarifying the protein lysates and removal of the supernatants for analysis. However, due to its advantages and available sample preparation methods to remove PEG before LC-MS/MS analysis, it is often used for protein extraction of FFPE tissues (Wiśniewski *et al*., 2011; Shen *et al*., 2015). However, to our knowledge, PEG efficacy with regard to protein extraction of human FFPE tissues has not been fully evaluated yet.

The aim of this study is to evaluate the effects of PEG within the protein extraction buffer using label-free LC-MS/MS analysis of manually micro-dissected FFPE human colorectal carcinoma resection samples. The sample pellets were also tested for residual protein, which was not extracted in the whole cell protein lysates (WCPLs).

3.2 Materials and Methods

3.2.1 FFPE human CRC resection samples

FFPE tissue blocks, which consisted of human colorectal carcinoma resection samples, were obtained from the Anatomical Pathology department at Tygerberg Hospital (Western Cape, South Africa) after obtaining ethics clearance from the Biomedical Science Research Ethics Committee (BMREC) of the University of the Western Cape (ethics reference number: BM17/7/15), as well as the Health Research

Ethics Committee (HREC) of Stellenbosch University (ethics reference number: S17/10/203). The FFPE blocks were anonymised prior to processing and archived since 2016/2017 (when the tissue was resected). Tissue processing and fixation times/conditions and storage conditions are unknown, since specimens were retrospectively collected. Three patient cases were reviewed and selected (Table 1).

Table 1. Information of three FFPE specimens selected for analysis.

	Patient 1	Patient 2	Patient 3
Block year	2017	2016	2016
Patient age (years)	60	47	60
Gender	Female	Male	Male
Diagnosis	Adenocarcinoma	Adenocarcinoma	Adenocarcinoma
Grade	low-grade	high-grade	low-grade
Stage	IIIB	IIIB	IIA
Location	Right colon	Right colon	Right colon

Patient samples diagnosed with low-grade or high-grade colorectal adenocarcinoma, after Haematoxylin and Eosin (H&E) staining, were reviewed by a pathologist(s) to ensure tissue quality and comparability (Fig. 14). The selected slides had carcinomas with more than 90% viable tumour nuclei.

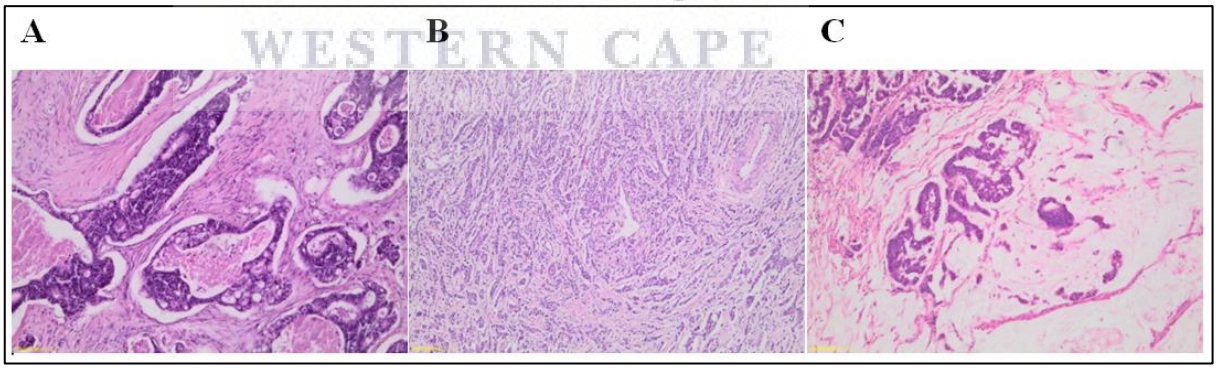

Figure 14. Colonic adenocarcinoma resection tissue samples. Representative H&E stained sections of patient cases analysed in this study; patient 1 (A), patient 2 (B), and patient 3 (C) at 100x magnification.

3.2.2 Protein extraction and quantification

The optimal protein extraction buffer (with or without PEG), as well as the optimal tissue size (measured area = length x breadth) and tissue thickness (µm) that would

produce a sufficient quantity of protein (1.25mg/ml in approximately 400 µl sample volume) for accurate mass spectrometry analysis was determined first.

Sample tumour areas were marked on H&E sections by the pathologist and the dimensions (length x breadth) of these tumour areas (mm^2) were calculated. This information was subsequently used to calculate the (approximate) total volume (mm^3) of tumour tissue per µm of sliced FFPE tissue sections. The volume of protein extraction buffer required per mm^3 of tissue to extract approximately 1.25mg/ml in 400 µl sample volume was determined, and the mass (µg) of extractable protein/protein yield per mm^3 tumour volume was calculated.

For protein extraction, the sample tissue sections were matched to the tumour areas marked on the H&E sections (by the pathologist) and manually micro-dissected, to include tumour tissue only. From each selected patient case, a number of 25µm sections (that were equivalent to 23 mm^3 of manually micro-dissected FFPE tumour tissue per sample) were cut and mounted onto generic glass microscopy slides. The sections were completely air dried and processed for protein extraction with or without the addition of 0.5% (w/v) PEG 20,000 in the protein extraction buffer (50 mM Ammonium bicarbonate (AmBic) (pH 8.0), 2% (w/v) Sodium dodecyl sulphate (SDS). In total, 12 samples were analysed (biological replicates only), including the whole cell protein lysates (WCPLs) as well as the sample pellets (Fig. 15).

The method used for sample processing and protein extraction was modified from the protocols used by Scicchitano *et al*. (2009), and Wiśniewski (2013). Briefly, tissue sections (mounted on glass slides) were heated on a heating block (65°C for 5 min), to melt the paraffin wax, followed by tissue deparaffinisation consisting of two consecutive incubations in xylene (Sigma-Aldrich, USA) for 2.5 min and 1.5 min each respectively, at room temperature. Tissue sections were then rehydrated by successive incubations in absolute ethanol (Merck, Germany), 70% (v/v) ethanol, and twice with distilled water, for 1 min each at room temperature. Slides were placed on tissue paper to absorb excess moisture and the tissues were collected in protein LoBind microcentrifuge tubes (Eppendorf, Germany) by scraping the tissue off the glass slides using a clean sterile scalpel blade. Protein extraction buffer (50 mM AmBic (pH 8.0) (Sigma-Aldrich, USA), 2% (w/v) SDS (Sigma-Aldrich, USA), either with or without addition of 0.5% (w/v) PEG 20,000 (Sigma-Aldrich, USA)) was

added to the samples at a volume of approximately 20 µl protein extraction buffer per mm^3 of tissue (approximately 23 mm^3 tissue per sample). Samples were mixed by vortexing and incubated at 99°C in a heating block with agitation set at 600 RPM for 1 hr, after which the samples were cooled/placed on ice before centrifugation at 16,000 x g and 18°C for 20 min to pellet the cell debris. The supernatant/WCPLs of each sample were transferred to new protein LoBind microcentrifuge tubes (Eppendorf, Germany) and an aliquot taken for protein yield determination. All samples (WCPLs and pellets) were stored at -80°C until further processing. For protein yield determination, the total protein extracted (WCPLs) from the FFPE tissues were quantified using the Pierce™ BCA Protein Assay Kit (Pierce Biotechnology, Thermo Fisher Scientific, USA) according to manufacturer's instructions.

Before sample processing for LC-MS/MS analysis, protein pellets were solubilised by resuspension in protein extraction buffer (50mM Triethylammonium bicarbonate (TEAB) (Sigma-Aldrich, USA), 4% (w/v) SDS (Sigma-Aldrich, USA), and either with or without addition of 0.5% (w/v) PEG 20,000) and incubation at 95˚C for 5 min. Thereafter samples were clarified by centrifugation at 10,000 x g for 5 min. The resultant supernatant was transferred to protein Lobind microcentrifuge tubes (Eppendorf, Germany). Total protein quantification was performed using the QuantiPro BCA assay kit (Sigma-Aldrich, USA) according to manufacturer's instructions. WCPLs were subsequently processed by the DRC (ThermoFisher Scientific, 2017), APFAR (Botelho *et al*., 2010; Doucette *et al*., 2014; Kachuk *et al*., 2015) and/or SP3/HILIC magnetic bead digestion method (Hughes *et al*., 2019), prior to LC-MS/MS analysis. Prior to LC-MS/MS analysis, sample pellets were processed by the APFAR and/or SP3/HILIC methods only, since 4% SDS is not compatible for DRC use (Fig. 15).

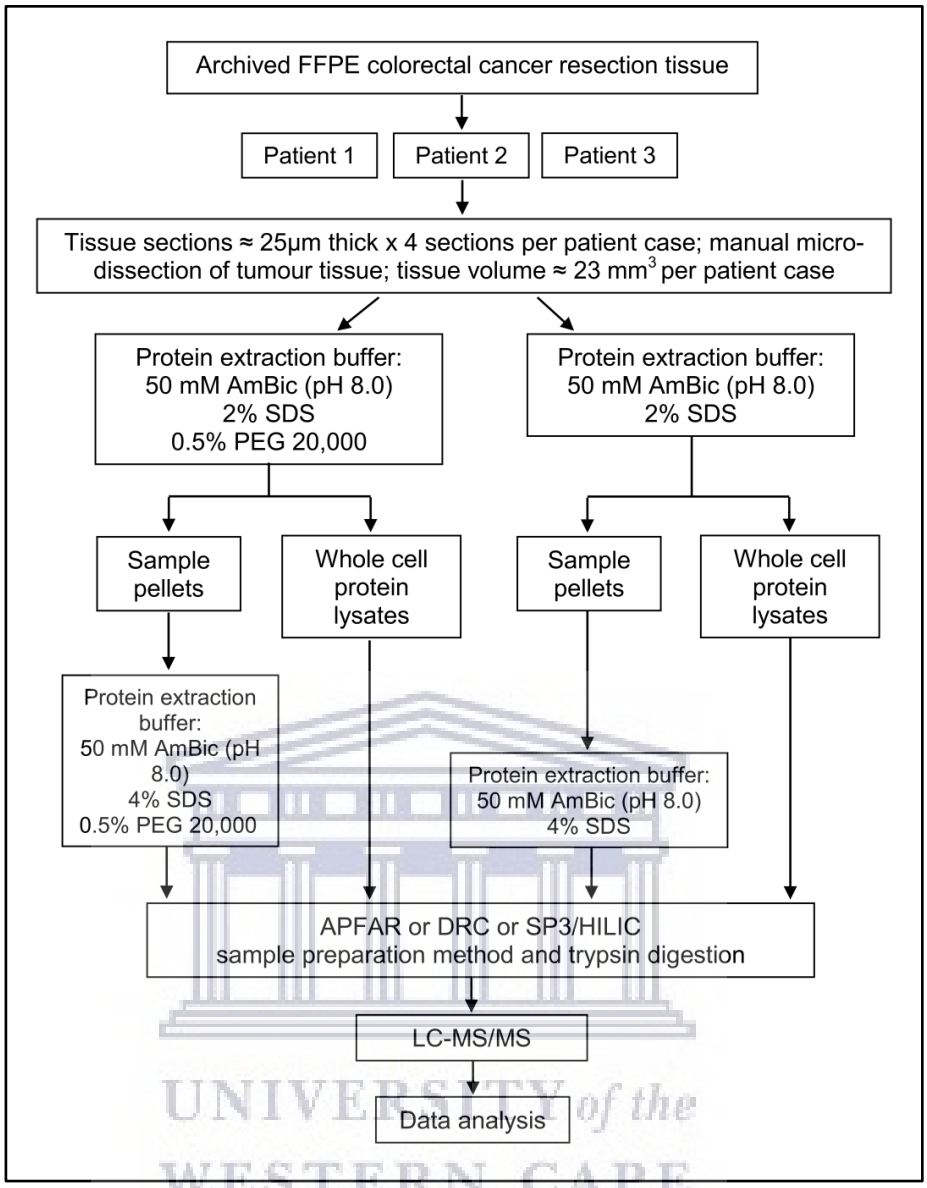

Figure 15. Experimental design and workflow used to evaluate the sample processing methods. FFPE human colorectal carcinoma resection tissues from three patients were cut at 25 µm thickness and tumour areas were manually micro-dissected for analysis. Four tissue sections (each 25 µm thick) from each patient, which corresponded to approximately 23 mm^3 tissue per patient/sample, were used per sample. Protein was extracted using protein extraction buffer with or without the addition of PEG. Sample pellets were analysed for residual protein by further protein extraction (using 4% SDS), followed by protein quantification, splitting each sample in two, and subsequent sample processing (for LC-MS/MS analysis) by either the APFAR or HILIC methods. WCPLs from each patient were quantified and split into three samples for processing by either the APFAR, HILIC or DRC sample preparation methods, followed by LC-MS/MS analysis. Data analysis was performed on all sample MS/MS spectra.

3.2.3 Sample preparation methods

3.2.3.1 Detergent removal columns (DRC)

Detergent removal was carried out using ThermoScientific Pierce® Detergent Removal Spin Columns (ThermoFisher Scientific, USA), according to manufacturer's instructions. Briefly, detergent removal columns were placed in 1.5 ml microcentrifuge tubes and the shipping solution removed by centrifugation at 1,500 x g for 1 min. The resin bed was equilibrated with two consecutive washes with 400 µl of 50 mM TEAB and subsequent removal by centrifugation at 1,500 x g for 1 min each. Thereafter, 100 µg of extracted protein was loaded onto the columns and incubated at room temperature for 2 min. This was followed by centrifugation at 1,500 x g for 2 min to elute the detergent-free protein into protein Lobind microcentrifuge tubes (Eppendorf, Germany). Samples were then dried down by vacuum centrifugation and resuspended in 30 µl of 50 mM TEAB.

3.2.3.2 Acetone precipitation and formic acid resolubilisation (APFAR) method

A total of 100 µg protein was transferred to each protein Lobind microcentrifuge tube and precipitated by addition of four volumes of ice cold acetone (Sigma-Aldrich, USA) followed by overnight incubation at -20˚C. Samples were then centrifuged at 21,000 x g for 15 min at 4˚C. The supernatant was discarded and the pellet washed with ice cold acetone. This process was repeated for a total of three pelleting steps. Thereafter, the pellets were air-dried and subsequently solubilised by re-suspension in 50mM TEAB.

3.2.3.3 In-solution digestion

In-solution digestion was carried out on samples processed by the APFAR (section 3.2.3.2) and DRC (section 3.2.3.1) methods. The protein was reduced by the addition of 0.1 volumes of 100 mM tris(2-carboxyethyl)phosphine (TCEP) (Sigma-Aldrich, USA) to each sample followed by incubation at 60˚C for 1 hour. Alkylation was accomplished by addition of 0.1 volumes of 100 mM methyl methanethiosulphonate (MMTS) (Sigma-Aldrich, USA), which was prepared in isopropanol (Sigma-Aldrich,

USA), to each sample and subsequent incubation at room temperature for 15 min. Protein digestion was accomplished by addition of 1:50 (trypsin: final protein ratio) trypsin (Promega, USA) in a solution with 50mM TEAB, and overnight incubation at 37˚C. Samples were dried down and resuspended in 0.1% trifluoroacetic acid (TFA) (Sigma-Aldrich, USA) prior to clean-up via Zip-Tip (Sigma-Aldrich, USA), after which the samples were again dried down and resuspended in a final volume of 12 µl liquid chromatography (LC) loading buffer (0.1% Formic Acid (FA) (Sigma-Aldrich, USA), 2% Acetonitrile (ACN) (Burdick & Jackson, USA).

3.2.3.4 SP3/HILIC method with on-bead digestion

In preparation for the HILIC magnetic bead workflow, MagReSyn® HILIC beads (ReSyn Biosciences, South Africa) were aliquoted into a new tube and the shipping solution removed. Beads were then washed with 250µl wash buffer (15% ACN, 100mM Ammonium acetate (Sigma-Aldrich, USA) pH 4.5) for 1 min then resuspended in loading buffer (30% ACN, 200mM Ammonium acetate, pH 4.5). The rest of the process, described hereafter, was performed using a Hamilton MassSTAR robotics liquid handler (Hamilton, Switzerland). A total of 50µg of protein from each sample was transferred to a protein LoBind plate (Merck, Germany). Protein was reduced with 10mM TCEP (Sigma-Aldrich, USA) and incubated at 60˚C for 1 hour. Samples were cooled to room temperature and alkylated with 10mM MMTS (Sigma-Aldrich, USA) at room temperature for 15 min. HILIC magnetic beads were added at an equal volume to that of the sample and a ratio of 5:1 total protein. The plate was incubated at room temperature on a shaker at 900 RPM for 30 min for binding of protein to beads. After binding, the beads were washed four times with 500µl of 95% ACN for 1 min each. For digestion, trypsin (Promega, USA) made up in 50mM TEAB was added at a ratio of 1:10 total protein, and the plate was incubated at 37˚C on the shaker for 4 hours. After digestion, the supernatant containing the peptides was removed and dried down. The samples were then resuspended in LC loading buffer (0.1% FA (Sigma-Aldrich, USA), 2% ACN (Burdick & Jackson, USA)).

3.2.4 Label–free LC–MS/MS analysis

LC-MS/MS analysis was conducted with a Q-Exactive quadrupole-Orbitrap mass spectrometer (Thermo Fisher Scientific, USA) coupled with a Dionex Ultimate 3000 nano-UPLC system. Peptides were dissolved in a solution of 0.1% FA and 2% ACN and loaded on a C18 trap column (PepMap100, 300µm × 5mm × 5µm). Samples were trapped onto the column and washed for 3 min before the valve was switched and peptides eluted onto the analytical column as described hereafter. A gradient of increasing organic proportion was used for peptide separation - chromatographic separation was performed with a Waters nanoEase (Zenfit) M/Z Peptide CSH C18 column (75µm × 25cm × 1.7µm) and the solvent system employed was solvent A (0.1% FA in LC water (Burdick & Jackson, USA)) and solvent B (0.1% FA in ACN). The multi-step gradient for peptide separation was generated at 300 nL/min as follows: time change 5 min, gradient change: 2 – 5% solvent B, time change 40 min, gradient change 5 – 18% solvent B, time change 10 min, gradient change 18 – 30% solvent B, time change 2 min, gradient change 30 – 80% solvent B. The gradient was then held at 80% solvent B for 10 min before returning it to 2% solvent B and conditioning the column for 15 min, as shown in Table 2.

Table 2. Peptide separation gradient setup.

Time (min):	Flow rate (µl/min):	Solvent A (%):	Solvent B (%):
0	0.3	98	2
3	0.3	98	2
8	0.3	95	5
48	0.3	82	18
58	0.3	70	30
60	0.3	20	80
70	0.3	20	80
70.1	0.3	98	2
80	0.3	98	2

All data acquisition was obtained using Proxeon stainless steel emitters (Thermo Fisher, USA). The mass spectrometer was operated in positive ion mode with a capillary temperature of 320°C. The applied electrospray voltage was 1.95 kV. The

mass spectra were acquired in a data-dependent manner using Xcalibur™ software version 4.1.31.9 (Thermo Fisher, USA), Chromeleon v6.8 (SR13), Orbitrap MS v2.9 (build 2926) and Thermo Foundations 3.1 (SP4). Details of data acquisition parameters are shown in Table 3.

Table 3. Data acquisition parameters.

Software function:	**Parameter:**	**Value:**
Full scan	Resolution	70,000 (@ *m/z* 200)
	AGC target value	3e6
	Scan range	350 – 2000 *m/z*
	Maximal injection time	100 ms
Data-dependent MS/MS	Inclusion	Off
	Resolution	17,500 (@ *m/z* 200)
	AGC target value	1e5
	Maximal injection time	50 ms
	Loop count	10 (Top-10 method)
	Isolation window width	3 Da
	NCE	27%
Data-dependent settings	Underfill ratio	1%
	Charge exclusion	Unassigned, 1, 7, 8, >8
	Peptide match	Preferred
	Exclusion isotopes	On
	Dynamic exclusion	60 s

3.2.5 Data analysis optimisations

3.2.5.1 Search engine performance evaluation

The protein sequence database search engine(s) is a major component in the data analysis process of a shotgun mass spectrometry experiment. Since there is no single top-performing, high-performance database search algorithm, and each one has its own advantages and disadvantages, it is important to use more than one search engine to achieve optimal results, however, also taking into consideration available

computational power and time limits (Vaudel *et al*., 2011; Shteynberg *et al*., 2013). Studies have found that by combining multiple search engines, it outperforms individual algorithm usage by increasing overall PSMs with high confidence levels (Martin *et al*., 2013; Shteynberg *et al*., 2013). The process of simultaneously running multiple search engines is, however, complicated due to each algorithm's distinct input parameters requirements and their individual communication interfaces. Therefore, for this purpose, SearchGUI was developed (Vaudel *et al*., 2011). SearchGUI (also available as SearchCLI) allows the user to save, as well as input the search parameters only once so as to configure and simultaneously start any number or combination of the search engines available on the platform (Vaudel *et al*., 2011).

To determine which of the most popular freely available, Linux-compatible search engines performed the best, five search engines (supported by SearchGUI version 3.3.3), namely OMSSA (version 2.1.9) (Geer *et al*., 2004), X!Tandem (version X!Tandem Vengeance 2015.12.15.2) (Craig & Beavis, 2004), MS Amanda (version 2.0.0.9706) (Dorfer *et al*., 2014), MS-GF+ (version v2018.04.09) (Kim & Pevzner, 2014), and MyriMatch (version 2.2.10165) (Tabb *et al*., 2007) were compared using SearchGUI (version 3.3.3) (Vaudel *et al*., 2011) and PeptideShaker version 1.16.31 (Vaudel *et al*., 2015) (results shown in Table 4 in section 3.2.5.1.4). Firstly, raw data (containing centroid MS/MS spectra), obtained from six WCPL raw files, were converted into mgf (Matrix Science, UK) files using msConvert from the Proteo-Wizard software suite (Kessner *et al*., 2008). Peak lists obtained from MS/MS spectra were identified using OMSSA (version 2.1.9) (Geer *et al*., 2004), X!Tandem (version X!Tandem Vengeance 2015.12.15.2) (Craig & Beavis, 2004), MS Amanda (version 2.0.0.9706) (Dorfer *et al*., 2014), MS-GF+ (version v2018.04.09) (Kim & Pevzner, 2014), and MyriMatch (version 2.2.10165) (Tabb *et al*., 2007). The search was conducted using SearchGUI (version 3.3.3) (Vaudel *et al*., 2011). Protein identification was conducted against a concatenated target/decoy set of sequences (Elias & Gygi, 2010) as described in section 3.2.5.1.1 and search engine results were collated using PeptideShaker as described in section 3.2.5.1.3.

3.2.5.1.1 Generating a target/decoy database from UniProtKB human reviewed Swiss-Prot proteome

The protein sequences database was generated by combining the 20,341 *Homo sapiens* sequences (obtained from UniProtKB human reviewed Swiss-Prot proteome) and one trypsin *Sus scrofa* sequence obtained from UniProtKB (Apweiler *et al*., 2004), downloaded on 21/05/2018. The decoy sequences were created by reversing the target sequences in SearchGUI. The identification settings were as follows: Trypsin, Specific, with a maximum of 2 missed cleavages; 10.0 ppm as MS1 and 0.02 Da as MS2 tolerances; fixed modifications: Methylthio of C (+45.987721 Da), variable modifications: Oxidation of M (+15.994915 Da), Deamidation of N and Q (+0.984016 Da); fixed modifications during refinement procedure: Methylthio of C (+45.987721 Da), variable modifications during refinement procedure: Acetylation of protein N-term (+42.010565 Da), Pyrolidone from E (--18.010565 Da), Pyrolidone from Q (--17.026549 Da), Pyrolidone from carbamidomethylated C (--17.026549 Da).

3.2.5.1.2 Generating a target/decoy database from UniProtKB human reference proteome database

Protein identification was conducted against a concatenated target/decoy (Elias & Gygi, 2010) version of the *Homo sapiens* (73,101, >99.9%), *Sus scrofa* (1, <0.1%) complement of the UniProtKB (Apweiler *et al*., 2004) human reference proteome (UP000005640; 9606-*Homo sapiens*) version downloaded on 29/10/2018, with 73,102 target sequences. The decoy sequences were created by reversing the target sequences in SearchGUI. The identification settings were as follows: Trypsin, Specific, with a maximum of 2 missed cleavages; 10.0 ppm as MS1 and 0.02 Da as MS2 tolerances; fixed modifications: Methylthio of C (+45.987721 Da), variable modifications: Oxidation of M (+15.994915 Da), Deamidation of N and Q (+0.984016 Da); fixed modifications during refinement procedure: Methylthio of C (+45.987721 Da), variable modifications during refinement procedure: Acetylation of protein N-term (+42.010565 Da), Pyrolidone from E (--18.010565 Da), Pyrolidone from Q (--17.026549 Da), Pyrolidone from carbamidomethylated C (--17.026549 Da).

3.2.5.1.3 Identification of peptides and proteins using PeptideShaker

Peptides and proteins were inferred from the spectrum identification results using PeptideShaker version 1.16.31 (Vaudel *et al*., 2015). Peptide Spectrum Matches (PSMs), peptides and proteins were validated at a 1% False Discovery Rate (FDR) estimated using the decoy hit distribution. Post-translational modification localizations were scored using the D-score (Vaudel *et al*., 2013) and the phosphoRS score (Taus *et al*., 2011) with a threshold of 95.0 as implemented in the compomics-utilities package (Barsnes *et al*., 2011).

3.2.5.1.4 Search engine performance evaluation results

Search engine performance was evaluated based on the number of PSMs, unique PSMs, unassigned PSMs and percentage identification rate (Table 4) using the same dataset (six WCPL raw files) described in section 3.2.5.1.

Table 4. Search engine performance evaluation.

Parameter tested:	OMSSA:	X!Tandem:	MS Amanda:	MS-GF+:	MyriMatch:
Number of PSM	5861 (±1134)	7343 (±1400)	7091 (±1399)	6987 (±1409)	6380 (±1238)
Unique PSMs	44 (±19)	258 (±62)	12 (±5)	56 (±22)	11 (±5)
Unassigned PSMs	17482 (±1250)	16000 (±1275)	16253 (±1278)	16356 (±1303)	16964 (±1277)
% Identification rate	25.0 (±3.5)	31.3 (±4.4)	30.3 (±4.4)	29.8 (±4.5)	27.2 (±3.9)

Based on these parameters, the overall top three performing search engines were found to be X!Tandem, MS Amanda, and MS-GF+. These three search engines will be used for all subsequent data analysis. Next, the protein sequence databases (sections 3.2.5.1.1 and 3.2.5.1.2) were evaluated to determine the best suited database for this study.

3.2.5.2 Protein sequence database evaluation

The protein sequence database is another crucial component of the data analysis process of a shotgun mass spectrometry experiment. The contents of the protein sequence database determine which proteins are discovered/identified in the sample analysed, as well as the subsequent biological conclusions derived from the experiment. A peptide cannot be identified if it is not present in the search database used, even when it is present within the sample analysed. It is therefore of utmost importance to select the appropriate database that is suitable for the specific experiment analysed (Kumar *et al*., 2017; Netzel & Dasari, 2017). Since the completeness of the repository-style databases as well as the accuracy of curated databases are required for the initial exploration of a sample's proteome, the UniProtKB sequence databases provide the best choice for a large number of organisms. UniProtKB contains the corresponding curated SwissProt entries as well as the translated TrEMBL entries (Netzel & Dasari, 2017). Other factors that need to be considered include database size (the number of protein sequences it contains) and search parameters selection (such as precursor tolerance, missed cleavages and PTM selection) affect an experiment's time complexity, as well as the number of peptides identified from the database search (Kumar *et al*., 2017; Netzel & Dasari, 2017). Time complexity and computational resource requirements increase with increased database size. The various search parameters also affect the search space and can magnify database size many folds. In addition, larger databases also result in more false-positive peptide identifications, and by increasing database size beyond expected proteome size tends to decrease overall numbers of identifications (Kumar *et al*., 2017; Netzel & Dasari, 2017). The best strategy is to select a well annotated, organism-specific, representative genome-wide protein sequence database (with highly robust mapping/linkage schemes, to ensure data linkage and integrity) and use it throughout a project, in all aspects of the project (Martin *et al*., 2013). Trying to translate across multiple different databases is not only a waste of time but also results in data loss and corruption, no matter how robust the implemented scheme is (Martin *et al*., 2013).

In order to make an informed choice on the optimal protein sequence database to use, two UniProt search databases, the UniProtKB human reviewed Swiss-Prot protein

sequence database (downloaded May 2018) (section 3.2.5.1.1) and the UniProtKB human reference proteome protein sequence database (downloaded October 2018) (section 3.2.5.1.2), were compared with regards to the number of proteins identified (with their respective % confidence of identification), to find the optimal database to use for this project. The same six WCPL mgf files (of section 3.2.5.1) were also used here. The three best performing search engines of section 3.2.5.1 (X!Tandem, MS Amanda, and MS-GF+) were used for the database search, as well as an in-house PTMs selection (section 3.2.5.3.1). The database search was performed using SearchGUI (version 3.3.3) (Vaudel *et al*., 2011) and PSM information was collated in PeptideShaker version 1.16.31 (Vaudel *et al*., 2015). Results obtained from the two protein sequence databases are shown in Table 5.

Table 5. Protein sequence database evaluation.

Samples[(a)]:	**UniProt reviewed No. peptides[(b)]:**	**UniProt reference No. peptides[(b)]:**	**UniProt reviewed No. proteins[(c)]:**	**UniProt reference No. proteins[(c)]:**
-PEG APFAR	5021 (88.19%)	5055 (86.02%)	1554 (83.36%)	1793 (85.81%)
-PEG DRC	7203 (81.92%)	7223 (80.33%)	1989 (89.13%)	2332 (89.78%)
-PEG HILIC	7717 (74.93%)	7736 (75.60%)	2121 (86.01%)	2500 (87.35%)
+PEG APFAR	5173 (81.22%)	5171 (78.47%)	1663 (88.31%)	1925 (92.95%
+PEG DRC	5173 (87.60%)	5228 (83.90%)	1488 (90.91%)	1751 (89.75%)
+PEG HILIC	6668 (77.67%)	6688 (77.85%)	1910 (66.50%)	2329 (71.84%)
Search duration:	3 hours 21 minutes 11.0 seconds	6 hours 40 minutes 52.0 seconds		
No. of target sequences[(d)]:	20,342	73,102		
Entries from:	Swiss-Prot only	TrEMBL and Swiss-Prot		

(a) All sample files analysed were the same as those in section 3.2.5.1
(b) The number of validated identified peptides is presented with % confidence of identification in parentheses
(c) The number of validated identified proteins is presented with % confidence of identification in parentheses
(d) The number of target protein sequences that each database contains (porcine trypsin is included) – decoy sequences not included

Based on the search accuracy, duration/time complexity and computational resource costs, it was decided to use the UniProtKB human reviewed Swiss-Prot proteome

protein sequence database (with 20,342 target sequences). Moreover, since 159 samples/files will be analysed for the block age and sample preparation methods comparison study of chapter 4, the duration/time complexity and computational resource costs will be too high when using a larger protein sequence database. In addition, the human reviewed Swiss-Prot database contains manually curated protein sequences without any isoforms or redundant sequences, unlike the human reference proteome database, which may result in more false-positive peptide and protein identifications (Kumar *et al*., 2017; Netzel & Dasari, 2017). Therefore, the UniProtKB human reviewed Swiss-Prot proteome protein sequence database will be used for all subsequent data analysis within this study. The next component evaluated is the search parameter post-translational modification (PTM) preselection, to determine which combination of PTMs gave optimal results.

3.2.5.3 Evaluation of formalin-induced protein post-translational modification (PTM) preselection during database search

To determine which PTM selection would be best suited for optimal PSM assignment, an in-house PTM selection was compared to a combination of PTMs selected from the literature (Guo *et al*., 2007; Zhang *et al*., 2015; Holfeld *et al*., 2018). The aim was to determine which PTM selection resulted in the highest number of identified peptides and proteins with sufficiently adequate confidence levels in the PSMs generated, as well as taking computing resources and time into consideration.

The same six WCPL mgf files used in sections 3.2.5.1 and 3.2.5.2 were also used here, together with the three best performing search engines of section 3.2.5.1 (X!Tandem, MS Amanda, and MS-GF+) and the UniProtKB human reviewed Swiss-Prot protein sequence database (downloaded May 2018) for the database search. Two different sets of PTMs were selected as described in sections 3.2.5.3.1 and 3.2.5.3.2. The database search was performed using SearchGUI (version 3.3.3) (Vaudel *et al*., 2011) and PSM information was collated in PeptideShaker version 1.16.31 (Vaudel *et al*., 2015) as described in section 3.2.5.1.3. The results are shown in Tables 6 and 7 of section 3.2.5.3.3.

3.2.5.3.1 In-house PTM selection

Identification parameters were set as follows: Trypsin, Specific, with a maximum of 2 missed cleavages; 10.0 ppm as MS1 and 0.02 Da as MS2 tolerances; fixed modifications: Methylthio of C (+45.987721 Da), variable modifications: Oxidation of M (+15.994915 Da), Deamidation of N and Q (+0.984016 Da); fixed modifications during refinement procedure: Methylthio of C (+45.987721 Da), variable modifications during refinement procedure: Acetylation of protein N-term (+42.010565 Da), Pyrolidone from E (--18.010565 Da), Pyrolidone from Q (--17.026549 Da), Pyrolidone from carbamidomethylated C (--17.026549 Da.

3.2.5.3.2 All PTM selections

Formalin-induced PTM preselection combinations from the literature (Guo *et al*., 2007; Zhang *et al*., 2015; Holfeld *et al*., 2018) were chosen for the identification settings, as follows: Trypsin, Specific, with a maximum of 2 missed cleavages; 10.0 ppm as MS1 and 0.02 Da as MS2 tolerances; fixed modifications: Methylthio of C (+45.987721 Da), variable modifications: Oxidation of M (+15.994915 Da), Acetylation of protein N-term (+42.010565 Da), Carbamilation of K (+43.005814 Da), Deamidation of N and Q (+0.984016 Da), Methylation of K (+14.01565 Da); fixed modifications during refinement procedure: Methylthio of C (+45.987721 Da), variable modifications during refinement procedure: Pyrolidone from E (--18.010565 Da), Pyrolidone from Q (--17.026549 Da), Pyrolidone from carbamidomethylated C (--17.026549 Da).

3.2.5.3.3 Formalin-induced protein PTMs pre-selection evaluation results

Table 6 shows that with increased number of PTM selected, the search time also increases (>8 hours), which is not ideal since 159 samples/files will be analysed for the block age and sample preparation methods comparison study of chapter 4, thereby unfavourably increasing the computational resource costs.

Table 6. PTM selection parameters.

In-house PTM selection:	Published PTM selection:
• Fixed Modifications: Methylthio of C • Variable Modifications: Oxidation of M, Deamidation of N, Deamidation of Q • Refinement Variable Modifications: Acetylation of protein N-term, Pyrolidone from E, Pyrolidone from Q, Pyrolidone from carbamidomethylated C • Refinement Fixed Modifications: Methylthio of C • Search was completed in 3 hours 21 minutes 11.0 seconds	• Fixed Modifications: Methylthio of C • Variable Modifications: Oxidation of M, Acetylation of protein N-term, Carbamilation of K, Deamidation of N, Deamidation of Q, Methylation of K • Refinement Variable Modifications: Pyrolidone from E, Pyrolidone from Q, Pyrolidone from carbamidomethylated C • Refinement Fixed Modifications: Methylthio of C • Search Completed in 8 hours 28 minutes 20.0 seconds

Table 7 shows the number of identified peptides and proteins (with respective % confidence levels of assignment) between the two groups of PTM selections. The in-house PTM selection resulted in more protein identifications for four out of the six files/samples analysed.

Table 7. PTM selection evaluation.

Samples[(a)]:	In-house PTM selection No. peptides[(b)]:	Published PTM selection No. peptides[(b)]:	In-house PTM selection No. proteins[(c)]:	Published PTM selection No. proteins[(c)]:
-PEG APFAR	5021 (88.19%)	5169 (86.01%)	1554 (83.36%)	1513 (83.95%)
-PEG DRC	7203 (81.92%)	7225 (81.88%)	1989 (89.13%)	1957 (89.69%)
-PEG HILIC	7717 (74.93%)	7764 (72.11%)	2121 (86.01%)	2136 (85.70%)
+PEG APFAR	5173 (81.22%)	5179 (80.07%)	1663 (88.31%)	1655 (90.22%)
+PEG DRC	5173 (87.60%)	5250 (84.77%)	1488 (90.91%)	1490 (85.28%)
+PEG HILIC	6668 (77.67%)	6677 (77.37%)	1910 (66.50%)	1879 (83.85%)

(a) All sample files analysed were the same as those in sections 3.2.5.1 and 3.2.5.2
(b) The number of validated identified peptides is presented with % confidence of identification in parentheses
(c) The number of validated identified proteins is presented with % confidence of identification in parentheses

It was decided to use the in-house PTM selection, since it gave the overall highest number of proteins identified with adequate % confidence levels (>66%) and is less computationally intensive. This PTM combination will be selected for all subsequent data analysis within this study. The next part of the study involved an evaluation of

the effect of PEG on the protein extraction efficiency and reproducibility of the protein extraction buffer used. In addition, a pilot study of the three different sample processing methods, to give an estimate of expected results and statistically significant sample size required for the larger block age and sample preparation methods comparison study (chapter 4), was performed.

3.2.6 Data and statistical analyses – evaluating the effect of PEG on protein extraction efficiency

Raw data containing centroid MS/MS spectra were converted into mgf (Matrix Science, UK) files using msconvert from the Proteo-Wizard software suite (Kessner *et al*., 2008). Peak lists obtained from MS/MS spectra were identified using X!Tandem (version X!Tandem Vengeance 2015.12.15.2) (Craig & Beavis, 2004), MS Amanda (version 2.0.0.9706) (Dorfer *et al*., 2014) and MS-GF+ (version 2018.04.09) (Kim & Pevzner, 2014) with parameter settings as described in section 3.2.5.3.1. The search was conducted using SearchGUI (version 3.3.3) (Vaudel *et al*., 2011) and spectrum identification was conducted against a concatenated target/decoy protein sequence database as described in sections 3.2.5.1.1 and 3.2.5.3.1. Peptides and proteins were inferred from the spectrum identification results as described in section 3.2.5.1.3, using PeptideShaker version 1.16.40 (Vaudel *et al*., 2015). (Refer to Appendix A for search algorithms specific settings).

Qualitative and quantitative data were exported from PeptideShaker and parsed using in-house scripts and graphs generated in Jupyter lab (using Pandas, NumPy, and Matplotlib Python packages), as well as Microsoft® Excel. Graphs and figures were annotated and/or resolution quality increased using Inkscape (version 0.92.4).

Venny version 2.1.0 (Oliveros, 2007) was used to generate Venn diagrams to visualise the consistency of peptide and/or protein identifications between samples.
Spectrum counting abundance indexes were estimated using the Normalised Spectrum Abundance Factor (NSAF) (Powell *et al*., 2004) adapted for better handling of protein inference issues and peptide detectability. The NSAF method followed here involves counting the number of spectra attributed to each protein in the result set, which is subsequently normalised to a relative abundance (Vaudel *et al*., 2011;

Vaudel, 2017). In the PeptideShaker implementation, this count is then normalised for the length of the protein, the presence of shared peptides, as well as redundant peptides. The spectrum counting indexes were exported from PeptideShaker and parsed using in-house scripts. The NSAF values (of common/shared proteins only) were multiplied by the lowest factor calculated for each pair of conditions compared, in order to deal with integers and facilitate comparisons. These NSAF values were then used to estimate the extent of differential protein abundance (of common/shared proteins only) by calculating the Pearson's correlation coefficient (PCC), for each pair of conditions compared, to assess the relationship/level of correlation between samples. PCC graphs (Appendix B – Supplementary figure S2) were generated in Jupyter lab, using Pandas, NumPy, and Matplotlib Python packages.

The physicochemical properties of the identified peptides, including the hydropathicity (Kyte-Doolittle scale), molecular weight, and isoelectric point were calculated for each sample using the Protein Property Analysis Software (ProPAS) version 1.1 (Wu & Zhu, 2012).

Protein annotations regarding subcellular localisation were retrieved from Ensembl (www.ensembl.org) using GOSlim UniProtKB-GOA (www.ebi.ac.uk/GOA) to minimise the number of terms retrieved. Hypergeometric testing was used to calculate the significance of gene ontology terms.

3.2.7 Data sharing information

The mass spectrometry data along with the identification results have been deposited to the PRIDE (Perez-Riverol *et al.*, 2019) archive (http://www.ebi.ac.uk/pride/archive/) via the PRIDE partner repository with the data set identifier PXD014419 and DOI: 10.6019/PXD014419.
Username: reviewer32243@ebi.ac.uk Password: NXFglOM7

3.3 Results and discussion

The objectives of this pilot study is to determine whether the presence or absence of PEG during protein extraction generated better results in a label-free quantitative

(LFQ) proteomics experiment, to optimise the experimental conditions and protocol and determine the sample size required (based on results obtained here) for the larger block age and sample preparation methods comparison study of chapter 4.

3.3.1 Protein extraction and quantification results

Initial protein extraction protocol optimisation experiments were performed to establish the approximate volume (tissue area mm^2 and tissue thickness µm) of manually micro-dissected patient tumour tissue (mm^3), as well as the volume of protein extraction buffer (µl) required (per mm^3 of tissue) to extract at least 1.25 mg/ml protein (in approximately 400 µl of total sample volume) for protein purification and accurate LC-MS/MS analysis.

Figure 16 shows the bicinchoninic acid (BCA) total protein quantitation assay results obtained after protein was extracted from approximately 15 mm^3 patient tumour tissue (described in sections 3.2.1 and 3.2.2) using 400 µl of protein extraction buffer.

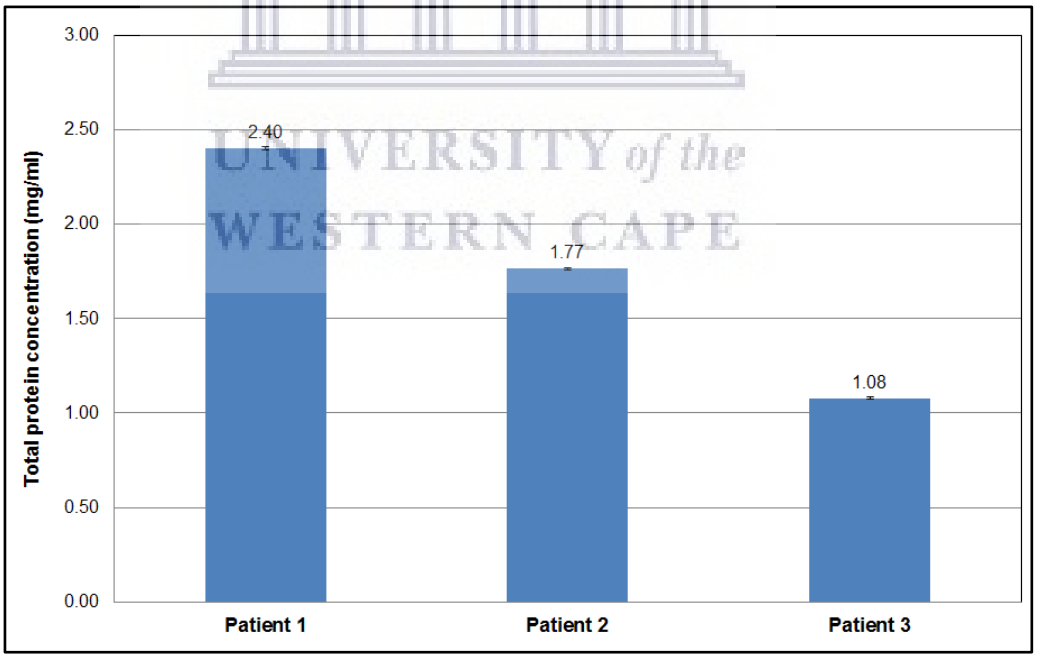

Figure 16. BCA total protein quantitation assay results. Protein was extracted from approximately 15 mm^3 patient tumour tissue using 400 µl protein extraction buffer per sample.

Although approximately 15 mm^3 of manually micro-dissected tumour tissue per sample was used for protein extraction, and the volume of protein extraction buffer kept constant at 400 µl per sample, the total amount of extractable protein and protein yield still differed among the patient samples (Fig. 17). Similar variations in protein yield, even between sample replicates, have been observed before in Wolff *et al.* (2011). The results also indicate that approximately 27 µl of protein extraction buffer per mm^3 of tumour tissue is adequate for sufficient protein extraction. This volume also falls within the range of previous studies; Bronsert *et al.* (2014) used 80 - 150 µl of protein extraction buffer per mm^3 of tissue, whereas Quesada−Calvo *et al.* (2017) used 20 µl protein extraction buffer per mm^3 tissue and Wiśniewski (2013) uses 10 µl of protein extraction buffer per mm^3 of tissue for larger amounts of sample (>1 mm^3). Overall, the average amount of protein extracted was 45 µg/mm^3 tumour tissue across all samples quantified (Fig. 17).

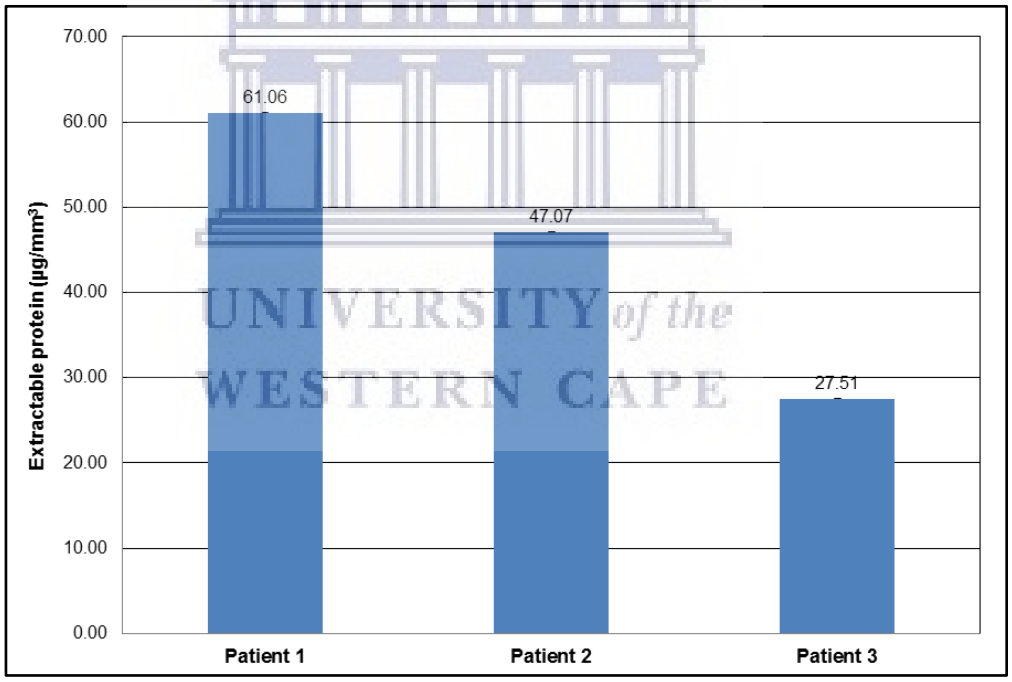

Figure 17. Total amount of extractable protein. The total amount of protein (µg) that was extracted from the tumour tissue per mm^3 was calculated as extractable protein (µg/ mm^3) when using 400 µl of protein extraction buffer per sample.

3.3.2 The effect of PEG on protein extraction efficiency

This pilot experiment was designed to determine whether the presence or absence of PEG 20,000 during protein extraction generated better results (with regard to protein

extraction efficiency, protein yield, and method reproducibility) with label-free LC-MS/MS analysis. In addition, the results will also give an idea of the statistically significant sample size required for the larger block age and sample preparation methods comparison study of chapter 4, to minimise the influence of biological variance between patient samples on the proteomic data.

Here FFPE colonic resection tumour tissues of three patients (diagnosed as indicated in Table 1) were processed using protein extraction buffer with or without the addition of PEG. To further determine protein extraction buffer efficiency, the sample pellets were also assessed for residual proteins that were not extracted in the initial extraction, which used 2% SDS. Extracted protein was purified by three different methods (APFAR, DRC, or HILIC) and, for preliminary analysis, the best method's data was used to evaluate proteome coverage, proportion of missed cleavages, and enrichment/selection bias based on protein extraction buffer components used.

3.3.2.1 Preliminary evaluation of the protein purification methods

Initially, to determine which sample preparation method performed the best, only the data from WCPL samples extracted without PEG were analysed, to evaluate the efficiency and reproducibility for each method (APFAR, DRC, or HILIC), at both protein and peptide level, with regards to proteome coverage and overlap (Fig. 18).

Overall, the HILIC sample preparation method showed adequate reproducibility and resulted in the highest numbers of identifications; 7068 ± 624 for validated peptides and 1952 ± 183 for validated proteins identified (Fig. 18 A and C). On the other hand, the APFAR method showed higher reproducibility at both peptide and protein level, but by comparison it had the lowest numbers of identifications; 5270 ± 348 for validated peptides and 1607 ± 104 for validated proteins identified. The DRC method performed intermediately between the other two methods with 6462 ± 667 validated peptides and 1879 ± 100 validated proteins identified.

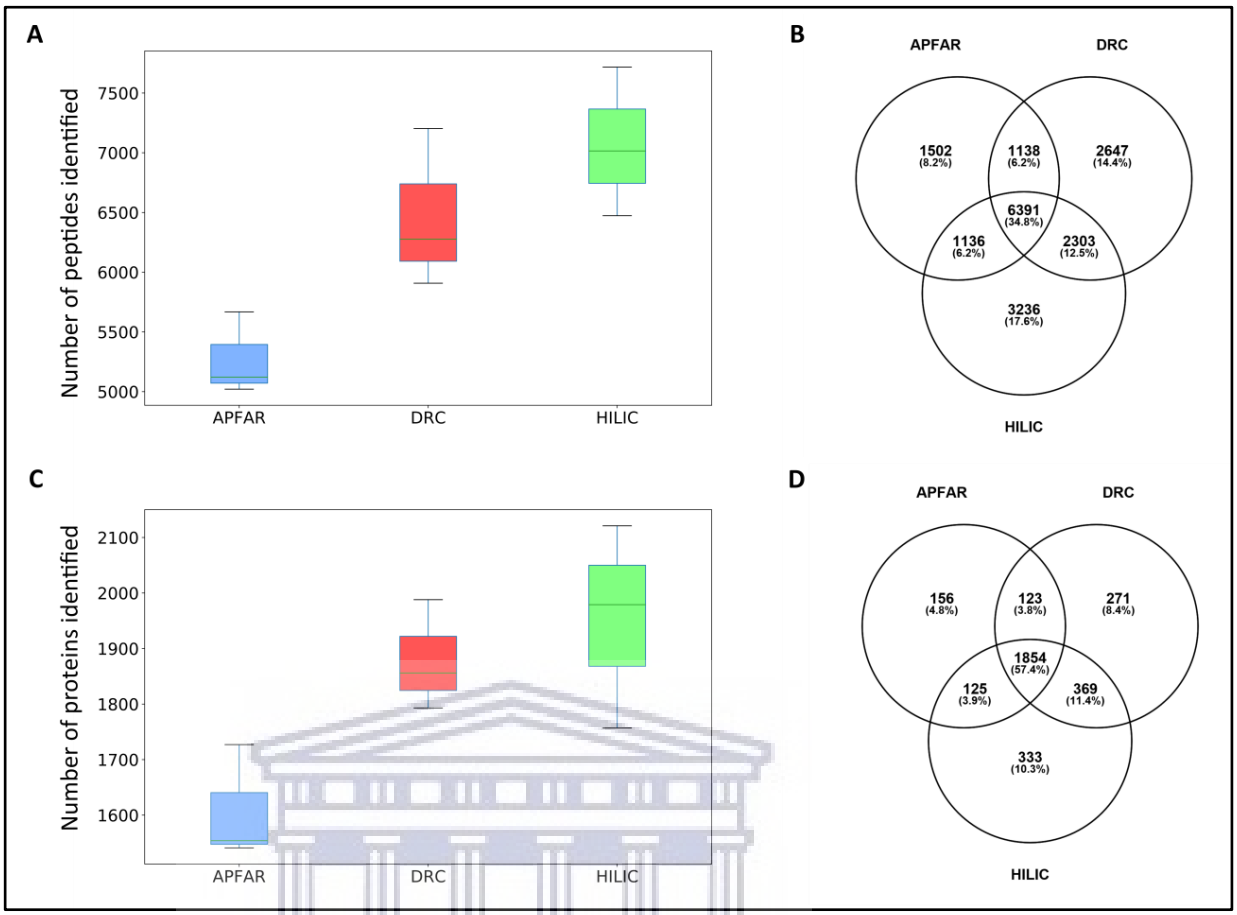

Figure 18. Comparison of the overall number of peptides and proteins identified for each sample preparation method (APFAR, DRC, or HILIC) for WCPLs (-PEG) only. (A) Box and whiskers plot of the number of peptides identified (for all three patient cases) per protein purification method – APFAR, DRC and HILIC (B) Venn diagram depicting the distribution of identified peptides (for all three patient cases) among all sample preparation methods (C) Box and whiskers plot of the number of proteins identified (for all three patient cases) per method – APFAR, DRC and HILIC (D) Venn diagram depicting the distribution of identified proteins (individual and protein groups) (for all three patient cases) among all sample preparation methods. Blue boxplots refer to the APFAR method; Red boxplots refer to the DRC method; Green boxplots refer to the HILIC method.

Figure 18 B shows the overall peptide identification overlap between the different sample preparation methods, calculated from the merged lists of peptide sequences identified in each method (group of three patients). This shows that the majority (34.8%) of identified peptides were shared/overlapped between all the sample preparation methods, with the APFAR method generating the lowest percentage of uniquely identified peptides (8.2%), compared to the DRC (14.4% unique peptides) and HILIC (17.6% unique peptides) methods. Furthermore, figure 18 D shows the overall protein identification overlap between the experimental conditions, calculated from the merged lists of protein accession numbers (individual as well as protein groups) identified in each method group, for all three patient cases. Here 57.4% of

identified proteins were shared/overlapped between all the experimental conditions, also with lower percentages of unique proteins identified for the APFAR method (4.8%), followed by DRC method (8.4%). The HILIC method has the highest percentage of unique proteins at 10.3%.

Since the HILIC protein purification method performed the best in this pilot study, the effect of PEG on the protein extraction buffer efficiency and reproducibility was assessed using only the HILIC-processed samples' data (WCPLs and pellets).

3.3.2.2 The effect of PEG on peptide and protein identifications

The efficiency and reproducibility for each experimental condition (WCPLs extracted with 2% SDS and either with or without PEG, pellets extracted with 4% SDS and either with or without PEG), at both protein and peptide level was assessed with regards to proteome coverage (number of peptides and proteins identified) (Fig. 19A and C) and percentage of overlap of identified peptides and proteins (Fig.19B and D).

Average results (with standard deviation) for all three patients (from non-fractionated LC–MS/MS analysis) show that overall, the WCPLs extracted with 2% SDS and PEG showed lower numbers of identifications ($p > 0.05$), at both peptide and protein levels; 6828 ± 560 for validated peptides and 1927 ± 125 for validated proteins identified (Fig. 19 A and C). On the other hand, the WCPLs extracted without PEG showed higher numbers of identifications ($p > 0.05$); 7068 ± 624 for validated peptides and 1952 ± 183 for validated proteins with adequate reproducibility. A summary of the statistical analysis is shown in Supplementary table 2. The pellet samples (extracted with 4% SDS) showed higher overall variability, at both peptide and protein levels, however the number of peptide and protein identifications were high at 6018 ± 2111 for validated peptides and 1601 ± 408 for validated proteins identified for pellets extracted without PEG and 4777 ± 1751 for validated peptides and 1332 ± 375 for validated proteins identified for pellets extracted with PEG (Fig. 19 A and C). Using HeLa cells, Wiśniewski *et al*. (2011) found that the addition of PEG to the protein extraction buffer improves protein extraction efficiency of samples that contained sub-microgram to microgram amounts of protein; however PEG's ability to improve protein extraction efficiency was compromised when

processing cell lysates that contained more than 10µg of protein. Shen *et al*. (2015) found that the addition of PEG to FFPE rat tissues, which contain >10µg protein, failed to increase the amount of peptide and protein identifications. Since the current study extracted protein in the range of approximately 400µg - 1000µg per sample (Fig. 16), it would explain why PEG's extraction efficiency was compromised and resulted in lower overall peptide and protein identifications.

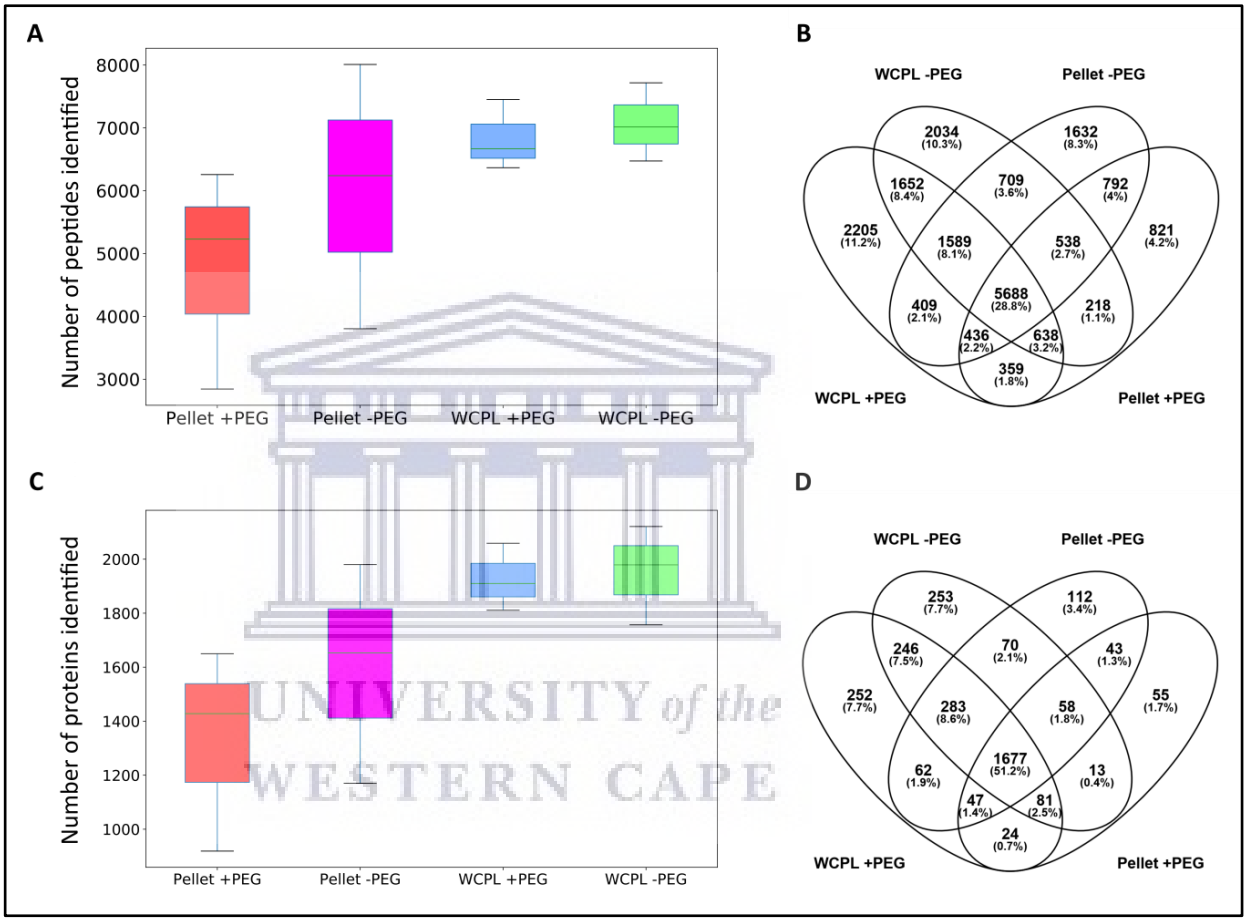

Figure 19. Comparison of the number of peptides and proteins identified using protein extraction buffer with or without addition of PEG, including the number of residual proteins remaining in the sample pellets. (A) Box and whiskers plot of the number of peptides identified (for all three patient cases) per condition – Pellet with PEG (4% SDS); Pellet without PEG (4% SDS); WCPL with PEG (2% SDS); WCPL without PEG (2% SDS) (B) Venn diagram depicting the distribution of identified peptides (for all three patient cases) among all conditions (C) Box and whiskers plot of the number of proteins identified (all patient cases) per condition. (D) Venn diagram depicting the distribution of identified proteins (individual and protein groups) (all three patient cases) among all conditions. (-PEG) refers to protein extracted without PEG and (+PEG) refers to protein extracted with PEG. Red boxplots refer to pellet samples extracted with PEG; Purple boxplots refer to pellet samples extracted without PEG; Blue boxplots refer to WCPL samples extracted with PEG; Green boxplots refer to WCPL samples extracted without PEG.

Figure 19 B shows the overall peptide identification overlap between the experimental conditions, calculated from the merged lists of peptide sequences identified in each sample group. This shows that 28.8% of identified peptides were shared/overlapped between all the experimental conditions, with lower percentages of unique peptides identified for the pellets (8.3% without PEG and 4.2% with PEG), compared to the WCPLs (10.3% without PEG and 11.2% with PEG).

Furthermore, figure 19 D shows the overall protein identification overlap between the experimental conditions, calculated from the merged lists of protein accession numbers (individual as well as protein groups) identified in each sample group, for all three patient cases. Here 51.2% of identified proteins were shared/overlapped between all the experimental conditions, also with lower percentages of unique proteins identified for the pellets (3.4% without PEG and 1.7% with PEG), compared to the WCPLs (7.7% with and without PEG). This indicates that the majority of proteins were extracted in the initial WCPLs using 2% SDS. Therefore, the extraction buffer containing 2% SDS, as well as the extraction protocol used was sufficiently efficient to extract the majority of proteins from the patient samples (WCPLs), and the main differences occurred due to the addition of PEG to the extraction buffer. Shi *et al*. (2006) found that 2% SDS is a critical chemical component for the successful extraction of protein from human FFPE tissue sections, which is also supported by other studies (Ikeda *et al*., 1998; Guo *et al*., 2007; Maes *et al*., 2013; Tanca *et al*., 2014). However, some studies recommend a concentration of 4% SDS for optimal protein extraction (Wiśniewski *et al*., 2009; Craven *et al*., 2013; Fu *et al*., 2013; Bronsert *et al*., 2014).

Shared/common peptides and proteins between the pellet samples and WCPLs are due to soluble fraction/liquid (containing protein) remaining trapped within the sample pellets, after protein extraction and homogenate clarification (by centrifugation) (Scopes, 1994). This is due to the fact that human tissues contain large amounts of insoluble cellular materials that greatly bind to water. As a result, the total loss of liquid (soluble fraction/sample protein) depends on the amount of insoluble cellular materials/debris present. When more protein extraction buffer is added, a larger proportion of the liquid/soluble fraction will be extracted, however, the extract will be more dilute, which is an unfavourable outcome for this current study.

Furthermore, the unique peptides of the pellet samples may also, in part, be attributed by the higher SDS concentration (4% SDS) used for extraction, since other studies have found greater protein extraction efficiency by using higher SDS concentrations (Wiśniewski *et al*., 2009; Craven *et al*., 2013; Fu *et al*., 2013; Bronsert *et al*., 2014). The qualitative reproducibility for each sample and experimental condition was also measured in terms of peptide identification overlap (Appendix B – Supplementary figure S1), calculated from the peptide sequences identified in each sample and experimental condition, irrespective of peptide abundance. From these results, the average physicochemical properties of the peptides (unique as well as shared) for all conditions were assessed for each patient (Appendix C – Supplementary table 1) and there were no substantial differences observed. The quantitative reproducibility between experimental conditions were expressed as PCC dot plots (Appendix B – Supplementary figure S2), which were calculated based on the NSAF abundance values for identified proteins in each sample and experimental condition. All samples/experimental conditions yielded comparable relative protein abundances, indicating that protein extraction with and without PEG did not introduce a significant observable bias with regard to proteome composition.

3.3.2.3 Evaluation of protein physicochemical properties and GO analysis of identified proteins

The effect of PEG on protein extraction buffer selection and/or enrichment bias with regards to protein physicochemical properties were assessed in the box and whisker plots of figure 20, which provides a statistical comparison between the samples and illustrates the peptide distribution according to hydropathicity, molecular weight and isoelectric point (pI). In addition, the protein extraction buffers' (with or without addition of PEG) protein selection bias, as well as residual proteins of the sample pellets, was assessed with regards to subcellular localisation, using Gene Ontology (GO) annotation whereby the distribution of the percentages of proteins belonging to each GO term was plotted (Fig. 21).

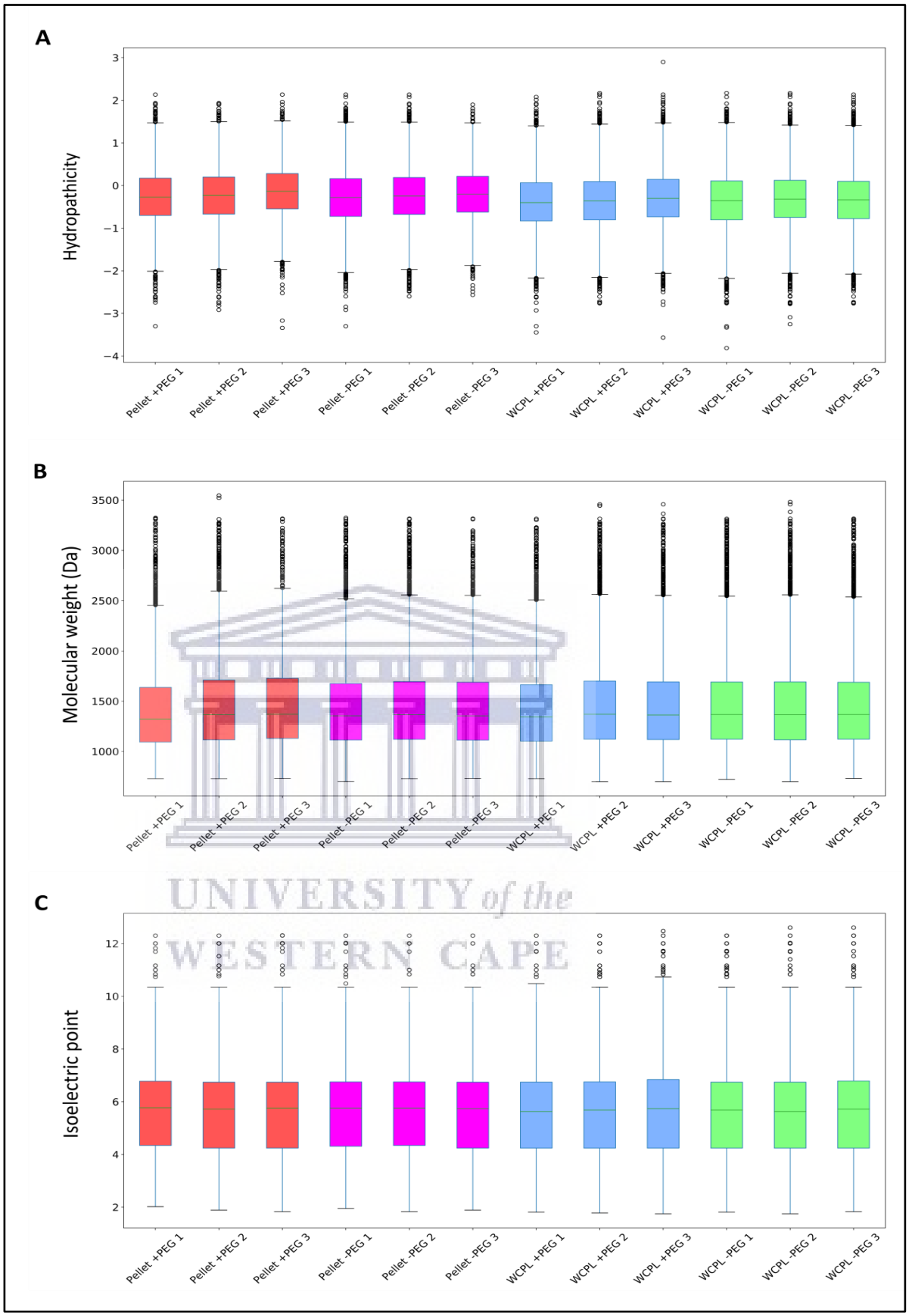

Figure 20. The physicochemical properties of peptides extracted under the different experimental conditions. (A) Hydropathicity was based on Kyte and Doolittle's (1982) grand average of hydropathicity index (GRAVY) scoring matrix, (B) Molecular weight (MW), (C) isolectric point (pI). (+PEG) refers to protein extracted with PEG and (-PEG) refers to protein extracted without PEG. Red boxplots refer to pellet samples extracted with PEG; Purple boxplots refer to pellet samples extracted without PEG; Blue boxplots refer to WCPL samples extracted with PEG; Green boxplots refer to WCPL samples extracted without PEG.

Overall, a comparison of the majority (upper and lower quartiles) of all peptides of all the experimental conditions shows that they share similar hydropathicity scales (Fig. 20 A). The average relative hydropathicity of all the samples are negative, which indicates that the majority of peptides extracted (with and/or without PEG) and processed via the HILIC sample preparation method are hydrophilic (Kyte & Doolittle, 1982; Farias *et al*., 2010). Some differences can be observed between pellet samples and WCPLs (extracted with and/or without PEG); the pellet samples seem slightly more hydrophobic or neutral (closer to 0) in nature compared to the WCPLs. However, neither the addition nor omission of PEG from the protein extraction buffer affects or shows a substantial hydropathicity preference/selection bias with regard to extracted peptides. In addition, the HILIC sample preparation method does not show a preference/selection bias with regard to protein hydropathicity either, which was also demonstrated in Hughes *et al*. (2014) and Moggridge *et al*. (2018).

Figure 20 B indicates that the molecular weight ranges of identified peptides are relatively constant across all samples and experimental conditions, with the majority >1000 Da and <2000 Da. Trypsin digestion efficiency influences the molecular weight of peptides (Hustoft *et al*., 2012), however all samples were subjected to the same digestion protocol, therefore the results show that the addition or omission of PEG to the protein extraction buffer does not significantly affect end-result molecular weight distributions, nor is there any significant differences in molecular weight distributions of residual proteins from the pellets. In addition, the pI ranges of identified peptides are relatively constant across all samples and experimental conditions, with the majority above pI 4 and below pI 7 (Fig. 20 C). Figure 20 therefore indicates that neither the addition nor omission of PEG to the protein extraction buffer had any significant selection bias with regard to extracted proteins' physicochemical properties. Similar results were observed by Hughes *et al*. (2014) and Moggridge *et al*. (2018); after processing protein extracts using the SP3/HILIC method, they found no obvious bias with regard to the molecular mass, isoelectric point, and/or average relative hydropathicity of resultant isolated peptides.

Overall, similar GO annotation profiles were obtained for all samples, therefore only GO terms that occurred at >15% frequency for all samples and experimental conditions were plotted (Fig. 21 A and B). The majority of proteins that were

preferentially extracted are involved in transport (>40%), signal transduction and stress response (>30%), as well as biosynthesis (>40%) (Fig. 21 A). The majority of proteins were preferentially extracted from the cytoplasm (>80%), organelles (>90%), intracellular region (>90%), and extracellular region (>50%) (Fig. 21 B). Approximately 30% of extracted proteins were membrane proteins and 50% were proteins associated with the nucleus. Wiśniewski *et al*. (2011) analysed FFPE colon cancer samples via LC-MS/MS, using the filter-aided sample preparation (FASP) method and protein extraction with PEG, and found the majority of extracted proteins to be membrane proteins (36 - 40%) (especially plasma membrane proteins (16 - 18%)) and proteins associated with the nucleus (36%). Overall, the current in-depth analysis demonstrates that without or without PEG, the SP3/HILIC sample preparation method is less biased with regard to extracted protein types.

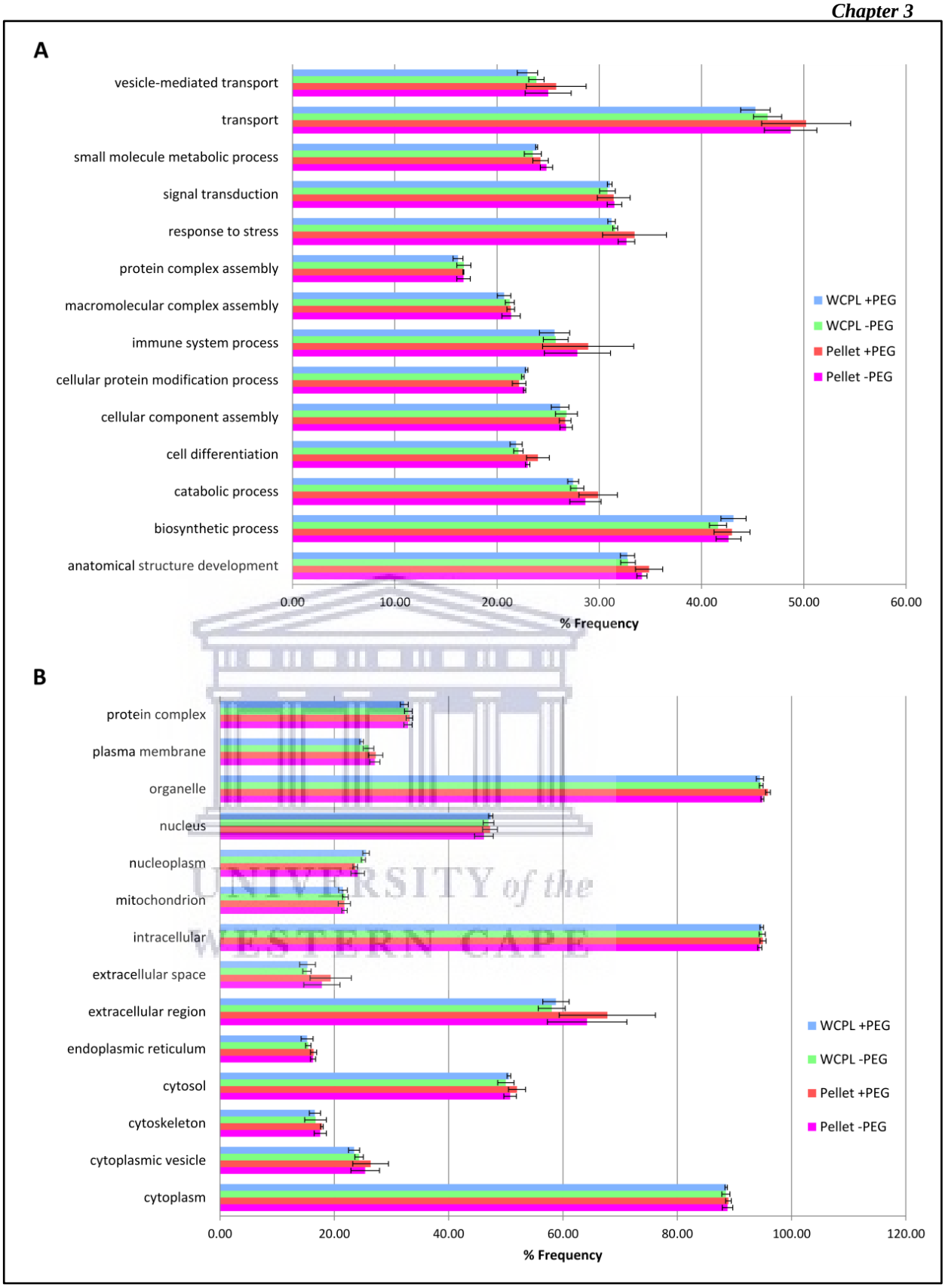

Figure 21. Gene Ontology annotation profiles for proteins identified from all samples/conditions. (A) GO profiles according to biological processes, (B) GO profiles according to cellular components. The average proportions for all three patients per condition are shown with error bars indicating the standard deviation. (-PEG) refers to protein extracted without PEG and (+PEG) refers to protein extracted with PEG. Red bar graphs refer to pellet samples extracted with PEG; Purple bar graphs refer to pellet samples extracted without PEG; Blue bar graphs refer to WCPL samples extracted with PEG; Green bar graphs refer to WCPL samples extracted without PEG.

3.3.2.4 Assessment of HILIC sample preparation method reproducibility and trypsin digestion efficiency

To assess the reproducibility of the HILIC sample preparation method and to determine if the protein extraction buffer components (PEG and/or SDS detergent) interfered with trypsin activity, the percentage of missed cleavages across all samples was analysed (Fig. 22).

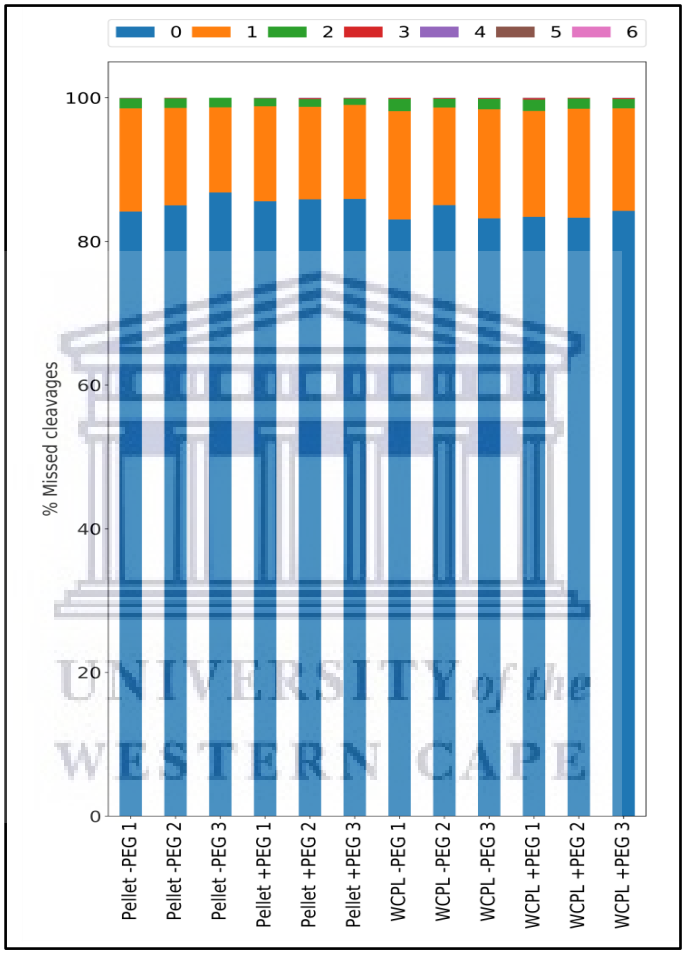

Figure 22. The number of missed cleavages for all samples. For each sample, the percentages of missed cleavages are plotted. (-PEG) refers to protein extracted without PEG and (+PEG) refers to protein extracted with PEG. The figure key on top shows the graph colours for corresponding number of missed cleavages, with 0 missed cleavages = blue, 1 missed cleavage = orange, 2 missed cleavages = green, 3 missed cleavages = red, etc.

Figure 22 illustrates that the percentage of missed cleavages were similar for all samples. All samples had a majority (>80%) of fully cleaved peptides (0 missed cleavages), with approximately 18% peptides with 1 missed cleavage, approximately 1.5% peptides with 2 missed cleavages, and 0.5% with >2 missed cleavages. This indicates that the protein extraction buffer components, PEG and/or SDS detergent

did not interfere with trypsin activity. In addition, the HILIC sample preparation method shows a similar range of missed cleavages in all samples and experimental conditions analysed. Therefore, the HILIC protocol/workflow was sufficiently reproducible across all samples and efficient at removing SDS, which interferes with trypsin activity (Pellerin *et al*., 2015). Batth *et al*., (2018), Hughes *et al*., (2018), and Moggridge *et al*. (2018) have also demonstrated the sensitivity, reproducibility, and efficiency of the SP3/HILIC sample preparation method in removing sample contaminants for optimal recovery of peptides for LC-MS/MS analysis.

3.4 Conclusions

Due to the importance of archival FFPE tissue repositories as a source for clinical proteomic studies and its convenient methods of storage and accessibility, it has become increasingly necessary to develop and standardise protocols for the proteomic analysis of FFPE tissues. We have demonstrated (using FFPE human colorectal cancer resection tissue) that the addition of 0.5% (w/v) PEG to protein extraction buffer resulted in overall lower peptide and protein identifications, compared to buffer without the addition of PEG. In addition, protein samples extracted without PEG showed higher reproducibility, however, addition of PEG to the protein extraction buffer generated lower percentages of unique peptides remaining in the sample pellets. We show here, by building on from previous studies, which found that higher protein concentrations (>10 µg) (of FFPE animal tissues and human cells) compromise the function of PEG, that this effect is also observed in FFPE human colon tissue.

Chapter 4: Evaluation of protein purification techniques and effects of storage duration on LC-MS/MS analysis of archived FFPE human CRC tissues

Abstract

Introduction: To elucidate cancer pathogenesis and its mechanisms at the molecular level, the collection and characterisation of large individual patient tissue cohorts are required. Since most pathology institutes routinely preserve biopsy tissues by standardised methods of formalin fixation and paraffin embedment, these archived FFPE tissues are important collections of pathology material that include patient's metadata (medical history/treatments). FFPE blocks can be stored under ambient conditions for decades, while retaining cellular morphology, due to modifications induced by formalin. However, the effect of long-term storage, at resource-limited institutions in developing countries, on extractable protein quantity/quality has not yet been investigated. In addition, the optimal sample preparation techniques required for accurate, reproducible results from label-free LC-MS/MS analysis across block ages remains unclear.

Methods: The impact of archival time, after approximately 1, 5 and 10 years of storage, on protein extraction efficiency from human colorectal carcinoma resection tissue samples was investigated. The performances of three different gel-free protein purification methods for label-free LC-MS/MS analysis, namely detergent removal plates (DRP), the APFAR method, and the SP3/HILIC method, across different sample/block ages were also assessed and compared. A sample size of $n = 17$ patients per experimental group (with experiment power = 0.7 and $\alpha = 0.05$, resulting in 70% confidence level) was selected based on results obtained in the pilot study of Chapter 3. Data were evaluated in terms of protein yield, peptide/protein identifications, method reproducibility and efficiency, sample proteome integrity (due to storage time), as well as protein/peptide distribution according to biological processes, cellular components, and physicochemical properties. Data are available via ProteomeXchange with identifier PXD017198.

Results: Total protein yield is significantly ($p < 0.0001$) dependent on block age, with older blocks (5 and 10-year-old) yielding less protein (at 2.46 ± 0.03 mg/ml and

1.65 ± 0.04 mg/ml, respectively) than approximately 1-year-old blocks (3.82 ± 0.03 mg/ml). Block age differences were also observed in tissue proteome composition, with greater proteome composition correlation detected between the 5 and 10-year-old blocks processed via the APFAR and DRP methods (r^2 values of 0.823 and 0.835, respectively), whereas the HILIC method yielded comparable relative protein abundances for all block ages. The DRP method resulted in the highest overall peptide and protein identifications, and the APFAR method resulted in the lowest. The different methods also introduced an observable bias with regard to proteome composition, which is also more pronounced for 1-year-old blocks, compared to older blocks. Differences in PCA variance were also shown, with the DRP method having the lowest variance (10.73%) between block ages, followed by the HILIC method (13.68%), and the APFAR method, which has the highest variance at 14.57%. The APFAR method had the highest overall digestion efficiency (with ≥85% of all peptides having no missed cleavages), and the HILIC method had the lowest overall digestion efficiency, with ≥80% of all peptides having no missed cleavages. However, no significant difference in methionine oxidation levels was found between 1, 5 and 10-year-old blocks for each sample preparation method.

Conclusions: Overall, the results indicate that long-term storage of FFPE tissues (at a resource-limited institution in a developing country) does not considerably interfere with retrospective proteomic analysis. In addition, variations in pre-analytical factors (spanning a decade) do not affect shotgun proteomic analysis to a significant extent. Sample/block age mainly affects initial protein extraction efficiency, with older blocks generating lower protein yields. Regarding the optimal protein purification technique required for archived tissues, the DRP and SP3/HILIC methods performed the best, with the SP3/HILIC method performing consistently across all block ages and requiring less protein (and therefore less starting material) than the other methods, therefore making it the most sensitive and efficient protein purification method evaluated here.

4.1 Introduction

The protein profiling of FFPE tissues has immense potential for biomarker discovery and validation. Pathology institutes routinely process and store patient biopsy and/or

surgery tissue samples via formalin fixation and paraffin embedment. Since FFPE blocks can be stored under ambient conditions for decades, most pathology archives consist of thousands of FFPE blocks, which often comprise recent as well as decades-old blocks. However, the effect of long-term storage, at resource-limited institutions in developing countries, on extractable protein quantity/quality has not yet been investigated. In addition, the optimal sample preparation techniques required for accurate, reproducible results from label-free LC-MS/MS analysis across block ages remains unclear.

Some top-down proteomic studies have found no significant difference in protein yield between younger and older FFPE blocks (Fowler *et al*., 2013), whereas others have found a significant decrease in protein yield as block age increases (Kroll *et al*., 2008; Wolff *et al*., 2011). The top-down proteomic approach analyses intact proteins, whereas the bottom-up and middle-down approaches involves the characterisation and analysis of proteins through proteolysis (of a protein mixture from a whole cell or tissue extract) and subsequent peptide generation and analysis (Zhang *et al*., 2013). Bottom-up proteomic studies found minimal or no impact of block age on protein yield and identifications (Gustafsson *et al*., 2015). The main detrimental pre-analytical factor appears to be tissue fixation time, with longer periods (>24 hours) leading to significant decreases in protein yield and number of proteins identified via LC-MS/MS (Sprung *et al*., 2009; Wolff *et al*., 2011; Tanca *et al*., 2011). Of interest to this study is the bottom-up proteomics approach (also referred to as shotgun MS), since it is difficult to obtain and maintain intact proteins during the sample processing stages for the top-down MS technique.

Due to formalin-induced protein cross-linking, strong detergents such as sodium dodecyl sulphate (SDS) are required for total tissue solubilisation and protein extraction from FFPE tissues (Wiśniewski *et al*., 2009; Botelho *et al*., 2010; Pellerin *et al*., 2015). However, SDS binds to amino acids and thereby changes the proteins' spatial conformational structures. This, in turn, inhibits proteases, such as trypsin, from accessing the proteins' cleavage sites (which have become distorted through SDS binding) and also inhibits protease activity by changing the enzymes' conformational structure (through SDS binding). In addition, SDS alters the chromatographic separation of peptides and also interferes with ESI mass

spectrometry by dominating mass spectra and significantly suppressing analyte ion signals since it is readily ionisabile and present in greater abundances than individual peptide ions. For these reasons, SDS must be completely depleted from a sample before enzymatic digestion and LC-ESI MS/MS analysis (Wiśniewski *et al*., 2009; Botelho *et al*., 2010; Kachuk *et al*., 2015; Pellerin *et al*., 2015). However, SDS removal with minimal sample loss is a challenging task and several gel-free approaches have been proposed over the years. These approaches include incorporating the use of detergent removal plates (DRP), protein precipitation with organic solvents, such as the APFAR method (Botelho *et al*., 2010; Doucette *et al*., 2014; Kachuk *et al*., 2015), and/or methods using hydrophilic interaction liquid chromatography (HILIC) and magnetic resin (Hughes *et al*., 2014) in the sample processing workflow prior to LC-MS/MS.

The aim of this study was to methodically characterise the effects of storage time (over 1, 5 and 10 years) on the quality of data produced via label-free LC-MS/MS analysis of FFPE tissue blocks from a resource-limited pathology archive. In addition, three different gel-free protein purification methods for label-free LC-MS/MS analysis was also assessed across all block ages. The best suited method for analysing archived colorectal carcinoma FFPE tissue was determined with regards to peptide and protein identifications, reproducibility, digestion efficiency, and any method-based protein selection bias.

4.2 Materials and Methods

4.2.1 Formalin-fixed paraffin-embedded (FFPE) human colorectal carcinoma (CRC) resection samples

FFPE tissue blocks, which consist of human colorectal carcinoma resection samples, were obtained from the Anatomical Pathology department at Tygerberg Hospital (Western Cape, South Africa) after obtaining ethics clearance from the Biomedical Science Research Ethics Committee (BMREC) of the University of the Western Cape (ethics reference number: BM17/7/15), as well as the Health Research Ethics Committee (HREC) of Stellenbosch University (ethics reference number: S17/10/203). The FFPE blocks were anonymised prior to processing. The 1-year-old

blocks were archived since 2016/2017 (when the tissue was resected), 5-year-old blocks were archived since 2012, and 10-year-old blocks were archived since 2007. Tissue processing and fixation times/conditions and storage conditions are unknown, since specimens were retrospectively collected. After performing a sample size power calculation, seventeen patient cases, per block age, were reviewed and selected (Table 8).

The power calculation was performed using previous protein identification results obtained by the pilot study of Chapter 3 (section 3.3.2.1) and an overall F-test for one-way ANOVA, which found that the sample size (n = 17) per group/block age resulted in a calculated power of 0.7 ($\alpha = 0.05$).

Patient samples diagnosed with colorectal adenocarcinoma, after H&E staining, were reviewed by a pathologist(s) to ensure tissue quality and comparability (Fig. 23). The selected slides had carcinomas with more than 90% viable tumour nuclei.

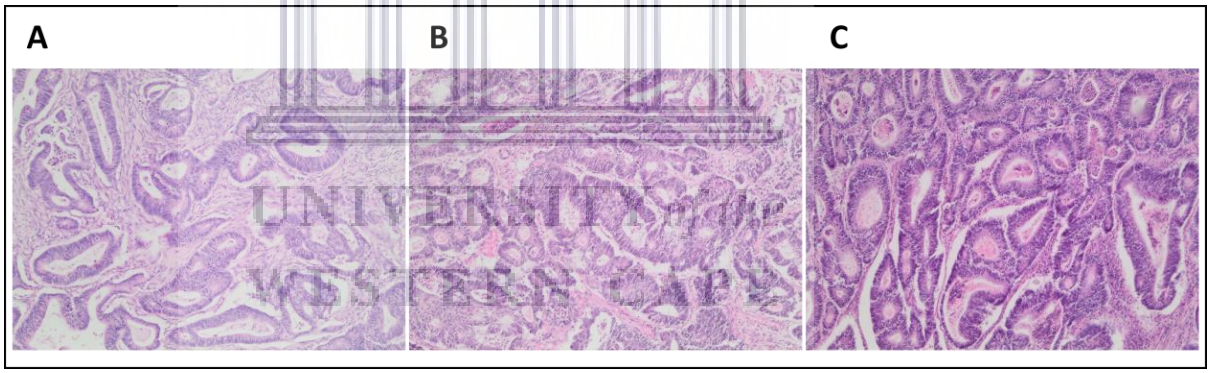

Figure 23. Colonic adenocarcinoma resection tissue samples. Representative H&E stained sections of patient cases/block ages analysed in this study; (A) 1-year-old block, (B) 5-year-old block, and (C) 10-year-old block at 100x magnification.

Table 8. Information of the FFPE specimens selected for analysis.

Patient number:	Block age (years):	Patient age (years):	Gender:	Diagnosis:	Grade:	Stage:	Location:
1	1	75	M	Adenocarcinoma	low-grade	IIA	Left colon
2	1	81	M	Adenocarcinoma	low-grade	IIA	Left colon
3	1	68	F	Adenocarcinoma	low-grade	IIA	Left colon
4	1	42	M	Adenocarcinoma	low-grade	IVA	Left colon
5	1	80	F	Adenocarcinoma	low-grade	I	Left colon
6	1	79	M	Adenocarcinoma	low-grade	IIA	Left colon
7	1	49	M	Adenocarcinoma	low-grade	IIA	Left colon
8	1	40	F	Adenocarcinoma	low-grade	IIA	Left colon
9	1	56	M	Adenocarcinoma	low-grade	IIA	Left colon
10	1	79	F	Adenocarcinoma	low-grade	IIA	Left colon
11	1	64	F	Adenocarcinoma	low-grade	IIA	Left colon
12	1	53	M	Adenocarcinoma	low-grade	IIIB	Left colon
13	1	78	M	Adenocarcinoma	low-grade	IIA	Left colon
14	1	51	F	Adenocarcinoma	low-grade	IIIB	Left colon
15	1	31	M	Adenocarcinoma	low-grade	IIIB	Left colon
16	1	73	F	Adenocarcinoma	low-grade	IIIB	Left colon
17	1	54	F	Adenocarcinoma	low-grade	IIIC	Left colon
18	5	51	F	Adenocarcinoma	low-grade	IIA	Left colon
19	5	56	F	Adenocarcinoma	low-grade	IIIB	Left colon
20	5	86	M	Adenocarcinoma	low-grade	IIA	Left colon
21	5	59	M	Adenocarcinoma	low-grade	IIC	Left colon
22	5	67	M	Adenocarcinoma	low-grade	IIA	Left colon
23	5	82	M	Adenocarcinoma	low-grade	IIA	Left colon
24	5	49	F	Adenocarcinoma	low-grade	IIIB	Left colon
25	5	54	M	Adenocarcinoma	low-grade	IIA	Left colon
26	5	58	M	Adenocarcinoma	low-grade	IIC	Left colon
27	5	44	F	Adenocarcinoma	low-grade	I	Left colon
28	5	50	M	Adenocarcinoma	low-grade	IIA	Left colon
29	5	74	F	Adenocarcinoma	low-grade	IIA	Left colon
30	5	54	M	Adenocarcinoma	low-grade	IIA	Left colon
31	5	47	F	Adenocarcinoma	low-grade	IIIA	Left colon
32	5	55	M	Adenocarcinoma	low-grade	IIIB	Left colon
33	5	83	M	Adenocarcinoma	low-grade	IIA	Left colon
34	5	60	M	Adenocarcinoma	low-grade	IIA	Left colon
35	10	69	M	Adenocarcinoma	low-grade	IIIB	Left colon
36	10	47	F	Adenocarcinoma	low-grade	IIA	Left colon
37	10	58	F	Adenocarcinoma	low-grade	IIA	Left colon
38	10	83	M	Adenocarcinoma	low-grade	IIA	Left colon
39	10	57	F	Adenocarcinoma	high-grade	IIA	Right colon
40	10	46	F	Adenocarcinoma	high-grade	IIA	Right colon
41	10	77	F	Adenocarcinoma	low-grade	IIA	Left colon
42	10	63	F	Adenocarcinoma	low-grade	IIA	Left colon
43	10	67	M	Adenocarcinoma	low-grade	IIIB	Left colon
44	10	50	F	Adenocarcinoma	low-grade	IIA	Left colon
45	10	42	M	Adenocarcinoma	low-grade	IIA	Left colon
46	10	71	F	Adenocarcinoma	low-grade	IIA	Left colon
47	10	70	M	Adenocarcinoma	low-grade	IIA	Left colon
48	10	69	M	Adenocarcinoma	low-grade	IIA	Left colon
49	10	62	F	Adenocarcinoma	low-grade	IIA	Right colon
50	10	78	M	Adenocarcinoma	low-grade	IIIB	Left colon
51	10	33	M	Adenocarcinoma	low-grade	IIA	Left colon

4.2.2 Protein extraction and quantification

The total volume (mm^3) of manually microdissected tumour tissue required to extract approx. 1.25mg/ml in approx. 500 µl sample volume was determined as described in section 3.2.2. Approximately 25 mm^3 of manually microdissected tumour tissue was used per patient sample (with 17 individual patient samples per group/block age) and protein extracted in 500 µl of 50 mM AmBic (pH 8.0) and 2% (w/v) SDS. The method used for sample processing and protein extraction is described in section 3.2.2. The protein lysates of each sample were transferred to new protein LoBind microcentrifuge tubes (Eppendorf, Germany) and the protein yield determined using the Pierce™ BCA Protein Assay Kit (Pierce Biotechnology, Thermo Fisher Scientific, USA) according to manufacturer's instructions.

The samples were subsequently processed by the DRC (ThermoFisher Scientific, 2017), APFAR (Botelho *et al*., 2010; Doucette *et al*., 2014; Kachuk *et al*., 2015) and/or HILIC (SP3) magnetic bead digestion method (Hughes *et al*., 2019), prior to LC-MS/MS analysis (Fig. 24).

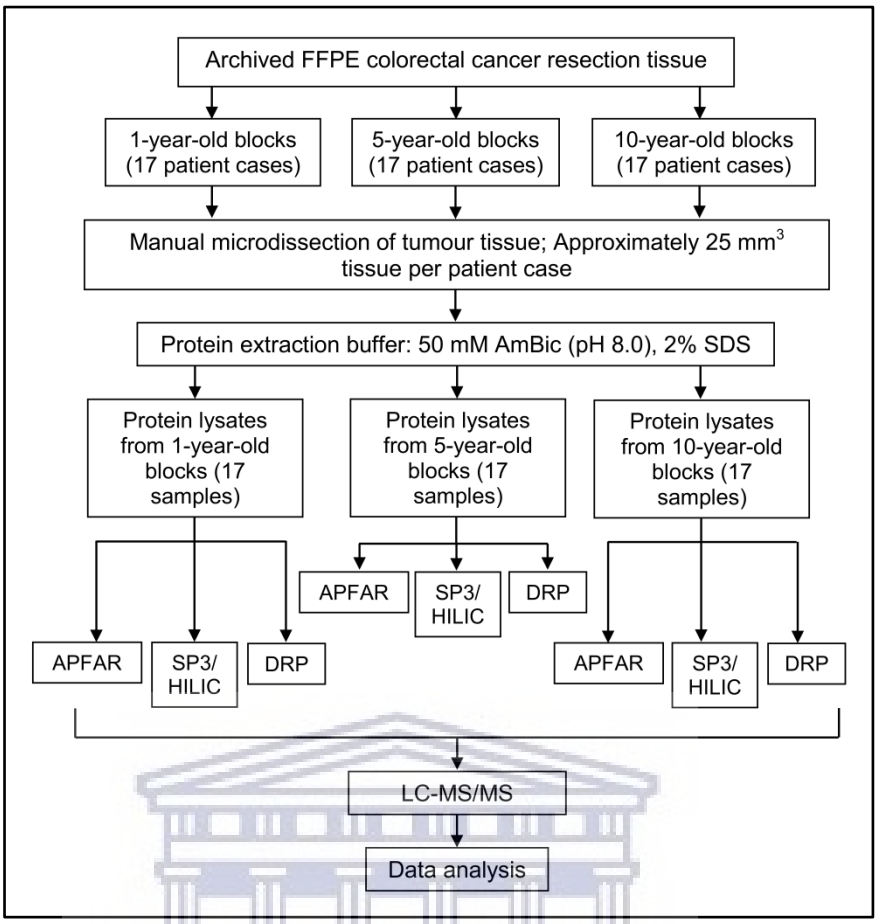

Figure 24. Experimental design and workflow used to evaluate the effects of block age and different sample processing methods. FFPE human colorectal carcinoma resection tissues from 17 patients per block age (1, 5 and 10-year old blocks) were cut and tumour areas were manually micro-dissected for analysis. From each patient, tissue sections, which corresponded to approximately 25 mm^3 tissue per patient/sample, were cut per sample. Protein was extracted and quantified, after which each patient sample was split in three, for subsequent sample processing by either the APFAR, DRP, or HILIC methods. Resultant peptides were analysed via LC-MS/MS and data analysis was performed on all sample MS/MS spectra.

4.2.3 Sample preparation methods

4.2.3.1 Detergent removal plates (DRP) method

Detergent removal was carried out using detergent removal spin plates (Pierce Biotechnology, Thermo Fisher Scientific, USA) according to the manufacturer's instructions. Briefly, a detergent removal plate was placed on top of a wash plate and the shipping solution spun out at 1,000 x g for 2 min. The resin bed was equilibrated with 300 µl of 50 mM TEAB and spun through as before, and this was repeated twice. Thereafter, 100 µg of protein was loaded onto the columns and incubated at room temperature for 2 min before spinning through at 1,000 x g for 2 min into the

sample collection plate. Samples were then transferred to protein Lobind tubes and dried down by vacuum centrifugation. Once dried, samples were resuspended in 30 µl of 50mM TEAB.

4.2.3.2 Acetone precipitation and formic acid resolubilisation (APFAR) method

Samples were processed via the APFAR method as described in section 3.2.3.2 (of Chapter 3).

4.2.3.3 In-solution digestion

In-solution digestion was carried out on samples processed by the APFAR (section 4.2.3.2) and DRC (section 4.2.3.1) methods as described in section 3.2.3.3 (of Chapter 3).

4.2.3.3 SP3/HILIC method with on-bead digestion

Samples were processed via the HILIC/SP3 method as described in section 3.2.3.4 (of Chapter 3).

4.2.4 Label–free LC–MS/MS analysis

LC-MS/MS analysis was conducted as described in section 3.2.4 of Chapter 3.

4.2.5 Peptide and protein identification

Raw data containing centroid MS/MS spectra were converted into mgf (Matrix Science, UK) files using msconvert from the Proteo-Wizard software suite (Kessner *et al*., 2008). Peak lists obtained from MS/MS spectra were identified using X!Tandem (version X!Tandem Vengeance 2015.12.15.2) (Craig & Beavis, 2004), MS Amanda (version 2.0.0.9706) (Dorfer *et al*., 2014) and MS-GF+ (version 2018.04.09) (Kim & Pevzner, 2014). The search was conducted using SearchGUI (version 3.3.3) (Vaudel *et al*., 2011) and protein identification was conducted against a concatenated target/decoy protein sequence database as described in sections

3.2.5.1.1 and 3.2.6 of Chapter 3 (refer to Appendix A for search algorithms specific settings). The decoy sequences were created by reversing the target sequences in SearchGUI. Peptides and proteins were inferred from the spectrum identification results as described in section 3.2.6 (of Chapter 3) using PeptideShake version 1.16.40.

4.2.6 Data and statistical analyses

Qualitative and quantitative data were exported from PeptideShaker and parsed using in-house scripts and graphs generated in Jupyter lab (using Pandas, NumPy, and Matplotlib Python packages), as well as Microsoft® Excel. Additional statistical analyses were performed using SAS® university edition and SAS® Studio version 3.8 (results of the statistical tests that were performed are listed in Appendix D Supplementary table 2). To determine if sample distributions were normal, a Kolmogorov–Smirnov or Shapiro–Wilk test was performed, with D denoting the test statistic for the Kolmogorov–Smirnov test and W denoting the test statistic for the Shapiro–Wilk test. For normal distributions, comparison of means across 3 (or more) groups was performed using the parametric ANOVA procedure, with F (F-ratio) denoting the test statistic. The Kruskal–Wallis nonparametric analysis of variance was used when data were from a non-normal distribution, and H denotes the test statistic. For all statistical reporting, the test statistic value is given along with the degrees of freedom (in brackets after the test statistic symbol) and p-value. Post hoc statistical analyses were performed on significant results using Bonferroni or Dunn's test (Field & Miles, 2010; Elliott & Hynan, 2011).

PeptideShaker uses spectrum counting based quantification, which relies on the reasoning that highly abundant peptides will have a higher intensity, and are therefore more likely to generate acquisition of MS/MS spectra (Vaudel *et al*., 2011; Vaudel, 2017). Consequently, peptides from abundant proteins are more likely to be identified and possess more spectra. The NSAF method followed here involves counting the number of spectra attributed to a protein (Powell *et al*., 2004). This count is then normalised for the length of the protein, the presence of shared peptides, as well as redundant peptides (Vaudel *et al*., 2011; Vaudel, 2017). The spectrum counting indexes were exported from PeptideShaker and parsed using in-house scripts. The

NSAF values (of common/shared proteins only) were multiplied by the lowest factor calculated for each pair of conditions compared, in order to deal with integers and facilitate comparisons. These NSAF values were then used to estimate the extent of differential protein abundance (of common/shared proteins only) by calculating the Pearson's correlation coefficient (PCC), for each pair of conditions compared, to assess the relationship/level of correlation between samples. PCC graphs were generated in Jupyter lab, using Pandas, NumPy, and Matplotlib Python packages.

Principal component analysis (PCA) was performed for each patient case/sample's list of identified proteins and corresponding NSAF values, with Jupyter lab, using Pandas, NumPy, Scikit-learn, Seaborn and Matplotlib Python packages.

The physicochemical properties of the identified peptides, including the hydropathicity (Kyte-Doolittle scale), molecular weight, and isoelectric point were calculated for each sample using the Protein property analysis software (ProPAS) version 1.1 (Wu & Zhu, 2012).

Venny version 2.1.0 (Oliveros, 2007) was used to generate Venn diagrams to visualise the consistency of peptide identifications between samples.

Protein annotations regarding subcellular localisation were retrieved from Ensembl (www.ensembl.org) using GOSlim UniProtKB-GOA (www.ebi.ac.uk/GOA) to minimise the number of terms retrieved. Hypergeometric testing was used to calculate the significance of gene ontology terms.

4.2.7 Data sharing information

The mass spectrometry proteomics data have been deposited to the ProteomeXchange Consortium (Deutsch *et al*., 2017) via the PRIDE (Perez-Riverol *et al*., 2019) partner repository with the dataset identifier PXD017198 and DOI: 10.6019/PXD017198.
Username: reviewer45507@ebi.ac.uk Password: R8Ep4gdw

4.3 Results and discussion

The objectives of this study were to evaluate three different sample processing methods (the APFAR or DRC methods followed by in-solution digestion, or the SP3/HILIC method with magnetic bead-based digestion) as well as the effect of storage time/FFPE tissue block age on protein extraction efficiency and reproducibility. Subsequent proteomic analysis by label-free LC-MS/MS evaluated the proteome coverage, proportion of missed cleavages, and enrichment/selection bias based on sample processing method used.

4.3.1 Protein extraction and quantification

The BCA total protein quantitation assay results of all samples (after protein was extracted from approximately 25 mm^3 patient tumour tissue using 500 µl of protein extraction buffer) are shown in figure 25.

A Kruskal–Wallis test was conducted to examine the differences in protein yield between block ages (Appendix D Supplementary table 2). Protein yield was significantly affected by block age ($H(2) = 23.92$, $p < 0.0001$), also seen in figure 25. Based on Dunn's post hoc testing results, there is evidence that the distribution of protein yields are significantly different for 1-year-old blocks vs 10-year-old blocks and for 1-year-old blocks vs 5-year-old blocks, but not for 5-year-old blocks vs 10-year-old blocks (results and conclusions are shown in Appendix D Supplementary table 2).

The 10-year-old FFPE tissues generated overall lower protein yields (an average of 1.65 ± 0.04 mg/ml) compared to the 5-year-old FFPE tissues, which generated an average of 2.46 ± 0.03 mg/ml protein, and the 1-year-old FFPE tissues, which generated an average of 3.82 ± 0.03 mg/ml protein. This corresponds to approximately 825 µg, 1230 µg, and 1910 µg protein extracted from the 10, 5 and 1-year-old FFPE tissues, respectively, by using approximately 25 mm^3 tissue.

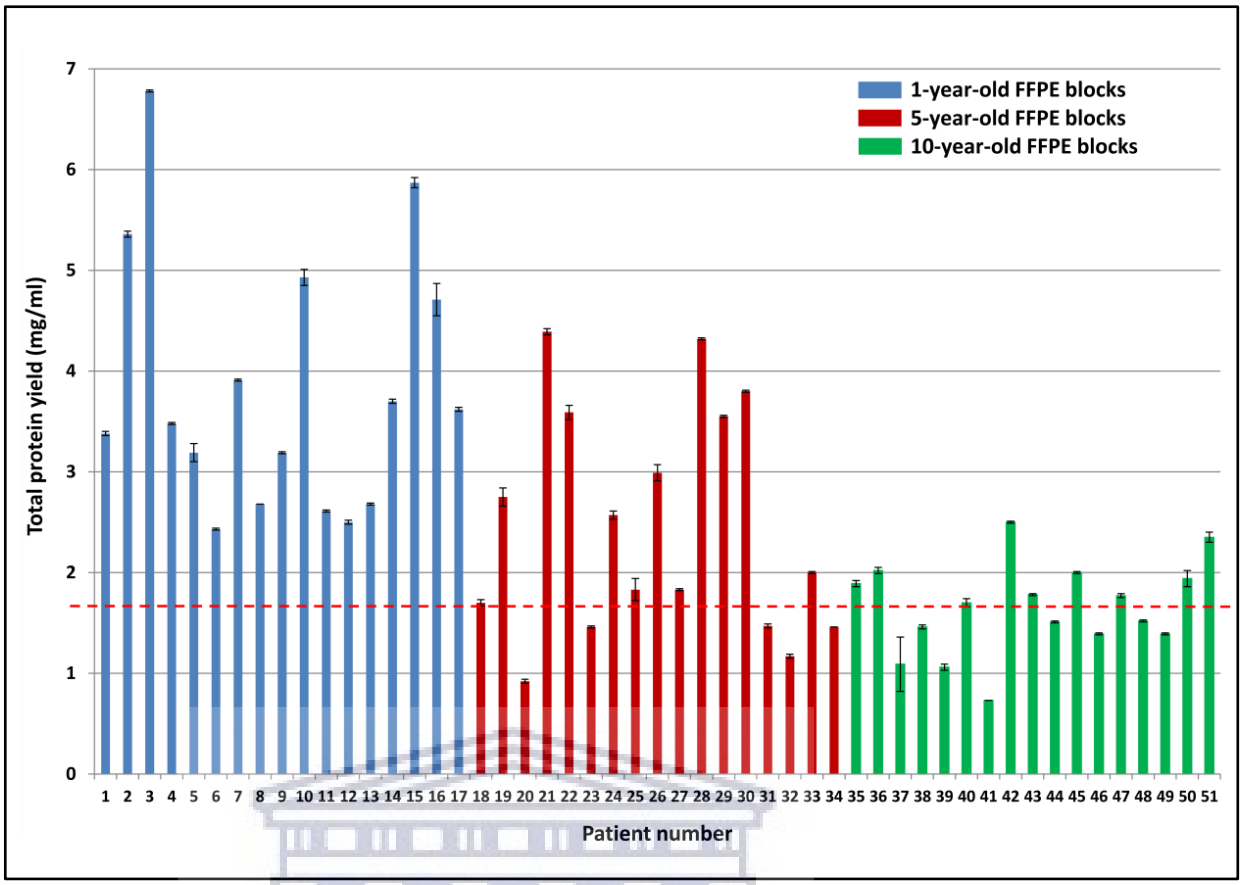

Figure 25. BCA total protein quantitation assay results for the different block ages. Protein was extracted from approximately 25 mm^3 patient tumour tissue using 500 µl protein extraction buffer per sample (n = 17 patients per group). The blue bars indicate protein yield from 1-year-old FFPE blocks, the red bars indicate protein yield from 5-year-old FFPE blocks, and the green bars indicate protein yield from 10-year-old FFPE blocks. The red dotted line indicates the average protein yield obtained from the 10-year-old FFPE blocks, which is 1.65 mg/ml protein.

Sprung *et al*. (2009) were able to extract 300 – 400 µg (0.14 mg/ml) protein from 1.18 mm^3 FFPE colon adenoma tissue (of 60 µm thickness and 5 mm diameter), which is approximately 4 times higher. However, they noted a suppressive effect of formalin-fixation on protein yield estimates, using the BCA assay, in colon adenoma tissue lysates. This effect occurs because the amino acids that contribute to the reduction of copper are also susceptible to reactions with formaldehyde. Therefore they empirically determined a correction factor for protein yield estimates of FFPE tissues (using the BCA assay) by comparing it to freshly frozen colon adenoma tissue replicates' protein yields. They then used this correction factor to measure the amount of protein generated from their FFPE samples. Since we are not comparing fresh tissues to FFPE tissues, we did not determine the correction factor of our dataset and we report the protein yield estimates only. In addition, Wiśniewski *et al*. (2012) also extracted higher protein yields at 100 mg/ml protein from 0.1 mm^3 FFPE colonic

adenoma tissue and Wolff *et al*. (2011) extracted 2.76 mg/ml protein from approximately 1-year-old and 1.48 mg/ml protein from approximately 21-year-old (1.5 mm^3) FFPE colon carcinoma tissue. On the other hand, Rodríguez-Rigueiro *et al*. (2011) extracted less protein than reported here, with 250 µg protein from approximately 18 mm^3 FFPE colon carcinoma tissues that were stored for less than 5 years. Therefore, the amount of protein extracted here falls within the published ranges for FFPE colon tissue.

Although approximately 25 mm^3 of manually microdissected tumour tissue per sample was used for protein extraction, and the volume of protein extraction buffer kept constant at 500 µl per sample, the total amount of extractable protein and protein yield still differed among the patient samples within the same block ages (Fig. 25). Similar variations in protein yields were also observed in section 3.3.1 (Fig. 16), as well as Wolff *et al*. (2011). This observation is also noted in FFPE protein extraction protocols elsewhere, with the Agilent Technologies (2009) manual explaining that protein yields obtained from FFPE protein lysates may vary between samples due to variance in pre-analytical factors, such as tissue handling and inconsistencies/differences in the formalin-fixation and paraffin-embedment protocol, which affects how well proteins will be preserved. They recommend increasing the amount of starting material/tissue if the quality of protein preservation in the FFPE sample is questionable (Agilent Technologies, 2009).

4.3.2 The effect of block age and sample preparation methods on peptide and protein identification

The efficiency and reproducibility for each sample preparation method, as well as the effect of storage time/block age, at both peptide and protein level was assessed with regards to proteome coverage (number of peptides and proteins identified) (Fig. 26 A and B) and known protein biomarkers (proteins deregulated in colon cancer) from the literature, which were also identified in the data (Table 9).

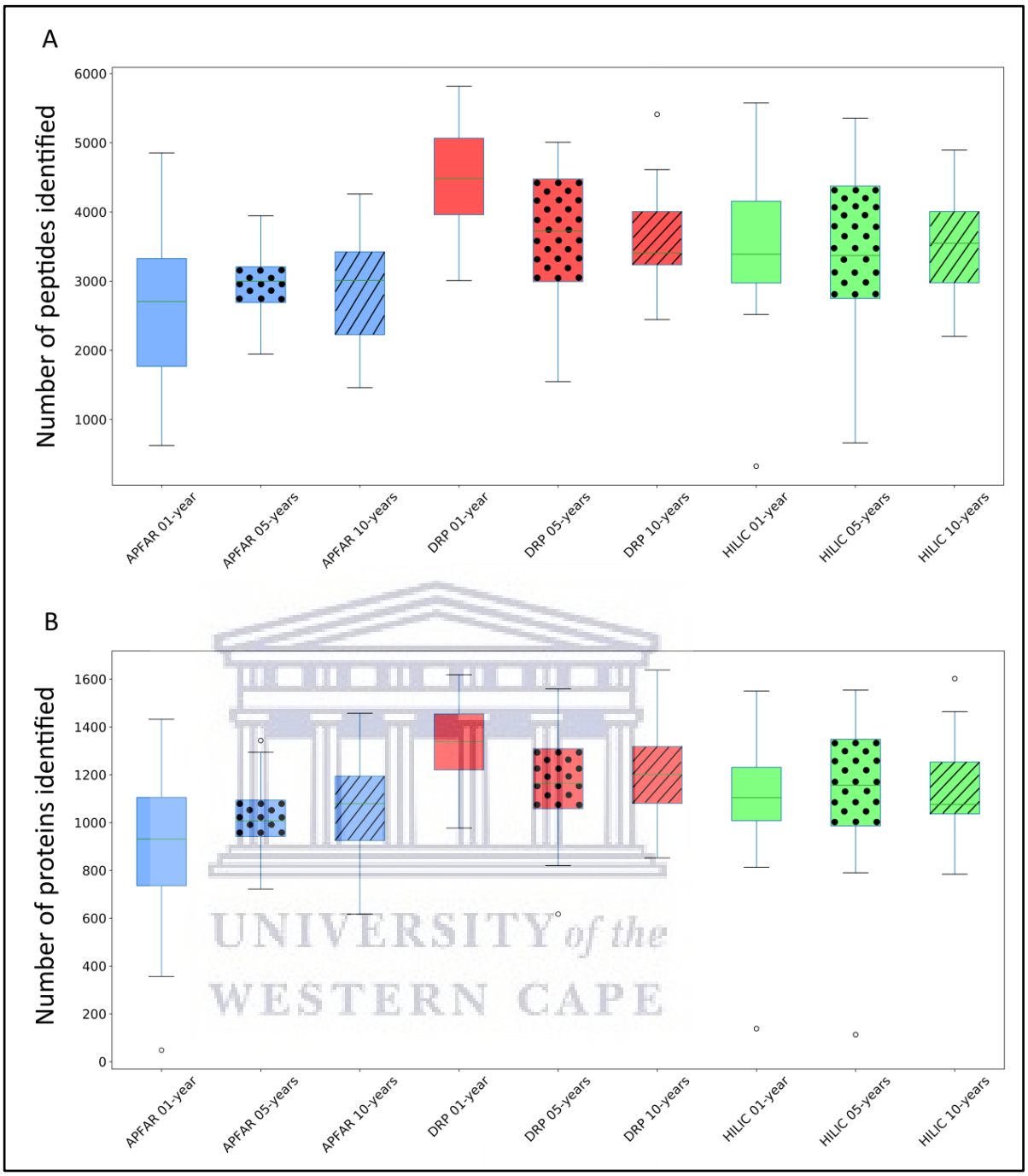

Figure 26. Comparison of the number of peptides and proteins identified for the different sample preparation methods for each block age. (A) Box and whiskers plots of the number of peptides identified (for all 17 patient cases) per block age ($p < 0.05$ for 1 and 10-year-old blocks), and protein purification method ($p = 0.0125$ for DRP) (B) Box and whiskers plots of the number of proteins identified (for all 17 patient cases) per block age ($p = 0.0002$ for 1-year-old blocks) and protein purification method. Blue boxplots refer to APFAR samples; Red boxplots refer to DRP samples; Green boxplots refer to HILIC samples. For all boxplots, 5-year-old samples are represented by dots; 10-year-old samples are represented by diagonal lines.

Average results (with standard deviation) for all samples (Fig. 26) show that overall, the DRP method performed the best with the highest overall peptide and protein

identifications; at 4436 ± 823 and 1319 ± 180 for validated peptides and proteins, respectively, for 1-year-old blocks; 3607 ± 1072 and 1155 ± 252 for validated peptides and proteins, respectively, for 5-year-old blocks; 3602 ± 786 and 1206 ± 214 for validated peptides and proteins, respectively, for 10-year-old blocks. This is followed by the SP3/HILIC method with 3446 ± 1151 and 1089 ± 313 for validated peptides and proteins, respectively, for 1-year-old blocks; 3386 ± 1182 and 1091 ± 335 for validated peptides and proteins, respectively, for 5-year-old blocks; 3472 ± 803 and 1150 ± 213 for validated peptides and proteins, respectively, for 10-year-old blocks. The APFAR method generated the lowest numbers of peptide and protein identifications; at 2627 ± 1128 and 883 ± 343 for validated peptides and proteins, respectively, for 1-year-old blocks; 3025 ± 608 and 1026 ± 173 for validated peptides and proteins, respectively, for 5-year-old blocks; 2882 ± 849 and 1039 ± 242 for validated peptides and proteins, respectively, for 10-year-old blocks.

One-way ANOVA or Kruskal–Wallis tests were conducted (as described in section 4.2.6 and results and conclusions are listed in Appendix D Supplementary table 2) to determine if the number of identified peptides and proteins were significantly different between block ages, as well as for each sample preparation method.

Statistical analyses comparing sample preparation method performance per block age indicated the following: For the 1-year-old blocks, based on post hoc Bonferroni (Dunn) t tests, the DRP method differs significantly ($F(2) = 12.78$, $p < 0.0001$, $\alpha = 0.05$) with regards to validated peptide identifications, however there was no significant difference between the numbers of validated peptides identified for the APFAR and SP3/HILIC methods. Based on Dunn's post hoc testing results, there is also evidence that the distribution of validated protein identifications (for 1-year old blocks) are significantly different ($p = 0.0002$) for DRP vs APFAR processing, but not for DRP vs HILIC and APFAR vs HILIC sample preparation methods. With regards to validated peptide and protein identifications, there is no significant difference ($p > 0.05$) between protein purification/sample preparation methods for 5-year old blocks. For the 10-year old blocks, based on post hoc Bonferroni (Dunn) t tests, the DRP and APFAR methods differ significantly ($F(2) = 3.78$, $p = 0.0299$, $\alpha = 0.05$) with regards to validated peptide identifications, however there is no significant difference between the APFAR and SP3/HILIC and the DRP and SP3/HILIC methods.

Statistical analyses comparing the differences between block ages (effect of block age on the number of peptide/protein identifications) within each sample preparation method indicated the following: Both the APFAR and SP3/HILIC methods performed most consistently across block ages, with no significant difference between 1, 5 and 10-year-old blocks (APFAR method: $F(2,48) = 0.88$, $p = 0.42$ for peptides identified and $H(2) = 2.28$, $p = 0.32$ for proteins identified; SP3/HILIC method: $F(2,48) = 0.03$, $p = 0.97$ for peptides identified and $H(2) = 0.101$, $p = 0.95$ for proteins identified). Only the DRP method showed a significant difference between the block ages with regard to numbers of peptides identified ($F(2) = 4.81$, $p = 0.0125$, $\alpha = 0.05$), with a significant difference between 1 and 5-year-old blocks, as well as 1 and 10-year-old blocks, but no significant difference between 5 and 10-year-old blocks. In addition, no significant difference was detected for the number of proteins identified ($F(2,48) = 2.53$, $p = 0.09$).

The sample preparation methods that did not show any significant differences between block ages, are in accordance with the findings of other studies (Sprung *et al*., 2009; Craven *et al*., 2013). Sprung *et al*. (2009) also assessed the effect of storage time/block age on FFPE colon adenoma tissue samples (stored for 1, 3, 5, or 10 years), using isoelectric focusing to fractionate peptides before LC-MS/MS analysis. They found no significant difference between the numbers of proteins identified for each block age and concluded that long-term storage of FFPE colon adenoma tissues did not compromise the samples. In general, the proteome coverage reported here (for all the block ages and sample preparation methods) falls within the range of several other studies of proteomic analysis of FFPE tissue (Sprung *et al*., 2009; Fu *et al*., 2013; Gámez-Pozo *et al*., 2013; Bronsert *et al*., 2014), with higher identification numbers reported by other studies (Craven *et al*., 2013; Wiśniewski *et al*., 2011; Wiśniewski *et al*., 2012; Wiśniewski *et al*., 2013). Table 9 shows known proteins that are deregulated in colon cancer that were also identified in the data. The % occurrence of these proteins within each group of 17 patients per experimental condition was calculated and shows that there are no observable differences due to block age. However, the DRP method shows overall higher % occurrence of these protein biomarkers, compared to the other sample preparation methods.

Table 9. Known proteins deregulated in colon cancer.

Main Accession:	Gene name:	Protein name:	MW (kDa):	Comments:	% Occurrence within 17 patient samples								
					APFAR:			DRP:			HILIC:		
					1 year old:	5 year old:	10 year old:	1 year old:	5 year old:	10 year old:	1 year old:	5 year old:	10 year old:
O95994	AGR2	Anterior gradient protein 2 homologue	19.97	Downregulated in CRC (Lee *et al.*, 2006)	88	100	94	94	100	94	100	94	100
Q13951	CBFB	Core-binding factor subunit beta	21.49	Frequently overexpressed in CRC (Andersen *et al.*, 2009)	12	41	24	35	35	47	0	12	6
P08174	CD55; DAF	Complement decay-accelerating factor	41.37	Upregulated in CRC (Mikesch *et al.*, 2006)	0	0	6	0	0	0	0	0	0
P10645	CHGA	Chromogranin-A	50.66	Downregulated in CRC (Helman *et al.*, 1988)	29	29	18	18	18	18	24	18	18
A8K7I4	CLCA1	Calcium-activated chloride channel regulator 1	100.16	Regulator of calcium channels, frequently downregulated in CRC (Bustin *et al.*, 2001)	59	53	41	59	59	47	53	53	47
Q96KP4	CNDP2	Cytosolic non-specific dipeptidase	52.84	Overexpressed in CRC (Toiyama *et al.*, 2011)	82	88	94	100	88	100	94	94	100
P07148	FABP1	FABP1 protein	14.20	Downregulated in CRC (Lee *et al.*, 2006)	100	100	71	94	100	88	94	100	88
Q9Y6R7	FCGBP	IgGFc-binding protein	571.64	Downregulated in CRC (Lee *et al.*, 2006)	76	94	82	76	94	76	82	88	82
P56470	LGALS4	Galectin-4	35.92	Downregulated in CRC (Lee *et al.*, 2006)	100	100	100	100	100	100	94	100	100
P09429	HMGB1	High mobility group protein B1	24.88	Overexpression in CRC correlates with poor prognosis (Yao *et al.*, 2010)	76	88	76	100	100	94	94	82	94
P01042	KNG1	Kininogen-1	71.91	Frequently overexpressed in CRC (Quesada-Calvo *et al.*, 2017)	29	41	53	53	59	82	29	47	65
Q9UHB6	LIMA1	LIM domain and actin-binding protein 1	85.17	Downregulated in CRC (Lee *et al.*, 2006)	0	0	6	0	0	24	6	6	0
P15941	MUC-1	Mucin-1	122.03	Frequently overexpressed in CRC, marker of poor prognosis (Li *et al.*, 2001)	0	6	12	6	6	12	0	6	6
Q02817	MUC-2	Mucin-2	539.96	Downregulation correlates with proliferation markers and with poor prognosis (Ogata *et al.*, 1992; Li *et al.*, 2001)	59	59	76	71	65	71	65	71	76
P06748	NPM1	Nucleophosmin	32.55	Protein involved in carcinogenesis, overexpressed in CRC (Nozawa *et al.*, 1996; Yung, 2007)	100	100	100	100	100	100	100	100	100
Q6UX06	OLFM4	Olfactomedin-4	57.24	Protein overexpressed in CRC (Quesada-Calvo *et al.*, 2017)	29	18	29	35	24	29	29	24	29
Q9Y617	PSAT1	Phosphoserine aminotransferase	40.40	Upregulated in CRC (Vie *et al.*, 2008)	0	0	6	18	12	12	18	12	18
P53992	Sec24C	Protein transport protein Sec24C	118.25	Overexpressed in early CRC stages, while downregulated in advanced CRC stages (Quesada-Calvo *et al.*, 2017)	0	0	0	0	6	6	6	0	0
P36952	SERPIN B5	Serpin B5	42.07	Upregulated in CRC (Zheng *et al.*, 2007)	29	6	29	35	6	29	29	6	29
P10599	TXN	Thioredoxin	11.73	Frequently overexpressed in CRC (Powis *et al.*, 2000)	94	100	100	94	100	100	94	94	94

4.3.3 The effect of block age and sample preparation methods on peptide-level reproducibility

The qualitative reproducibility for each sample and experimental condition was also measured in terms of peptide identification overlap (Fig. 27), calculated from the peptide sequences identified in each sample and experimental condition, irrespective of peptide abundance.

Figure 27 A illustrates that the APFAR method showed the highest peptide overlap/common peptides (46.5%) between samples of different block ages. This was followed by the HILIC method, with 45.4% peptide overlap, and the lowest peptide overlap was seen for the DRP method at 43%. Overall, there was no significant difference between uniquely identified peptides of the different block ages (ranging from 11.3% to 13.2%) for the APFAR and HILIC methods. However, the 1-year-old blocks processed with the DRP method had the highest percentage of uniquely identified peptides at 20.4%.

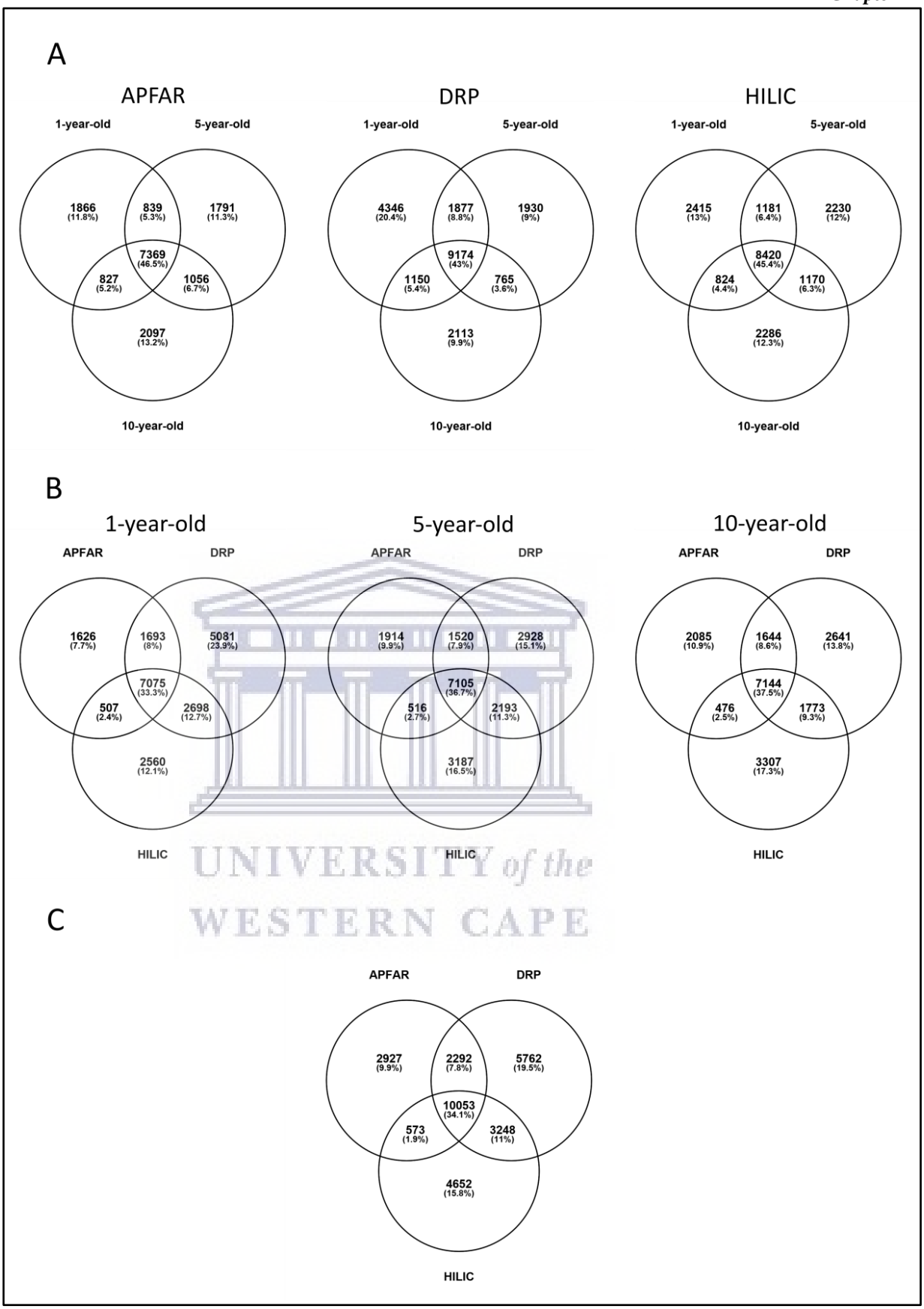

Figure 27. Comparison of the qualitative reproducibility of the experimental conditions in terms of peptide identification overlap for block ages and sample preparation methods. (A) Venn diagrams depicting the distribution of identified peptides for 1, 5 and 10-year-old blocks within each sample preparation method (B) Venn diagrams depicting the distribution of identified peptides for each sample preparation method within each block age (C) Venn diagrams showing the overlap of combined identified peptides (of all block ages) for each sample preparation method.

The shared peptides for each sample preparation method within a specific block age are shown in Figure 27 B. The 10-year-old blocks showed the highest peptide overlap/common peptides (37.5%) between the different sample preparation methods. This was followed by the 5-year-old blocks, with 36.7% peptide overlap, and the lowest peptide overlap was seen for the 1-year-old blocks at 33.3%. This could be due, in part, to similar proteins extracted from the older blocks (since formaldehyde-induced cross-linking continues with time), compared to more diverse sets of proteins extracted from the more recently preserved 1-year-old blocks (Lemaire *et al*., 2007). Due to the continuation and extent of formaldehyde-induced protein cross-linking with time, the extraction of full-length proteins from older FFPE blocks is also more difficult. In addition, Paine *et al*. (2018) were able to identify small proteins, without antigen retrieval and enzymatic digestion steps, via mass spectrometry imaging. They hypothesise that not all proteins, especially small proteins (with short amino acid sequences and low lysine content), react with formaldehyde to the same extent. However, larger proteins (with longer amino acid sequences and greater lysine content) were more challenging to detect via mass spectrometry, and therefore have a greater probability of being more extensively crosslinked by formaldehyde. On average, for all block ages and sample preparation methods, the identified proteins were in the range of 40 – 60 kDa (data not shown). This therefore indicates that mostly low and medium molecular weight proteins were extracted from the FFPE tissues at all block ages.

Figure 27 C shows that, when all the identified peptides for each block age is combined within a sample preparation method, there is 34.1% overlapping peptides shared between the different methods. The DRP method had the highest percentage of uniquely identified peptides at 19.5%, followed by the HILIC method, with 15.8% unique peptides, and the lowest uniquely identified peptides was seen for the APFAR method at 9.9%.

4.3.4 Physicochemical properties of extracted and processed peptides for all block ages

The effect of archival time/block age as well as sample preparation method protein selection/enrichment bias was assessed with regards to peptide sequence

physicochemical properties in figure 28, which illustrates the peptide distribution according to hydropathicity, molecular weight and isoelectric point (pI). Kruskal–Wallis tests were conducted to determine if there were significant differences between experimental conditions (Appendix D Supplementary table 2).

Overall, a comparison of the majority (upper and lower quartiles) of all peptides of all experimental conditions shows that they share similar hydropathicity scales (Fig. 28 A). There is a significant difference ($p < 0.0001$) between the hydropathicity of peptides generated in all experimental conditions, however, the average relative hydropathicity of all the samples are negative (below zero), which indicates that the majority of peptides that were extracted and processed, by all three sample preparation methods and across all block ages are hydrophilic (Kyte & Doolittle, 1982; Farias *et al*., 2010).

Figure 28 B indicates that the molecular weight ranges of identified peptides are relatively constant across all samples and experimental conditions, with the majority >1000 Da and <2000 Da. There is a significant difference ($p < 0.0001$) between the molecular weights of peptides generated via the different sample preparation methods for 1, 5 and 10-year old blocks. With regards to block age differences, there is no significant difference ($p = 0.26$) between the molecular weights of peptides generated via the DRP method, however there is a significant difference ($p < 0.05$) between the molecular weights of peptides generated using the APFAR and/or HILIC methods.

There is a significant difference ($p < 0.0001$) between the pI ranges of peptides generated in all experimental conditions, however, the pI range values are relatively similar across all samples and experimental conditions, with the majority above pI 4 and below pI 7 (Fig. 28 C). These results are in accordance with previous studies that used the APFAR and HILIC methods (Doucette *et al*., 2014; Hughes *et al*., 2014; Kachuk *et al*., 2015; Moggridge *et al*., 2018).

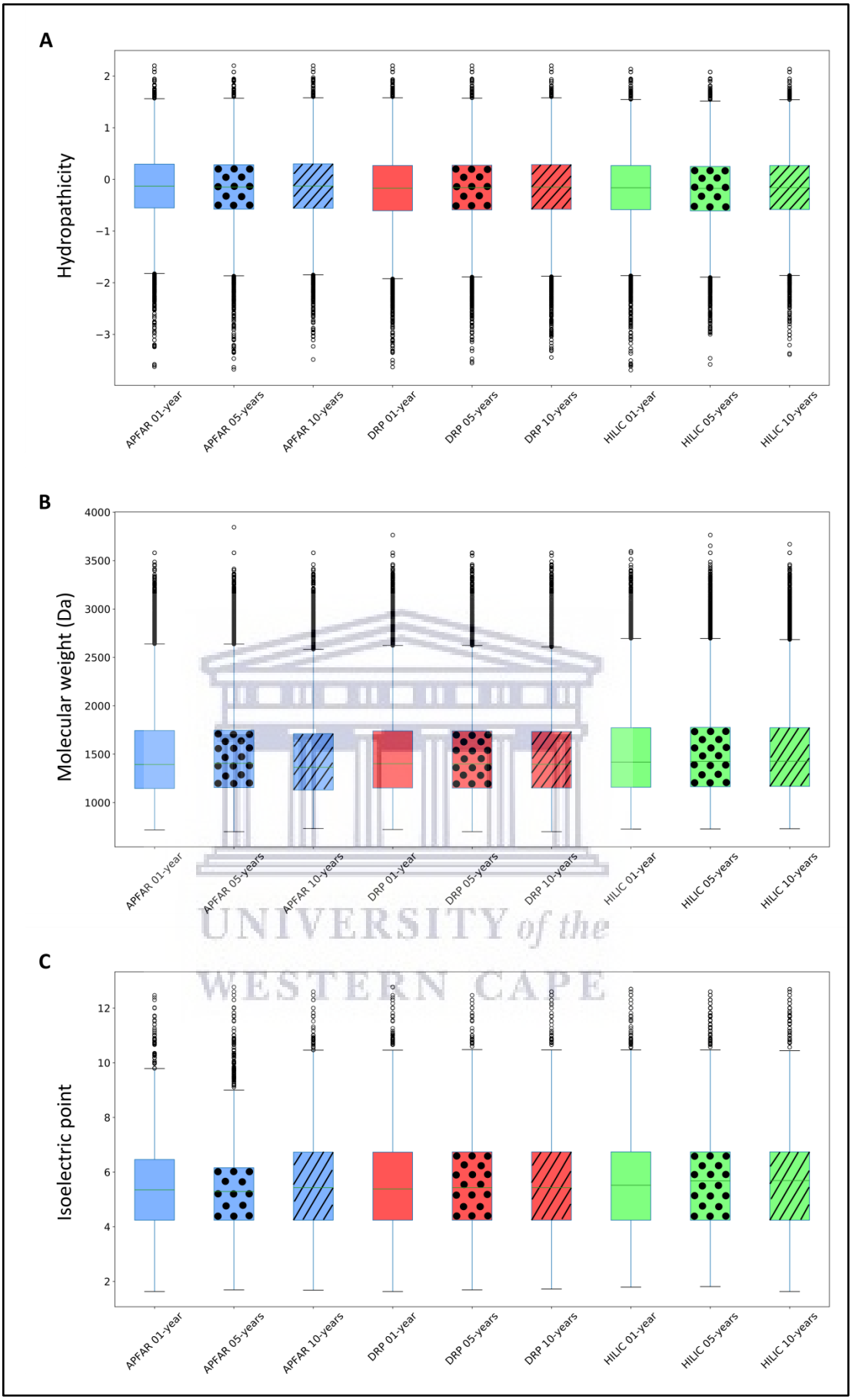

Figure 28. Physicochemical properties of identified peptides for all experimental conditions. (A) Hydropathicity based on GRAVY scoring matrix, *n* = 17 for each boxplot, (B) Molecular weight (MW), *n* = 17 for each boxplot, (C) Isoelectric point (pI), *n* = 17 for each boxplot. Blue boxplots refer to APFAR samples; Red boxplots refer to DRP samples; Green boxplots refer to HILIC samples. For all boxplots, 5-year-old samples are represented by dots; 10-year-old samples are represented by diagonal lines.

4.3.5 The effect of block age and sample preparation methods on protein-level reproducibility

The quantitative reproducibility between experimental conditions were expressed as PCC dot plots (Fig. 29 and Fig. 30), which were calculated based on the NSAF abundance values for common/shared identified proteins in each sample and experimental condition. PCA plots were also generated from this data to assess the variance between block ages and the sample preparation methods (Fig. 31).

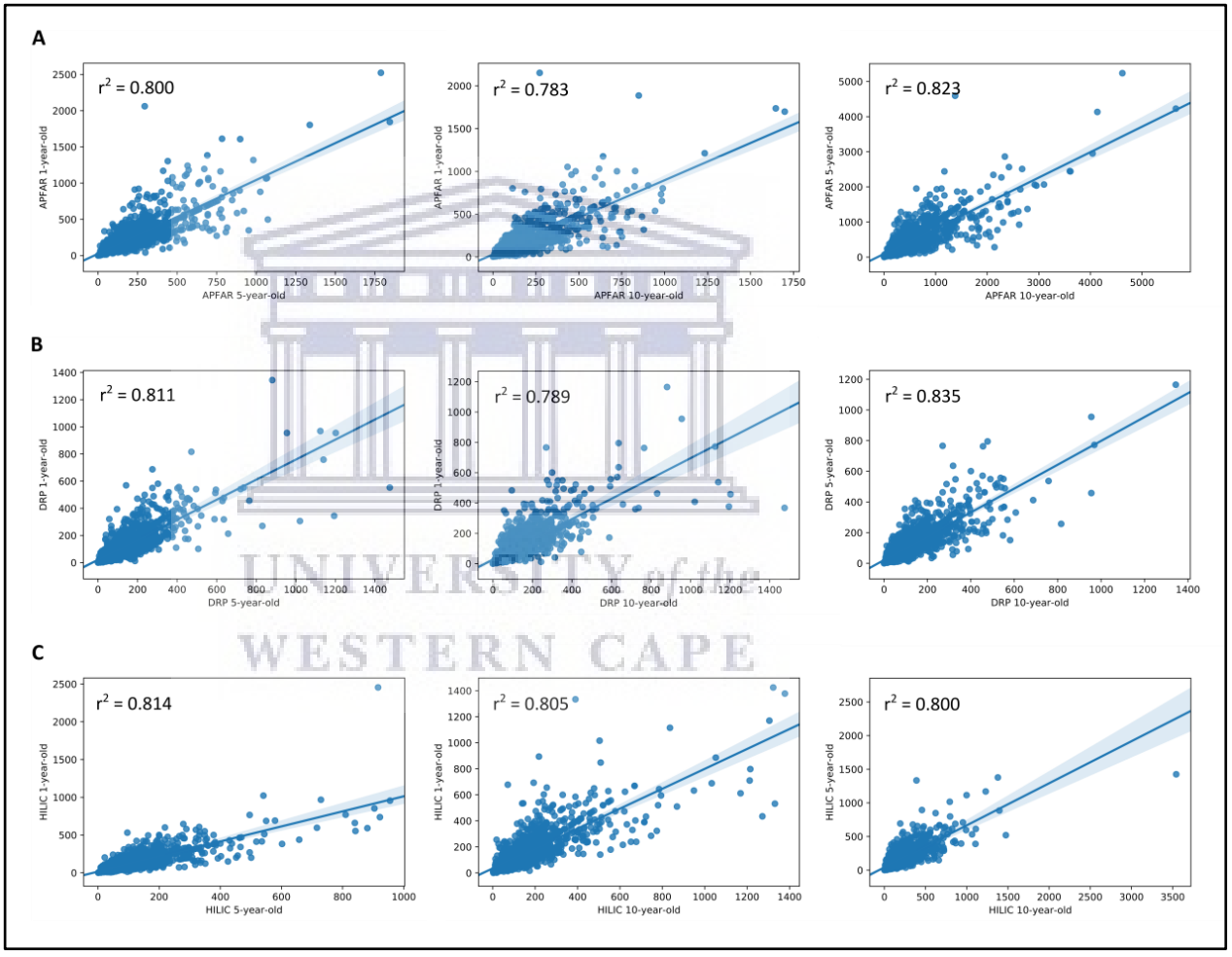

Figure 29 . Correlation of protein abundance between all block ages for each patient sample. (A) Correlation of protein abundance for all APFAR processed samples for all block ages (1, 5 and 10-year old blocks) (B) Correlation of protein abundance for all DRP processed samples for all block ages (1, 5 and 10-year old blocks) (C) Correlation of protein abundance for all HILIC processed samples for all block ages (1, 5 and 10-year old blocks). The Pearson correlation coefficients (r^2) are indicated on each plot and plot axes values are the normalised NSAF values for proteins present in both condition compared per plot.

Fig. 29 shows the correlation of protein abundance for all block ages for each sample preparation method. This demonstrates that, for the APFAR and DRP methods, there were greater proteome composition correlation between the 5 and 10-year-old blocks (PCC values of 0.823 and 0.835, respectively), compared to the correlation between their other block age samples (PCC values ranging between 0.783 and 0.811), as well as the 5 and 10-year-old blocks processed via the HILIC method (PCC value of 0.800). The HILIC method yielded comparable relative protein abundances for all block ages, with PCC values of 0.814 for 1 and 5-year-old blocks, 0.805 for 1 and 10-year-old blocks, and 0.800 for 5 and 10-year-old blocks. For the APFAR and DRP methods, proteome composition correlation was lowest between 1 and 10-year-old blocks (PCC values of 0.783 and 0.789, respectively), compared to 1 and 5-year-old blocks (PCC values of 0.800 and 0.811, respectively) and 5 and 10-year-old blocks (PCC values of 0.823 and 0.835, respectively).

These results indicate that block age may introduce an observable bias with regard to proteome composition, depending on the sample processing method used for LC-MS/MS analysis. This bias is also more pronounced for older blocks processed via the APFAR and DRP methods. Craven *et al*. (2013) found overall higher proteome composition correlation between approximately 1-year-old and 10-year-old normal FFPE kidney tissue (PCC value of 0.954) and FFPE renal cell carcinoma tissue (PCC values of 0.885).

Fig. 30 shows the correlation of protein abundance for all sample preparation methods for each block age. This illustrates that, for 1-year-old blocks, the DRP and HILIC methods yielded comparable relative protein abundances (PCC value of 0.863), whereas proteome composition correlation was lower for the AFFAR and DRP (PCC value of 0.755) as well as APFAR and HILIC (PCC value of 0.789) methods. Overall, the 5 and 10-year-old blocks show similar proteome composition correlation between the sample preparation methods.

For 5-year-old blocks, the PCC values for the APFAR and HILIC, as well as DRP and HILIC methods are approximately equal, 0.838 and 0.839, respectively. The APFAR and DRP method has a higher PCC value of 0.859, indicating slightly higher correlation in proteome composition between these two sample preparation methods.

For 10-year-old blocks, the PCC values for the APFAR and DRP as well as DRP and HILIC methods were the same. The APFAR and HILIC method has a lower PCC value of 0.804, indicating slightly lower correlation in proteome composition between these two sample preparation methods. These results indicate that sample processing with the different methods introduces an observable bias with regard to proteome composition. This bias is also more pronounced for 1-year-old blocks, compared to older blocks.

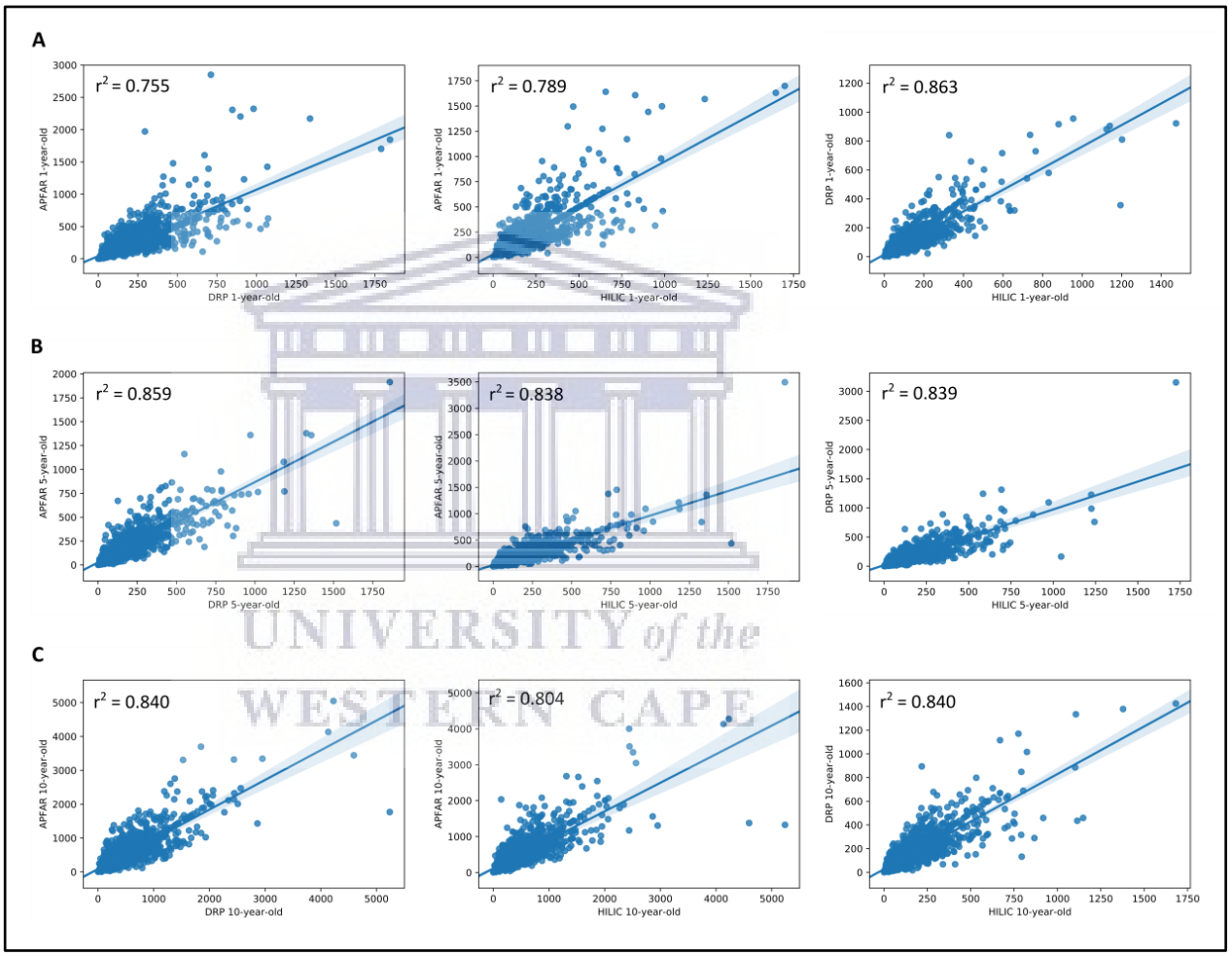

Figure 30. Correlation of protein abundance between all sample preparation methods for each patient sample. (A) Correlation of protein abundance for all sample preparation methods for 1-year-old blocks/samples (B) Correlation of protein abundance for all sample preparation methods for 5-year-old blocks/samples (C) Correlation of protein abundance for all sample preparation methods for 10-year-old blocks/samples. The Pearson correlation coefficients (r^2) are indicated on each plot and plot axes values are the normalised NSAF values for proteins present in both condition compared per plot.

PCA plots showing clusters of samples, based on their similarities, were generated for all block ages and sample preparation methods (Fig. 31). The samples that have similar expression profiles are clustered together. Figures 31 A – B show the clustering of different block ages (1, 5 and 10 years) for each sample preparation method, with the DRP method having the lowest variance (10.73%) between block ages, followed by the HILIC method (13.68%), and the APFAR method, which has the highest variance at 14.57%.

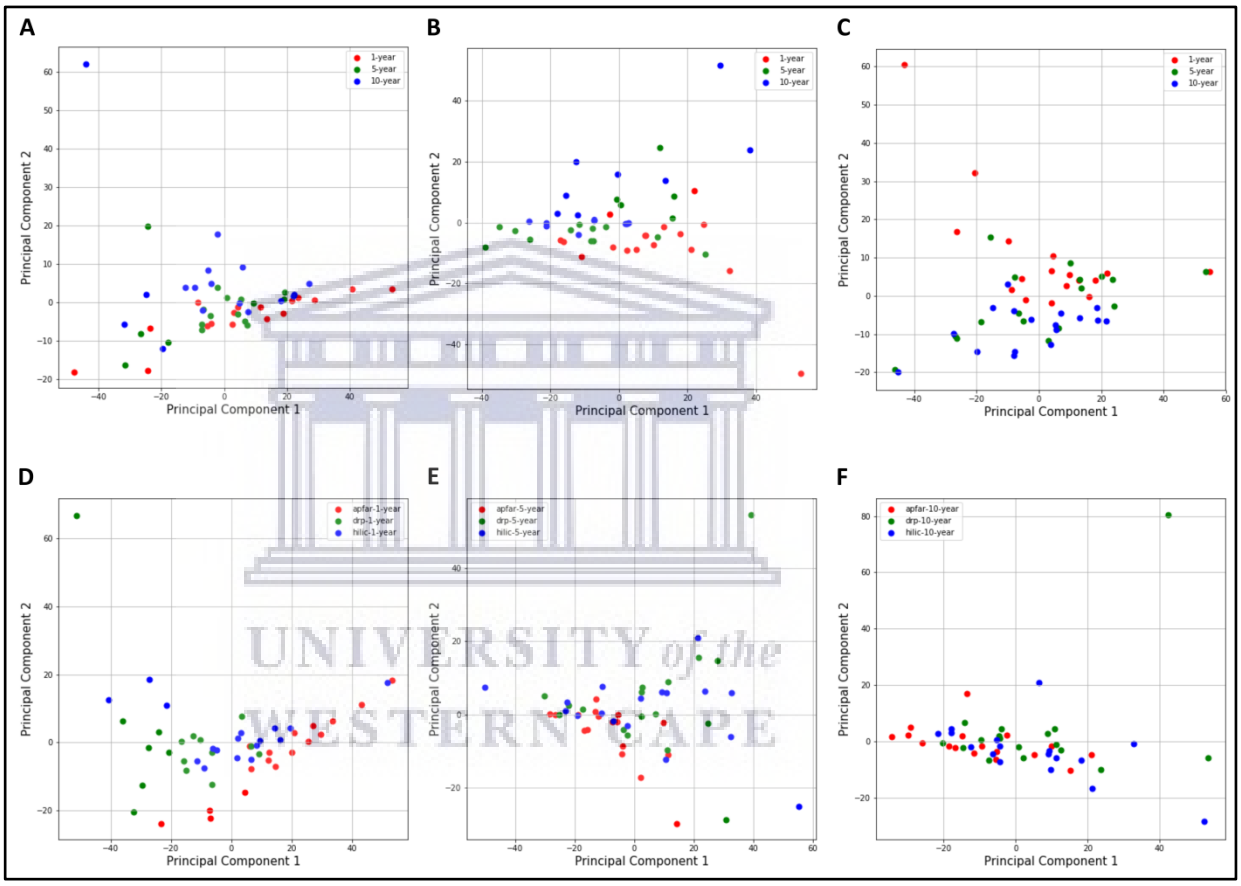

Figure 31. PCA plots for all block ages and sample preparation methods. The NSAF values for proteins identified from each patient case were normalised and dimensionality reduced by principal component analysis of the datasets. (A) PCA plot of all block age (1-year-old = red; 5-year-old = green; 10-year-old = blue) samples processed via the APFAR method, (B) PCA plot of all block age (1-year-old = red; 5-year-old = green; 10-year-old = blue) samples processed via the DRP method, (C) PCA plot of all block age (1-year-old = red; 5-year-old = green; 10-year-old = blue) samples processed via the HILIC method, (D) PCA plot of 1-year-old samples for all sample preparation methods (APFAR = red; DRP = green; HILIC = blue), (E) PCA plot of 5-year-old samples for all sample preparation methods (APFAR = red; DRP = green; HILIC = blue), (F) PCA plot of 10-year-old samples for all sample preparation methods (APFAR = red; DRP = green; HILIC = blue).

For the sample preparation methods (Figures 31 D – F), the 10-year-old blocks/samples shows the lowest variance between the different methods (11.4%), followed by the 5-year-old blocks/samples. This could be due, in part, to similar proteins extracted from the older blocks because the formaldehyde-induced protein cross-linking process is continual and becomes more extensive with time (as discussed in section 4.3.3). The 1-year-old blocks/samples (Fig. 31 D) shows the highest variance (15.86%) between the different methods.

4.3.6 GO analysis of identified proteins

The effect of storage time/block age as well as the sample preparation methods' protein selection biases were assessed with regards to the main biological processes and cellular components present within the identified proteins, using Gene Ontology (GO) annotation. The distribution of the percentages of proteins belonging to each GO term was plotted for GO terms that occurred at >15% frequency for all samples and experimental conditions (Fig. 32).

Overall, similar GO profiles were obtained for all samples, therefore only the GO terms that showed some observable difference between experimental conditions were plotted. Figure 32 A shows the percentage frequency at which the identified proteins (of all experimental conditions) occurs for each of the plotted GO terms for biological processes, and Fig. 32 B shows GO terms for cellular components. The lack of observable differences in GO term frequency between the different block ages and sample preparation methods indicate that neither had an observable protein-selection bias. Therefore all block ages and sample preparation methods used in this study demonstrate more or less equivalent usability for proteomic analysis.

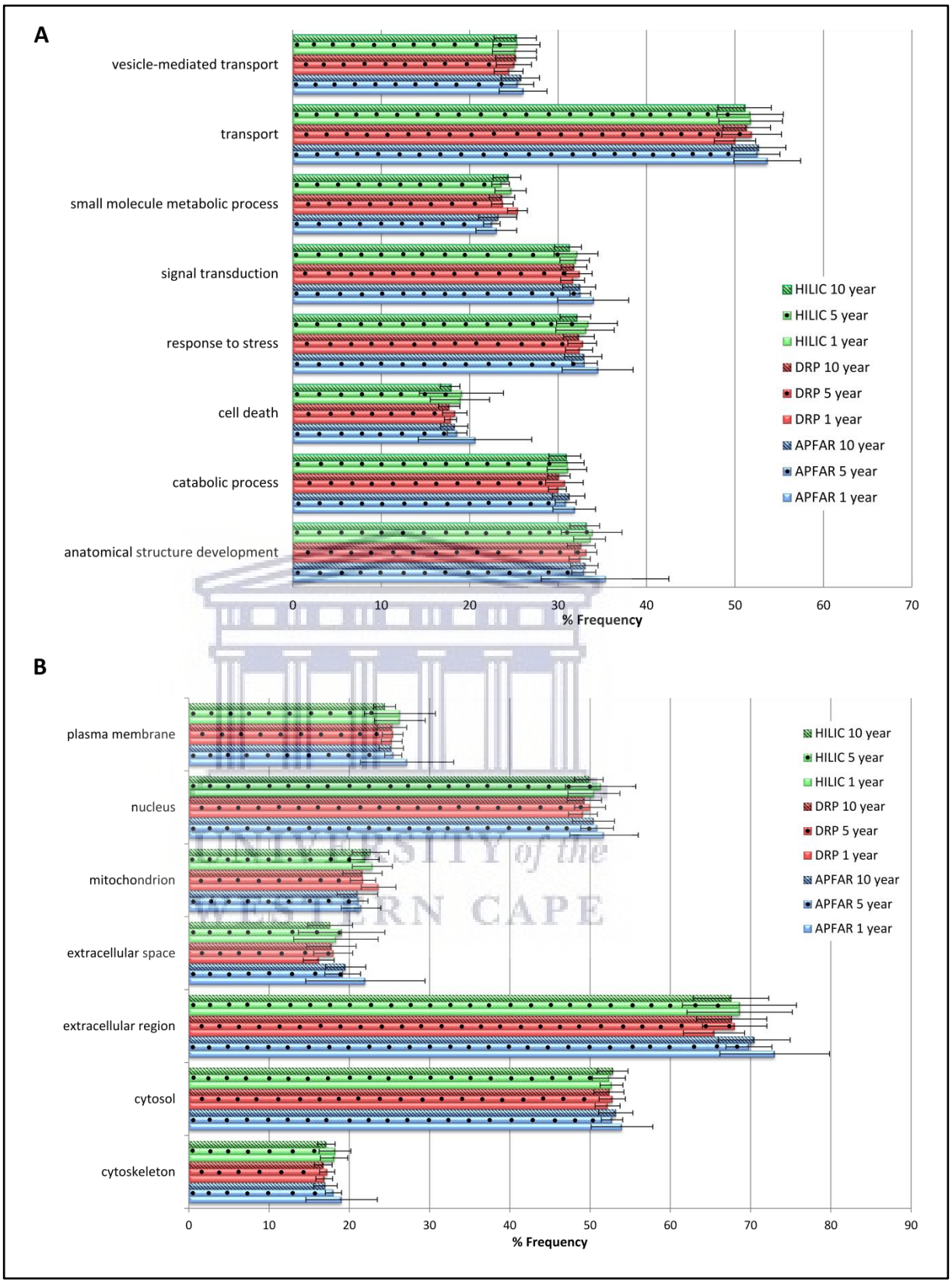

Figure 32. Gene Ontology annotation profiles for proteins identified from all block ages and sample preparation methods. (A) GO profiles according to biological processes, (B) GO profiles according to cellular components. The average proportions for all 17 patients per condition are shown with error bars indicating the standard deviation. Blue bars refer to APFAR samples; Red bars refer to DRP samples; Green bars refer to HILIC samples. For all samples, 5-year-old samples are represented by dots; 10-year-old samples are represented by diagonal lines.

4.3.7 Assessment of the digestion efficiency of the sample preparation methods for all block ages

To assess the reproducibility and digestion efficiency of the different sample preparation methods, the percentages of missed cleavages across all samples were analysed (Fig. 33). To successfully analyse FFPE tissues requires overcoming the issue of the formaldehyde cross-linking between molecules (Magdeldin & Yamamoto, 2012; Fowler *et al*., 2013; Avaritt *et al*., 2014; Gustafsson *et al*., 2015). The most important aspect to take into consideration for accurate protein extraction from FFPE tissues is the cleavage of these methylene bridges to allow for proper trypsin digestion. The methylene bridges prevent trypsin from reaching its cleavage sites. If the methylene bridges are not adequately cleaved, it will result in improperly digested, cross-linked peptides that will not produce correct MS results. Therefore, the effect of storage time/block age on trypsin digestion efficiency was also determined by comparing the percentage of missed cleavages across all block ages.

Fig. 33 shows that overall, all sample preparation methods and all block ages generated low numbers of missed cleavages. The APFAR method (Fig. 33 A) generated the lowest percentages of missed cleavages with ≥85% of all peptides for 1-year-old samples having no missed cleavages, and ≥90% of all peptides for 5 and 10-year-old samples having no missed cleavages. This was followed by the DRP method (Fig. 33 B), with ≥85% of all peptides (except for sample number DRP-9) for 1-year-old samples having no missed cleavages, and ≥85% of all peptides for 5 and 10-year-old samples having no missed cleavages (except for sample number DRP-34 of the 5-year-old cohort). The HILIC method (Fig. 33 C) had overall lower digestion efficiency with ≥80% of all peptides for 1 and 5-year-old samples having no missed cleavages, and ≥80% of all peptides for 10-year-old samples having no missed cleavages (except for samples HILIC-37 and HILIC-41).

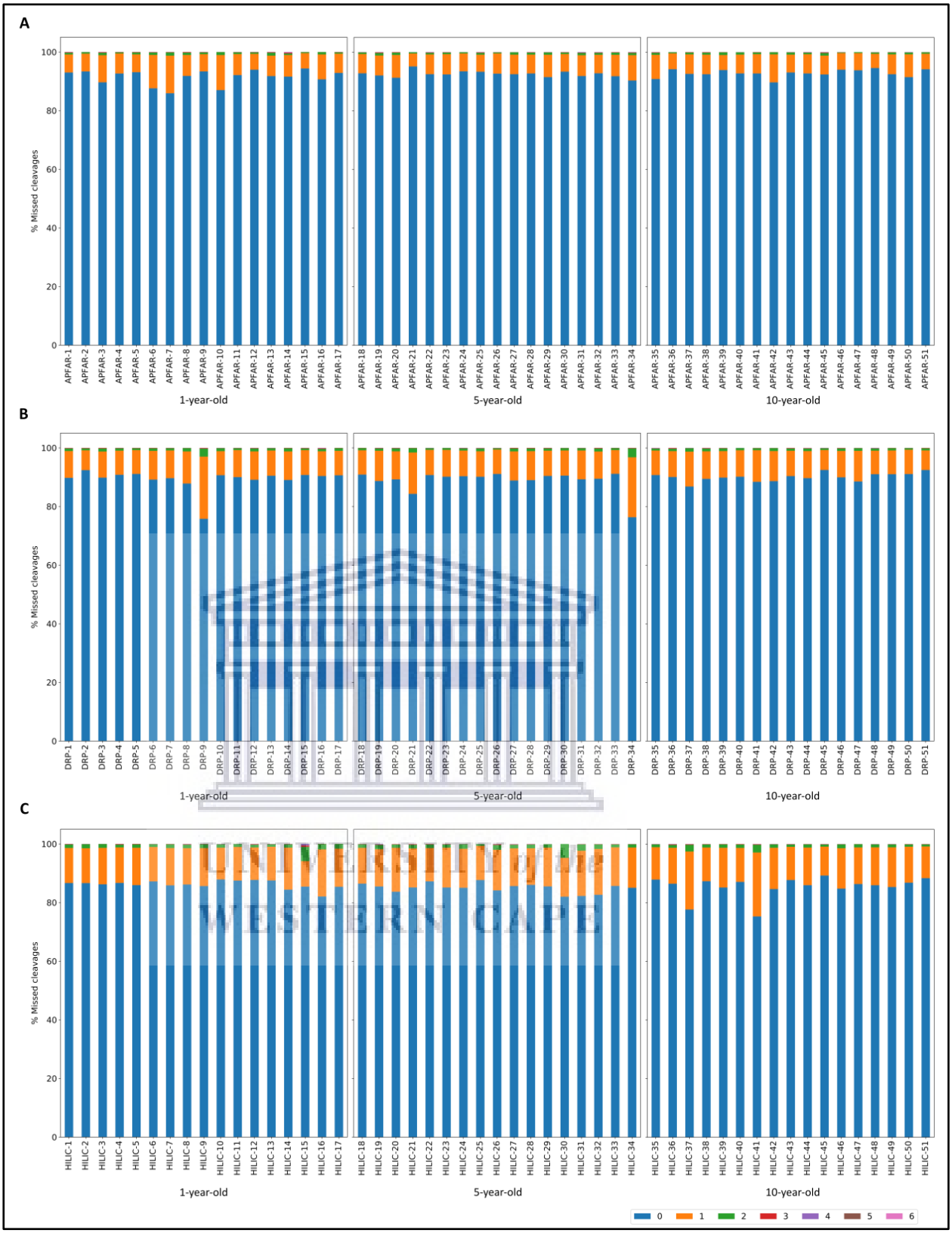

Figure 33. The numbers of missed cleavages for all block ages and sample preparation methods. For each sample preparation method and block age, the percentages of missed cleavages are plotted. (A) APFAR 1, 5 and 10-year-old blocks (B) DRP 1, 5 and 10-year-old blocks (C) HILIC 1, 5 and 10-year-old blocks. The figure key in the bottom right corner shows the graph colours for corresponding number of missed cleavages, with 0 missed cleavages = blue, 1 missed cleavage = orange, 2 missed cleavages = green, etc.

The sample preparation methods' digestion efficiency therefore does not appear to be only affected by the age of the sample, since older and newer blocks gave varying results depending on the processing method used. Sprung *et al*. (2009) found that after deparaffinisation and rehydration, cross-linked proteins are efficiently digested with trypsin, without the need for additional specialised reagents, even under mild conditions typically used for fresh tissues. This is also observed here, since all block ages and sample preparation methods used demonstrate sufficient trypsin activity/cleavage efficiency, with all samples showing low levels of missed cleavages. Generally, the percentage of missed cleavages of the present study was in the range of several other recent reports (Batth *et al*., 2018; Hughes *et al*., 2018; Moggridge *et al*., 2018), with lower percentage of missed cleavages reported in Kachuk *et al*. (2015).

4.3.8 Effects of block age and sample preparation methods on sample proteome integrity

The oxidation of methionine is a major protein modification, which converts methionine to methionine sulfoxide, and targets the affected protein for degradation, both *in vivo* and *in vitro* (Liu *et al*., 2013). Methionine oxidation is linked to processes relating to aging and pathology (*in vivo*) as well as *in vitro* conditions caused by protein purification, storage, light exposure, and exposure to free radicals generated in the presence of metals during LC-MS/MS analysis (Liu *et al*., 2013). To determine the impact of long-term storage, the percentage of peptides containing methionine oxidation (out of the total number of peptides identified) was calculated for all block ages and sample preparation methods (Fig. 34).

Kruskal–Wallis tests were conducted to determine if the percentage of peptides containing methionine oxidation were significantly different between block ages for each sample preparation method (Appendix D Supplementary table 2). No significant differences were found between 1, 5 and 10-year old blocks/samples processed via the APFAR ($H(2) = 1.23$, $p = 0.54$), DRP ($H(2) = 0.86$, $p = 0.65$), or HILIC ($H(2) = 3.38$, $p = 0.18$) methods. Fig. 34 shows that for the 10-year-old blocks/samples the percentage of peptides with methionine oxidation are 8.77 ± 3.41%, 7.77 ± 2.41%, and 5.47 ± 2.13%, for APFAR, DRP and HILIC respectively. Similar percentages of

peptides with methionine oxidation (7.65 ± 2.05% and 7.38 ± 2.15%) are observed for 1 and 5-year-old blocks/samples processed via the APFAR method. The same is seen for 1 and 5-year-old blocks/samples processed via the DRP method (7.24 ± 2.11% and 6.83 ± 1.69%). The HILIC method has lower percentages of peptides with methionine oxidation for all block ages, with 4.34 ± 1.36%, 4.43 ± 1.16% and 5.47 ± 2.13%, for 1, 5 and 10-year-old blocks/samples respectively. Therefore, the choice of sample preparation/protein purification method may contribute to methionine oxidation artefacts (Liu *et al*., 2013). Zhang *et al*. (2012) found that methionine oxidation increases during enzymatic digestion, with the presence of residual metals in the digestion buffer, sample contact with metal surfaces, as well as chromatography separation.

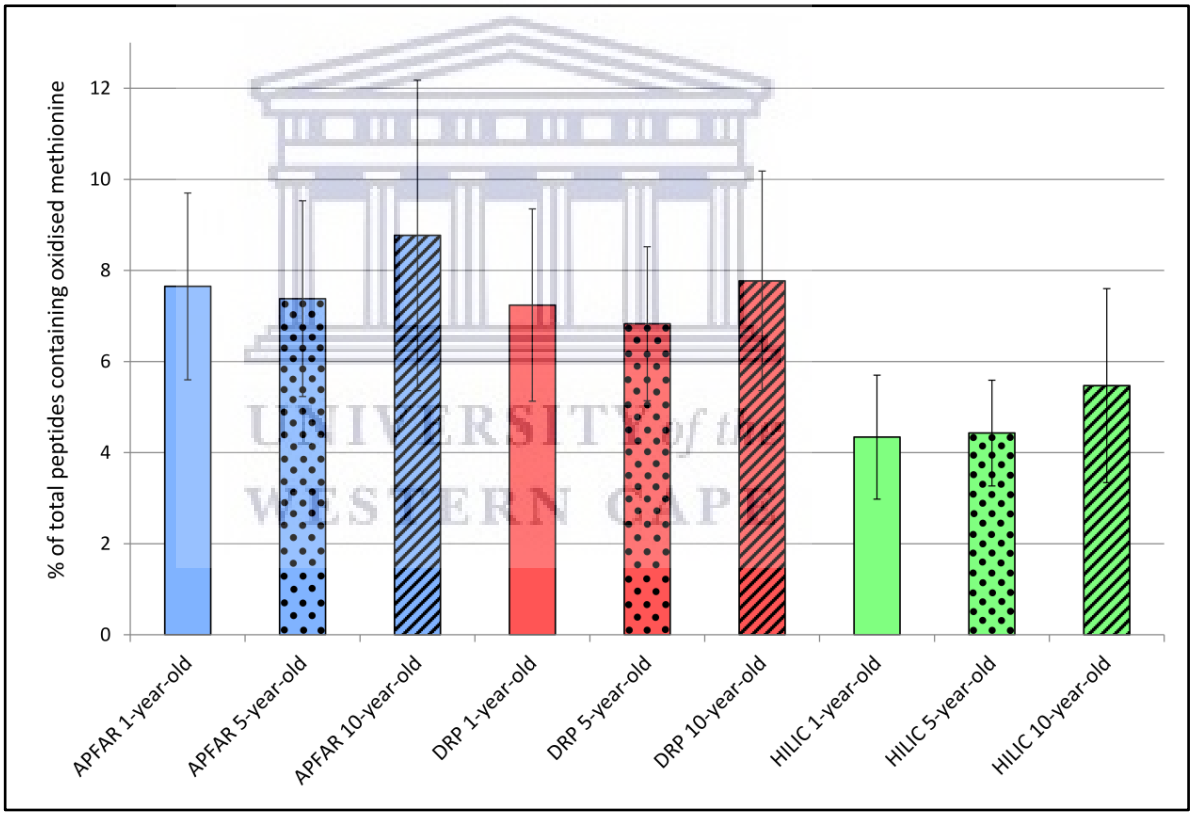

Figure 34. Percentages of peptides containing oxidised methionine for all block ages and sample preparation methods. The percentages of peptides containing oxidised methionine, relative to the total number of identified peptides, were calculated for each patient sample analysed (n = 17, p > 0.05 for all) per block age and sample preparation method, and the averages plotted here. Error bars refer to the standard deviation. Blue bars refer to APFAR samples; Red bars refer to DRP samples; Green bars refer to HILIC samples. For all bars, 5-year-old samples are represented by dots; 10-year-old samples are represented by diagonal lines.

The SP3/HILIC method's results are in agreement with results reported by Bronsert *et al*. (2014) for newly preserved (<1-year-old) FFPE samples (processed using acetone precipitation and sodium hydroxide resolubilisation for protein purification), which had methionine oxidation ratios of 3.9 – 4.5% for all identified peptides. In contrast, Sprung *et al*. (2009) reported higher methionine oxidation levels and found that archived colon adenoma tissues displayed an increase in methionine oxidation with block age - from 16.8% after one year of storage, 18.2% for 5-year-old samples up to 25.2% after 10 years of storage.

4.4 Conclusions

Archived FFPE tissue repositories are precious sources of clinical material, often stored for decades, for clinical proteomic studies. Since these preserved blocks may be conveniently stored at ambient temperatures, it makes them easily accessible and cost effective. However, standardised protocols for the proteomic analysis of FFPE tissues have not been determined yet. In addition, the effect of block age and storage at resource-limited institutions, on protein quality remains unclear. We have demonstrated (using FFPE human colorectal cancer resection tissue) that, overall, block age mainly affects protein yields during the protein extraction phase. Therefore greater amounts of starting material are required for older blocks prior to LC-MS/MS analysis. Analysed samples' peptide and protein identifications mainly differed according to the protein purification method used and not block age, which mainly impacted on tissue proteome composition.

This study is also of particular relevance, since it assessed the performance of different protein purification techniques on tissues derived from samples stored over a long period of time (1 to 10 years). The different methods show differences in the number of peptides and proteins identified and sample proteome composition, differences in reproducibility in terms of peptide identification overlap, PCA variance, as well as protocol digestion efficiency. Overall, the DRP and SP3/HILIC methods performed the best, with the SP3/HILIC method requiring less protein than the other methods, therefore making it the most sensitive and efficient protein purification method tested here.

These results are encouraging since they indicate that long-term storage of FFPE tissues does not significantly interfere with retrospective proteomic analysis. In addition, variations in pre-analytical factors (spanning a decade), such as tissue harvesting, handling, the fixation protocol used as well as storage conditions, does not affect protein extraction and shotgun proteomic analysis to a significant extent.

Chapter 5: Conclusions and recommendations

5.1 Key findings and future recommendations

FFPE tissue archives are valuable sources of clinical material for clinical proteomic studies (Fowler *et al*., 2013; Avaritt *et al*., 2014; Bronsert *et al*., 2014; Gustafsson *et al*., 2015). These preserved blocks may be conveniently stored for decades, at ambient temperatures, and are easily accessible and cost effective. In addition, they are accompanied by patient records and metadata, which may facilitate and enhance clinical studies (Fowler *et al*., 2013; Avaritt *et al*., 2014; Bronsert *et al*., 2014; Gustafsson *et al*., 2015). However, standardised analytical protocols, such as protein extraction, digestion and sample purification for proteomic analysis of FFPE tissues have not been determined yet. In addition, the impact of block age and storage at resource-limited institutions, on protein quantity/quality remains unclear.

Protein yields from this study were within the ranges of previously reported values for FFPE tissue (Sprung *et al*., 2009; Rodríguez-Rigueiro *et al*., 2011; Wolff *et al*., 2011). Here it was demonstrated that the addition of 0.5% (w/v) PEG 20,000 to protein extraction buffer (for protein extraction from FFPE human colorectal carcinoma resection tissue) impacted on MS analysis and resulted in overall lower peptide and protein identifications, compared to buffer without the addition of PEG. In addition, protein samples extracted without PEG showed higher reproducibility. The analysis of the sample pellets also showed that the protein extraction buffer was efficient enough to extract the majority of proteins. Therefore, by building on from previous studies, which found that higher protein concentrations (>10 µg) (of FFPE animal tissues and human cells) compromise the function of PEG (Wiśniewski *et al*., 2011; Shen *et al*., 2015), it was also demonstrated here that this effect is also observed in FFPE human colon tissue.

Using FFPE human colorectal carcinoma resection tissue, stored for approximately 1, 5 and 10 years, it was found that block age mainly affects protein yields during the protein extraction phase. Therefore, it is advised to use greater amounts of starting material/tissue during the protein extraction phase for older blocks. In addition,

changes in tissue proteome composition were also found between newer and older blocks, therefore this should also be considered when performing MS-based proteomic analysis on FFPE samples.

This study is also of particular relevance, since it assessed the performance of different sample preparation techniques for shotgun MS analysis of FFPE tissues stored for up to a decade. The different methods demonstrated differences in the number of peptides and proteins identified and tissue proteome composition, differences in reproducibility in terms of peptide identification overlap, PCA variance, as well as protocol digestion efficiency. The DRP and HILIC sample preparation methods performed the best overall and indicates that long-term storage of FFPE tissues do not significantly interfere with retrospective MS-based proteomic analysis. This is also encouraging since it shows that variations in pre-analytical factors, spanning a decade, (including tissue harvesting, handling, fixation protocol used as well as storage time and conditions) does not significantly affect shotgun MS-based proteomic analysis of older FFPE samples, and known proteins that are deregulated in colon cancer are still detected in older samples.

This study forms part of a larger project of studies towards improvement of FFPE sample preparation methods for MS analysis, as well as identification of possible biomarkers for CRC in South African populations. The project lays the initial groundwork required towards CRC biomarker discovery.

The main limitation of the study was the inability to control or account for the impact of pre-analytical factors on the downstream proteomic analysis of the samples analysed. These factors may affect the number of identifiable peptides and especially peptides with labile PTMs, such as phosphopeptides (Thompson *et al*., 2013; Piehowski *et al*., 2018). In addition, the impact of biological variance was also a confounding factor (Thompson *et al*., 2013; Piehowski *et al*., 2018). This was somewhat compensated for in the subsequent block age analysis by choosing a 70% statistically significant sample size (n = 17 patients per experimental condition) based on previous protein identifications, to ensure that results reflect analytical differences and not biological variance.

5.2 Concluding remarks

Even with the great advances made in molecular medicine, genomics, proteomics and translational research in the past decades, the most common cancer mortality rates have not been significantly reduced (Diamandis, 2004). Successful cancer treatment still includes primary prevention, earlier diagnosis and improved therapeutic treatments. Primary prevention strategies still lag behind since cancer pathogenesis and tumour progression mechanisms still remain largely unknown. New, non-invasive cancer biomarkers and diagnostic techniques that will further enhance our ability to diagnose, prognose and predict therapeutic response are still required for many types of cancer, including CRC (Diamandis, 2004).

Genomic and proteomic studies are able to generate a broad perspective into the molecular events in a transformed cell; however, many factors need to be taken into consideration for experiments to be accurate and reproducible. Therefore, experimental validation remains one of the challenges that need to be overcome for future biomarker discovery (Baak *et al*., 2005). Future prospects for CRC diagnostic techniques include developing and defining biomarkers that are robust and reproducible and unaffected by slight changes in sample handling and experimental methodology. To retrieve as much information from patient biopsies as possible, genomic and proteomic techniques may be used in conjunction in future. Of current importance is the necessity to develop high-throughput experimental systems to validate these methods (Punt *et al*., 2016).

References

Adeola, H., Goosen, R.W., Goldberg, P., Blackburn, J. (2014). Prospects of 'Omics based molecular approaches in colorectal cancer diagnosis and treatment in the developing world: A case study in Cape Town, South Africa. In Khan, J.S. (ed.), *Colorectal cancer – Surgery, diagnostics and treatment* (Chapter 15). Rijeka: InTech. http://dx.doi.org/10.5772/57485

Aebersold, R., Mann, M. (2003). Mass spectrometry-based proteomics. *Nature, 422*, 198–207.

Agilent Technologies. (2009). FFPE protein extraction solution protocol. Retrieved from https://www.chem-agilent.com/pdf/strata/400925.pdf

Aguilar, M. (2004). HPLC of peptides and proteins: Basic theory and methodology. In Aguilar, M. (ed.), *Methods in Molecular Biology (Vol. 251) - HPLC of Peptides and Proteins: Methods and Protocols* (pp. 3 – 8). New Jersey: Humana Press Inc.

Alpert, A.J. (1990). Hydrophillic-interaction chromatography for the separation of peptides, nucleic acids and other polar compounds. *J. Chromatogr*., *499*, 177-196.

Alpert, A.J. (2008). Electrostatic repulsion hydrophilic interaction chromatography for isocratic separation of charged solutes and selective isolation of phosphopeptides. *Anal. Chem., 80*, 62-76.

Andersen, C.L., Christensen, L.L., Thorsen, K., Schepeler, T., Sorensen, F.B., Verspaget, H.W., Simon, R., Kruhoffer, M., Aaltonen, L.A., Laurberg, S., Orntoft, T.F. (2009). Dysregulation of the transcription factors SOX4, CBFB and SMARCC1 correlates with outcome of colorectal cancer. *Br. J. Cancer*, *100*(3), 511–23.

Apweiler, R., Bairoch, A., Wu, C.H., Barker, W.C., Boeckmann, B., Ferro, S., Gasteiger, E., Huang, H., Lopez, R., Magrane, M., Martin, M.J., Natale, D.A., O'Donovan, C., Redaschi, N., Yeh, L.L. (2004). UniProt: the Universal Protein knowledgebase. *Nucleic Acids Research, 32*, D115 - D119. DOI: 10.1093/nar/gkh131

Avaritt, N.L,, Shalin, S., Tackett, A.J. (2014) Decoding the proteome in formalin-fixed paraffin-embedded (FFPE) tissues. *J Proteomics Bioinform, 7: e25*. DOI:10.4172/jpb.10000e25.

Baak, J.P.A., Janssen, E.A.M, Soreide, K., Heikkilæ, R. (2005). Genomics and proteomics - the way forward. Annals of Oncology, 16(Supplement 2), ii30–ii44. DOI:10.1093/annonc/mdi728.

Balboa, E., Carracedo, A., Barros, F. (2014). The complexity of colorectal cancer biology — putting bricks on the path to personalized medicine. In Khan, J.S. (ed.), *Colorectal cancer – Surgery, diagnostics and treatment* (Chapter 17). Rijeka: InTech. http://dx.doi.org/10.5772/57485

Ballinger, A., Patchett, S. (2003). Clinical Medicine (3rd edition). In Kumar, P. & Clark, M. (eds.), *Saunders' Pocket Essentials series* (pp. 93 – 97). Philadelphia: Elsevier Limited.

Barsnes, H., Vaudel, M., Colaert, N., Helsens, K., Sickmann, A., Berven, F.S., Martens, L. (2011). Compomics-utilities: an open-source Java library for computational proteomics. *BMC Bioinf*., *12*, 70.

Bass, B.P., Engel, K.B., Greytak, S.R., Moore, H.M. (2014). A review of preanalytical factors affecting molecular, protein, and morphological analysis of formalinfixed, paraffin-embedded (FFPE) tissue: how well do you know your FFPE specimen? *Arch Pathol Lab Med*., *138*(11), 1520–30.

Batth, T.S., Tollenaere, M.A.X., Rüther, P.L., et al. (2018). Protein aggregation capture on microparticles enables multi-purpose proteomics sample preparation. *Mol Cell Proteomics*., Preprint at https://www.biorxiv.org/content/early/2018/10/25/447904.

Bell, A.W., Deutsch, E.W., Au, C.E., *et al*. (2009). A HUPO test sample study reveals common problems in mass spectrometry–based proteomics. *Nature Methods*, *6*(6), 423–546.

Bessant, C. (2017). Introduction to proteome informatics. In Bessant, C. (ed.), *New developments in mass spectrometry no. 5: Proteome informatics* (pp. 1 – 12). Cambridge: The Royal Society of Chemistry.

Bielas, J.H., Loeb, K.R., Rubin, B.P., True, L.D., Loeb, L.A. (2006). Human cancers express a mutator phenotype. *National Academy of Sciences of the United States of America*, 103(48), 18238 - 18242.

Blein-Nicolas, M., Zivy, M. (2016). Thousand and one ways to quantify and compare protein abundances in label-free bottom-up proteomics. *BBA - Proteins and Proteomics*, DOI:10.1016/j.bbapap.2016.02.019.

Botelho, D., Wall, M.J., Vieira, D.B., Fitzsimmons, S., Liu, F., Doucette, A. (2010). Top-down and bottom-up proteomics of SDS-containing solutions following mass-based separation. *J Proteome Res*., *9*, 2863−2870.

Bronsert, P., Weiber, J., Biniossek, M.L., Kuehs, M., Mayer, B., Drendel, V., Timme, S., Shahinian, H., Küsters, S., Wellner, U.F., Lassmann, S., Werner, M., Schilling, O. (2014). Impact of routinely employed procedures for tissue processing on the proteomic analysis of formalin-fixed paraffin-embedded tissue. *Proteomics Clin. Appl*., *8*, 796–804. DOI: 10.1002/prca.201300082

Busby, T.F., Ingham, K.C. (1980). Removal of polyethylene glycol from proteins by salt-induced phase separation. *Vox Sang*., *39*, 93-100.

Bustin, S.A., Li, S.R., Dorudi, S. (2001). Expression of the Ca^{2+}-activated chloride channel genes CLCA1 and CLCA2 is downregulated in human colorectal cancer. *DNA Cell Biol*., *20*(6), 331–8.

Chambers, M.C., Maclean, B., Burke, R., et al., (2012). A cross-platform toolkit for mass spectrometry and proteomics. *Nature Biotechnology*, *30*(10), 918–920.

Chen, E.I., Yates, J.R. (2007). Cancer proteomics by quantitative shotgun proteomics. *Mol Oncol*., *1*(2), 144–159.

Christin, C., Bischoff, R., Horvatovich, P. (2011). Data processing pipelines for comprehensive profiling of proteomics samples by label-free LC–MS for biomarker discovery. *Talanta*, *83*, 1209–1224. DOI:10.1016/j.talanta.2010.10.029.

Chugunova, A., Navalayeu, T., Dontsova, O., Sergiev, P. (2018). Mining for Small Translated ORFs. *J. Proteome Res*., *17*, 1−11.

Coetzee, E.D.T., Thomson, S.R. (2013). Inherited colorectal cancer: a plea for a national registry. *S Afr J Surg*, *51*(2), 42-43. DOI:10.7196/SAJS.1742.

Craig, R., Beavis, R.C. (2004). TANDEM : matching proteins with tandem mass spectra, *Bioinformatics*, *20*(9), 1466–1467.

Craven, R.A., Cairns, D.A., Zougman, A., Harnden, P., Selby, P.J., Banks, R.E. (2013). Proteomic analysis of formalin-fixed paraffin-embedded renal tissue samples by label-free MS: Assessment of overall technical variability and the impact of block age. *Proteomics Clin. Appl*., *7*(3-4), 273–282.

Daniele, L., D'Armento, G., Bussolati, G. (2011). Preanalytical time interval (PATI) and fixation. In Stanta, G. (ed.), Guidelines for molecular analysis in archive tissues. (pp. 5 – 11). Berlin: Springer-Verlag.

Deutsch, E.W. (2012). File formats commonly used in mass spectrometry proteomics. *Molecular & Cellular Proteomics*, *11.12*, 1612–1621. DOI:10.1074/mcp.R112.019695.

Deutsch, E.W., Csordas, A., Sun, Z., et al., (2017). The ProteomeXchange Consortium in 2017: supporting the cultural change in proteomics public data deposition. *Nucleic Acids Res*, *54*(D1), D1100-D1106.

Diamandis, E.P. (2004). Mass spectrometry as a diagnostic and a cancer biomarker discovery tool – opportunities and potential limitations. *Molecular & Cellular Proteomics*, *3*, 367–378.

Doerr, A. (2013). Mass spectrometry of intact protein complexes. *Nature Methods*, *10*(1), 38.

Dorfer, V., Pichler, P., Stranzl, T., Stadlmann, J., Taus, T., Winkler, S., Mechtler, K., (2014). MS Amanda, a universal identification algorithm optimized for high accuracy tandem mass spectra, *J. Proteome Res*., *13*, 3679–3684.

Doucette, A.A, Vieira, D.B., Orton, D.J., Wall, M.J. (2014). Resolubilization of precipitated intact membrane proteins with cold formic acid for analysis by mass spectrometry. J. Proteome Res., 13(12), 6001–6012.

Duncan, M.W., Aebersold, R., Caprioli, R.M. (2010). The pros and cons of peptide-centric proteomics. *Nature Biotechnology*, *28*(7), 659–664.

Elias, J.E., Gygi, S.P. (2010). Target-Decoy search strategy for mass spectrometry-based proteomics. *Methods Mol Biol*., *604*, 55–71. DOI:10.1007/978-1-60761-444-9_5.

Elliott, A.C., Hynan, L.S. (2011). A SAS® macro implementation of a multiple comparison post hoc test for a Kruskal–Wallis analysis. *Computer methods and programs in biomedicine*, *102*, 75-80.

Farias, S.S., Kline, K.G., Klepacki, J., Wu, C.C. (2010). Quantitative improvements in peptide recovery at elevated chromatographic temperatures from μLC/MS analyses of brain using SRM mass spectrometry. *Anal. Chem*., *82*(9), 3435–3440. DOI:10.1021/ac100359p.

Field, A., Miles, J. (2010). *Discovering statistics using SAS*, London: SAGE Publications Ltd.

Feist, P., Hummon, A.B. (2015). Proteomic challenges: sample preparation techniques for microgram-quantity protein analysis from biological samples. *Int. J. Mol. Sci*, *16*, 3537-3563.

Findeisen, P., Neumaier, M. (2009). Mass spectrometry-based clinical proteomics profiling: Current status and future directions. *Expert Rev. Proteomics*, *6*(5), 457–459.

Foster, P.R., Dunnill, P., Lilly, M.D. (1973). The precipitation of enzymes from cell extracts of *Saccharomyces Cerevisiae* by polyethyleneglycol. *Biochim. Biophys. Acta*, *317*, 505-516.

Fowler, C.B., O'Leary, T.J., Mason, J.T. (2013). Toward improving the proteomic analysis of formalin-fixed paraffin-embedded tissue. *Expert Rev Proteomics*, *10*(4), 389-400.

French, W.R., Zimmerman, L.J., Schilling, B., et al. (2015). Wavelet-based peak detection and a new charge inference procedure for MS/MS implemented in ProteoWizard's msConvert. *J. Proteome Res.*, *14*, 1299−1307.

Fu, Z., Yan, K., Rosenberg, A., Jin, Z. et al. (2013). Improved protein extraction and protein identification from archival formalin-fixed paraffin-embedded human aortas. *Proteomics Clin. Appl*., *7*, 217–224.

Gámez-Pozo, A., Ferrer, N. I., Ciruelos, E., Lopez-Vacas, R. et al. (2013). Shotgun proteomics of archival triple-negative breast cancer samples. *Proteomics Clin. Appl.*, *7*, 283–291.

Geer, L.Y., Markey, S.P, Kowalak, J.A., Wagner, L., Xu, M., Maynard, D.M., … Bryant, S.H. (2004). Open mass spectrometry search algorithm, *J. Proteome Res*., *3*(5), 958–964.

Gustafsson, O.J.R., Arentz, G., Hoffmann, P. (2015). Proteomic developments in the analysis of formalin-fixed tissue. *Biochimica et Biophysica Acta*, *1854*, 559–580.

Guo, T., Wang, W., Rudnick, P.A., Song, T., Li, J., Zhuang, Z., Weil, R.J., DeVoe, D.L., Lee, C.S., Balgley, B.M. (2007). Proteome analysis of microdissected formalin-fixed and paraffin-embedded tissue specimens. *J. Histochem. Cytochem.*, *55*(7), 763–772.

Helman, L.J., Gazdar, A.F., Park, J.G., Cohen, P.S., Cotelingam, J.D., Israel, M.A. (1988). Chromogranin A expression in normal and malignant human tissues. *J. Clin. Invest*., *82*(2), 686–90.

Holfeld, A., Valdés, A., Malmström, P., Segersten, U., Bergström Lind, S., (2018). A parallel proteomic workflow for mass spectrometric analysis of tissue samples preserved by different methods. *Anal. Chem*., *90*(9), 5841-5849.

Hubbard, S.J. (2010). Computational approaches to peptide identification via tandem MS. In Hubbard, S.J. & Jones, A.R. (eds.), *Proteome Bioinformatics, Methods*

in Molecular Biology, Vol. 604 (pp. 23 – 42). New York: Humana Press (Springer Science+Business Media). DOI: 10.1007/978-1-60761-444-9_3

Hughes, C.S., Foehr, S., Garfield, D.A., Furlong, E.E., Steinmetz, L.M., Krijgsveld, J. (2014). Ultrasensitive proteome analysis using paramagnetic bead technology. Mol. Syst. Biol., 10(10), 1–10.

Hughes, C.S., Moggridge, S., Müller, T., Sorensen, P.H., Morin, G.B., Krijgsveld, J. (2018). Single-pot, solid-phase-enhanced sample preparation for proteomics experiments. *Nature protocols, 14*(1), 1 – 18.

Hughes, C.S., Sorensen, P.H., Morin, G.B. (2019). A standardized and reproducible proteomics protocol for bottom-up quantitative analysis of protein samples using SP3 and mass spectrometry. In Brun, V. & Coute´, Y. (eds.), *Proteomics for Biomarker Discovery: Methods and Protocols, Methods in Molecular Biology, Vol. 1959* (pp. 65 – 87). New York: Springer Nature.

Hustoft, H.K., Malerod, H., Wilson, S.R., Reubsaet, L., Lundanes, E., Greibrokk, T. (2012). A critical review of trypsin digestion for LC-MS based proteomics. In Leung, H-C. (ed.), *Integrative proteomics* (pp. 73 – 92). Croatia: InTech.

Ikeda, K., Monden, T., Kanoh, T., et al. (1998). Extraction and analysis of diagnostically useful proteins from formalin-fixed, paraffin-embedded tissue sections. *J Histochem Cytochem., 46*(3), 397-403.

Juckes, I.R.M. (1971). Fractionation of proteins and viruses with polyethylene glycol. *Biochim. Biophys. Acta, 229*, 535-546.

Kachuk, C., Stephen, K., Doucette, A. (2015). Comparison of sodium dodecyl sulfate depletion techniques for proteome analysis by mass spectrometry. Journal of Chromatography A, 1418, 158-166.

Karpievitch, Y.V., Dabney, A.R., Smith, R.D. (2012). Normalization and missing value imputation for label-free LC-MS analysis. *BMC Bioinformatics, 13*(Suppl 16):S5. DOI: 10.1186/1471-2105-13-S16-S5.

Keerthikumar, S., Mathivanan, S. (2017). Proteomic data storage and sharing. In Keerthikumar, S. & Mathivanan, S. (eds.), *Proteome Bioinformatics, Methods in Molecular Biology, Vol. 1549* (pp. 5 – 16). New York: Springer Nature.

Kessner, D., Chambers, M., Burke, R., Agus, D., Mallick, P. (2008). ProteoWizard: open source software for rapid proteomics tools development. Bioinformatics, 24, 2534–2536.

Kim, S., Pevzner, P.A. (2014). MS-GF+ makes progress towards a universal database search tool for proteomics, *Nat. Commun., 5*, 5277.

Klockenbusch, C., O'Hara, J.E., Kast, J. (2012). Advancing formaldehyde cross-linking toward quantitative proteomic applications. *Anal Bioanal Chem, 404*, 1057–1067. DOI 10.1007/s00216-012-6065-9.

Kumar, D., Yadav, A.K., Dash, D. (2017). Choosing an optimal database for protein identification from tandem mass spectrometry data. In Keerthikumar, S. & Mathivanan, S. (eds.), *Proteome Bioinformatics, Methods in Molecular Biology, Vol. 1549* (pp. 17 – 29). New York: Springer Nature.

Kyte, J., Doolittle, R.F. (1982). A simple method for displaying the hydropathic character of a protein. *J. Mol. Biol*., *157*, 105–132.

Lai, X., Wang, L., Witzmann, F.A. (2013). Issues and applications in label-free quantitative mass spectrometry. *International Journal of Proteomics*, *2013*, 1-3. http://dx.doi.org/10.1155/2013/756039

Lee, S., Bang, S., Song, K., Lee, I. (2006). Differential expression in normal-adenoma-carcinoma sequence suggests complex molecular carcinogenesis in colon. *Oncol. Rep*., *16*(4), 747–54.

Lemaire, R., Desmons, A., Tabet, J.C., Day, R., Salzet, M., Fournier, I. (2007). Direct analysis and MALDI imaging of formalin-fixed, paraffin-embedded tissue sections. *Journal of Proteome Research*, *6*, 1295-1305.

Li, A., Goto, M., Horinouchi, M., Tanaka, S., Imai, K., Kim, Y. S., Sato, E., Yonezawa, S. (2001). Expression of MUC1 and MUC2 mucins and relationship with cell proliferative activity in human colorectal neoplasia. *Pathol. Int*., *51*(11), 853–60.

Liu, H., Ponniah, G., Neill, A., Patel, R., Andrien, B. (2013). Accurate determination of protein methionine oxidation by stable isotope labeling and LC-MS analysis. *Anal*. *Chem*., *85*, 11705−11709.

Maes, E., Valkenborg, D., Mertens, I., et al. (2013). Proteomic analysis of formalin-fixed paraffin embedded colorectal cancer tissue using tandem mass tag protein labelling. *Mol Biosyst*., *9*, 2686–2695.

Magdeldin, S., Yamamoto, T. (2012). Toward deciphering proteomes of formalin-fixed paraffin-embedded (FFPE) tissues. Proteomics, 12, 1045-1058.

Martens, M., Chambers, M., Sturm, M., et al., (2011). mzML - a community standard for mass spectrometry data. Molecular & Cellular Proteomics, 10.1, 1–7. DOI:10.1074/mcp.R110.000133

Martin, S.F., Falkenberg, H., Dyrlund, T.F., Khoudoli, G.A., Mageean, C.J., Linding, R. (2013). PROTEINCHALLENGE: Crowd sourcing in proteomics analysis and software development. *J. Proteomics*, *88*, 41–46.

Michalski, A., Damoc, E., Hauschild, J., Lange, O., Wieghaus, A., Makarov, A., Nagaraj, N., Cox, J., Mann, M., Horning, S. (2011). Mass spectrometry-based proteomics using Q Exactive, a high-performance benchtop quadrupole Orbitrap mass spectrometer. *Molecular & Cellular Proteomics*, *10.9* (10.1074/mcp.M111.011015), 1–11.

Mikesch, J. H., Buerger, H., Simon, R., Brandt, B. (2006). Decayaccelerating factor (CD55): a versatile acting molecule in human malignancies. *Biochim. Biophys. Acta*, *1766*(1), 42–52.

Mishra, A., Verma, M. (2010). Cancer biomarkers: Are we ready for the prime time? *Cancers*, *2*, 190-208. DOI:10.3390/cancers2010190

Moggridge, S., Sorensen, P.H., Morin, G.B., Hughes, C.S. (2018). Extending the compatibility of the SP3 paramagnetic bead processing approach for proteomics. *J Proteome Res*, *17*(4), 1730–1740.

Nahnsen, S., Bielow, C., Reinert, K., Kohlbacher, O. (2013). Tools for label-free peptide quantification. *Molecular & Cellular Proteomics*, *12*, 549–556. DOI:10.1074/mcp.R112.025163.

Netzel, B., Dasari, S. (2017). Peptide spectrum matching via database search and spectral library search. In Bessant, C. (ed.), *New developments in mass spectrometry no. 5: Proteome informatics* (pp. 39 – 68). Cambridge: The Royal Society of Chemistry.

Nibbe, R.K., Chance, M.R. (2009). Approaches to biomarkers in human colorectal cancer: looking back, to go forward. *Biomark Med*., *3*(4), 385–396. DOI:10.2217/BMM.09.33.

Nozawa, Y., Van Belzen, N., Van der Made, A.C., Dinjens, W.N., Bosman, F.T. (1996). Expression of nucleophosmin/B23 in normal and neoplastic colorectal mucosa. *J. Pathol*., *178*(1), 48–52.

Ogata, S., Uehara, H., Chen, A., Itzkowitz, S.H. (1992). Mucin gene expression in colonic tissues and cell lines. *Cancer Res*., *52*(21), 5971–8.

Oliveros, J.C. (2007-2015) Venny. An interactive tool for comparing lists with Venn's diagrams. http://bioinfogp.cnb.csic.es/tools/venny/index.html

Ogorzalek Loo, R.R., Dales, N., Andrews, P.C. (1994). Surfactant effects on protein structure examined by electrospray ionization mass spectrometry. Protein Sci, 3, 1975-1983.

Paine, M.R.L., Ellis, S.R., Maloney, D., Heeren, R.M.A., Verhaert, P.D.E.M. (2018). Digestion-free analysis of peptides from 30-year-old formalin-fixed, paraffin-embedded tissue by mass spectrometry imaging. *Anal. Chem*., *90*, 9272-9280.

Pellerin, D., Gagnon, H., Dubé, J., Corbin, F. (2015). Amicon-adapted enhanced FASP: an in-solution digestion-based alternative sample preparation method to FASP. *F1000Research*, *4*, 1-18. DOI:10.12688/f1000research.6529.1.

Perez-Riverol, Y., Alpi, E., Wang, R., Hermjakob, H., Vizcaíno, J.A. (2015). Making proteomics data accessible and reusable: Current state of proteomics databases and repositories. *Proteomics*, *15*, 930–949.

Perez-Riverol, Y., Csordas, A., Bai, J., et al., (2019). The PRIDE database and related tools and resources in 2019: improving support for quantification data. *Nucleic Acids Res*, *47*(D1), D442-D450.

Piehowski, P.D., Petyuk, V.A., Sontag, R.L., et al. (2018). Residual tissue repositories as a resource for population‐based cancer proteomic studies. *Clin Proteom*, *15*:26. https://doi.org/10.1186/s12014-018-9202-4

Powell, D.W., Weaver, C.M., Jennings, J.L., McAfee, K.J., He, Y., Weil, P.A., Link, A.J. (2004). Cluster analysis of mass spectrometry data reveals a novel component of SAGA. *Molecular and cellular biology*, *24*, 7249-7259.

Powis, G., Mustacich, D., Coon, A. (2000). The role of the redox protein thioredoxin in cell growth and cancer. *Free Radic. Biol. Med*., *29*(3–4), 312–22.

Punt, C.J.A., Koopman, M., Vermeulen, L. (2016). From tumour heterogeneity to advances in precision treatment of colorectal cancer. *Nature Reviews Clinical Oncology*, Advance online publication. DOI:10.1038/nrclinonc.2016.171.

Quesada-Calvo, F., Massot, C., Bertrand, V., Longuespée, R., Blétard, N., Somja, J., Mazzucchelli, G., Smargiasso, N., … Louis, E. (2017). OLFM4, KNG1 and Sec24C identified by proteomics and immunohistochemistry as potential markers of early colorectal cancer stages. *Clin Proteom*, *14*(9). DOI:10.1186/s12014-017-9143-3.

Rodríguez-Rigueiro, T., Valladares-Ayerbes, M., Haz-Conde, M., Blanco, M., Aparicio, G., Fernandez-Puente, P., Blanco, F.J., Lorenzo, M.J., Aparicio, L.A., Figueroa, A. (2011). A novel procedure for protein extraction from formalin-fixed paraffin-embedded tissues. *Proteomics*, *11*, 2555–2559.

Ruderman, D. (2017). Designing successful proteomics experiments. In Comai, L., Katz, J.E., Mallick, P. (eds.), *Proteomics: Methods and Protocols* (pp. 271 – 288). New York: Humana Press (Springer Science+Business Media). DOI: 10.1007/978-1-4939-6747-6_19

Scheerlinck, E., Dhaenens, M., Van Soom, A., Peelman, L., De Sutter, P., Van Steendam, K., Deforce, D. (2015). Minimizing technical variation during sample preparation prior to label-free quantitative mass spectrometry. *Analytical Biochemistry*, *490*, 14-19.

Scicchitano, M.S., Dalmas, D.A., Boyce, R.W., Thomas, H.C., Frazier, K.S. (2009). Protein extraction of formalin-fixed, paraffin-embedded tissue enables robust proteomic profiles by mass spectrometry. *Journal of Histochemistry & Cytochemistry*, *57*(9), 849–860.

Scopes, R.K. (1994). Making an extract. In Cantor, C.R. (ed.), *Protein purification: Principles and practice, 3rd edition*, (pp. 22 – 43). New York: Springer.

Shen, T., Noon, K.R. (2004). Liquid chromatography–and tandem mass spectrometry of peptides and proteins. In Aguilar, M. (ed.), *Methods in molecular biology Vol. 251: HPLC of Peptides and Proteins – Methods and Protocols* (pp. 111 - 139). New Jersey: Humana Press Inc.

Shen, K., Sun, J., Cao, X., Zhou, D., Li, J. (2015). Comparison of different buffers for protein extraction from formalin-fixed and paraffin-embedded tissue specimens. *PLoS ONE*, *10*(11): e0142650. DOI:10.1371/journal.pone.0142650.

Shi, S.R., Key, M.E., Kalra, K.L. (1991). Antigen retrieval in formalin-fixed, paraffin-embedded tissues: an enhancement method for immunohistochemical staining based on microwave oven heating of tissue sections. *J Histochem Cytochem*, *39*(6), 741-748. DOI: 10.1177/39.6.1709656.

Shi, S., Liu, C., Balgley, B.M., Lee, C., Taylor, C.R. (2006). Protein extraction from formalin-fixed, paraffin-embedded tissue sections: quality evaluation by mass spectrometry. *J Histochem Cytochem*, *54*, 739 – 743.

Shteynberg, D., Nesvizhskii, A.I., Moritz, R.L., Deutsch, E.W. (2013). Combining results of multiple search engines in proteomics. *Molecular & Cellular Proteomics*, *12*, 2383–2393.

Speers, A.E., Wu, C.C. (2007). Proteomics of integral membrane proteins – theory and application, *Chem. Rev.*, *107*, 3687–3714.

Sprung, R. W., Brock, J. W. C., Tanksley, J. P., Li, M. et al. (2009). Equivalence of protein inventories obtained from formalin-fixed paraffin-embedded and

frozen tissue in multidimensional liquid chromatography-tandem mass spectrometry shotgun proteomic analysis. *Mol. Cell. Proteomics, 8*, 1988–1998.

Tabb, D.L., Fernando, C.G., Chambers, M.C. (2007). MyriMatch: highly accurate tandem mass spectral peptide identification by multivariate hypergeometric analysis, *J. Proteome Res*., *6*(2), 654–661.

Tanca A, Pagnozzi D, Falchi G, Biosa G, Rocca S, Foddai G, Uzzau S, Addis MF. (2011). Impact of fixation time on GeLC-MS/MS proteomic profiling of formalinfixed, paraffin-embedded tissues. J Proteomics 2011, 74:1015–1021.

Tanca, A., Abbondio, M., Pisanu, S., Pagnozzi, D., Uzzau, S., Addis, M.F. (2014). Critical comparison of sample preparation strategies for shotgun proteomic analysis of formalin-fixed, paraffin-embedded samples: insights from liver tissue. *Clinical Proteomics, 11*(28), 1–11.

Taus, T., Kocher, T., Pichler, P., Paschke, C., Schmidt, A., Henrich, C., Mechtler, K. (2011). Universal and confident phosphorylation site localization using phosphoRS. *J. Proteome Res*., *10*(12), 5354–5362.

Taylor, C.F., Paton, N.W., Lilley, K.S., Binz, P-A., Julian, R.K., Jones, A.R. … Hermjakob, H. (2007). The minimum information about a proteomics experiment (MIAPE). *Nature Biotechnology*, *25*(8), 887 – 893.

ThermoFisher Scientific Detergent removal columns, retrieved on 25 April 2017: https://www.thermofisher.com/order/catalog/product/87777

Thompson, S.M., Craven, R.A., Nirmalan, N.J., Harnden, P., Selby, P.J., Banks, R.E. (2013). Impact of pre-analytical factors on the proteomic analysis of formalin-fixed paraffin-embedded tissue. *Proteomics Clin. Appl*, *7*, 241–251.

Toiyama, Y., Inoue, Y., Yasuda, H., Saigusa, S., Yokoe, T., Okugawa, Y., Tanaka, K., Miki, C., Kusunoki, M. (2011). DPEP1, expressed in the early stages of colon carcinogenesis, affects cancer cell invasiveness. *J. Gastroenterol*., *46*, 153–63.

Vaudel, M., Barsnes, H., Berven, F.S., Sickmann, A., Martens, L. (2011). SearchGUI: An open-source graphical user interface for simultaneous OMSSA and X!Tandem searches, *Proteomics, 11*, 996–999.

Vaudel, M., Breiter, D., Beck, F., Rahnenfuhrer, J. et al., (2013). Dscore: a search engine independent MD-score. *Proteomics*, *13*(6), 1036–1041.

Vaudel, M., Venne, A.S., Berven, F.S., Zahedi, R.P., Martens, L., Barsnes, H. (2014). Shedding light on black boxes in protein identification. *Proteomics*, *14*, 1001–1005. DOI: 10.1002/pmic.201300488

Vaudel, M., Burkhart, J.M., Zahedi, R.P., Oveland, E., Berven, F.S., Sickmann, A., Martens, L., Barsnes, H. (2015). PeptideShaker enables reanalysis of MS-derived proteomics data sets. *Nature Biotechnology*, *33*(1), 22 - 24.

Vaudel, M. (2017). MS2-based quantitation. In Bessant, C. (ed.), *New developments in mass spectrometry no. 5: Proteome informatics* (pp. 155 – 177). Cambridge: The Royal Society of Chemistry.

Vehus, T., Roberg-Larsen, H., Waaler, J., Aslaksen, S., Krauss, S., Wilson, S.R., Lundanes, E. (2016).Versatile, sensitive liquid chromatography mass spectrometry – Implementation of 10 μm OT columns suitable for small molecules, peptides and proteins. *Nature Scientific Reports, 6,* 37507, DOI: 10.1038/srep37507.

Vie, N., Copois, V., Bascoul-Mollevi, C., Denis, V., Bec, N., Robert, B., Fraslon, C., Conseiller, E., Molina, F., Larroque, C., Martineau, P., Del Rio, M., Gongora, C. (2008). Overexpression of phosphoserine aminotransferase PSAT1 stimulates cell growth and increases chemoresistance of colon cancer cells. *Mol. Cancer*, *7*, 14.

Villar, E.L., Cho, W.C. (2013). Proteomics and cancer research. In Wang, X. (ed.), *Translational Bioinformatics, Vol. 3: Bioinformatics of human proteomics* (pp. 75 - 100). Dordrecht: Springer Science+Business Media. DOI: 10.1007/978-94-007-5811-7_4

Vizcaíno, J.A., Perkins, S., Jones, A.R., Deutsch, E.W. (2017). Data formats of the Proteomics Standards Initiative. In Bessant, C. (ed.), *New developments in mass spectrometry no. 5: Proteome informatics* (pp. 231 – 258). Cambridge: The Royal Society of Chemistry.

Wiśniewski, J.R., Zougman, A., Nagaraj, N., Mann, M. (2009). Universal sample preparation method for proteome analysis. *Nature Methods*, *6*(*5*), 359–362.

Wiśniewski, J.R., Ostasiewicz, P., Mann, M. (2011). High recovery FASP applied to the proteomic analysis of microdissected formalin fixed paraffin embedded cancer tissues retrieves known colon cancer markers. *J. Proteome Res., 10,* 3040–3049. DOI:10.1021/pr200019m

Wiśniewski, J.R., Duś, K., Mann, M. (2012). Proteomic workflow for analysis of archival formalin-fixed and paraffin-embedded clinical samples to a depth of 10 000 proteins. *Proteomics Clin. Appl., 7,* 1–9. DOI:10.1002/prca.201200046

Wiśniewski, J.R. (2013). Proteomic sample preparation from formalin fixed and paraffin embedded tissue. *J Vis Exp*, *79*, e50589, 1–6.

Wiśniewski, J.R., Duś, K., Mann, M. (2013). Proteomic workflow for analysis of archival formalin-fixed and paraffin-embedded clinical samples to a depth of 10 000 proteins. *Proteomics Clin Appl*, *7*, 225–233.

Wiśniewski, J.R., Duś-Szachniewicz, K., Ostasiewicz, P., Ziółkowski, P., Rakus, D., Mann, M. (2015). Absolute proteome analysis of colorectal mucosa, adenoma, and cancer reveals drastic changes in fatty acid metabolism and plasma membrane transporters. *J. Proteome Res., 14*, 4005−4018. DOI: 10.1021/acs.jproteome.5b00523

Wolff, C., Schott, C., Porschewski, P., Reischauer, B., Becker, K-F. (2011) Successful protein extraction from over-fixed and long-term stored formalin-fixed tissues. *PLoS ONE*, *6*(1), e16353. DOI:10.1371/journal.pone.0016353

Wright, J.C., & Choudhary, J.S (2017). PSM scoring and validation . In Bessant, C. (ed.), *New developments in mass spectrometry no. 5: Proteome informatics* (pp. 69 – 92). Cambridge: The Royal Society of Chemistry.

Wu, S., Zhu, Y. (2012). ProPAS: standalone software to analyze protein properties. *Bioinformation*, *8*(3), 167–169.

Yamagishi, H., Kuroda, H., Imai, Y., Hiraishi, H. (2016). Molecular pathogenesis of sporadic colorectal cancers. *Chin J Cancer*, *35*(4), 1-8. DOI: 10.1186/s40880-015-0066-y.

Yao, X., Zhao, G., Yang, H., Hong, X., Bie, L., Liu, G. (2010). Overexpression of high-mobility group box 1 correlates with tumor progression and poor prognosis in human colorectal carcinoma. *J. Cancer Res. Clin. Oncol*., *136*(5), 677–84.

Yung, B.Y. (2007). Oncogenic role of nucleophosmin/B23. *Chang Gung Med*. J., *30*(4), 285–93.

Zhang, L., Carlage, T., Murphy, D., Frenkel, R., Bryngelson, P., Madsen, M., Lyubarskaya, Y. (2012). Residual metals cause variability in methionine oxidation measurements in protein pharmaceuticals using LC-UV/MS peptide mapping. *J. Chromatogr. B, 895−896*, 71−76.

Zhang, Y., Fonslow, B.R., Shan, B., Baek, M-C, Yates, J.R. (2013). Protein analysis by shotgun/bottom-up proteomics. *Chem. Rev*., *113*(4), 2343–2394. DOI:10.1021/cr3003533.

Zhang, Y., Muller, M., Xu, B., Yoshida, Y., Horlacher, O., Nikitin, F., Garessus, S., Magdeldin, S., Kinoshita, N., Fujinaka, H., Yaoita, E., Hasegawa, M., Lisacek, F., Yamamoto, T. (2015). Unrestricted modification search reveals lysine methylation as major modification induced by tissue formalin fixation and paraffin embedding. *Proteomics*, *15*, 2568–2579.

Zhao, C., O'Connor, P.B. (2007). Removal of polyethylene glycols from protein samples using titanium dioxide. *Anal Biochem*, *365*(2), 283–285.

Zheng, H., Tsuneyama, K., Cheng, C., Takahashi, H., Cui, Z., Murai, Y., Nomoto, K., Takano, Y. (2007). Maspin expression was involved in colorectal adenoma-adenocarcinoma sequence and liver metastasis of tumors. *Anticancer Res*., *27*(1A), 259–65.

Appendix A: Search algorithms specific settings

Project Details

1: PeptideShaker Version: 1.16.40
2: Date:
3: Experiment:
4: Sample:
5: Replicate Number: 1
6: Identification Algorithms: X!Tandem, MS Amanda and MS-GF+

Database Search Parameters

1: Precursor Tolerance Unit: ppm
2: Precursor Ion m/z Tolerance: 10.0
3: Fragment Ion Tolerance Unit: Da
4: Fragment Ion m/z Tolerance: 0.02
5: Cleavage: Enzyme
6: Enzyme: Trypsin
7: Missed Cleavages: 2
8: Specificity: Specific
9: Database: uniprot-human-reviewed-trypsin-may-2018_concatenated_target_decoy.fasta
10: Forward Ion: b
11: Rewind Ion: y
12: Fixed Modifications: Methylthio of C
13: Variable Modifications: Oxidation of M, Deamidation of N, Deamidation of Q
14: Refinement Variable Modifications: Acetylation of protein N-term, Pyrolidone from E, Pyrolidone from Q, Pyrolidone from carbamidomethylated C
15: Refinement Fixed Modifications: Methylthio of C

Input Filters

1: Minimal Peptide Length: 8
2: Maximal Peptide Length: 30
3: Precursor m/z Tolerance: 10.0
4: Precursor m/z Tolerance Unit: Yes
5: Unrecognized Modifications Discarded: Yes

PTM Scoring Settings

1: Probabilistic Score: PhosphoRS
2: Accounting for Neutral Losses: No
3: Threshold: 95.0

Spectrum Counting Parameters

1: Method: NSAF

2: Validated Matches Only: No

Annotation Settings

1: Intensity Limit: 0.75
2: Automatic Annotation: Yes
3: Selected Ions: y, b
4: Neutral Losses: H2O, NH3, CH4OS
5: Neutral Losses Sequence Dependence: Yes
6: Fragment Ion m/z Tolerance: 0.02

Appendix B: Supplementary figures

Table of contents

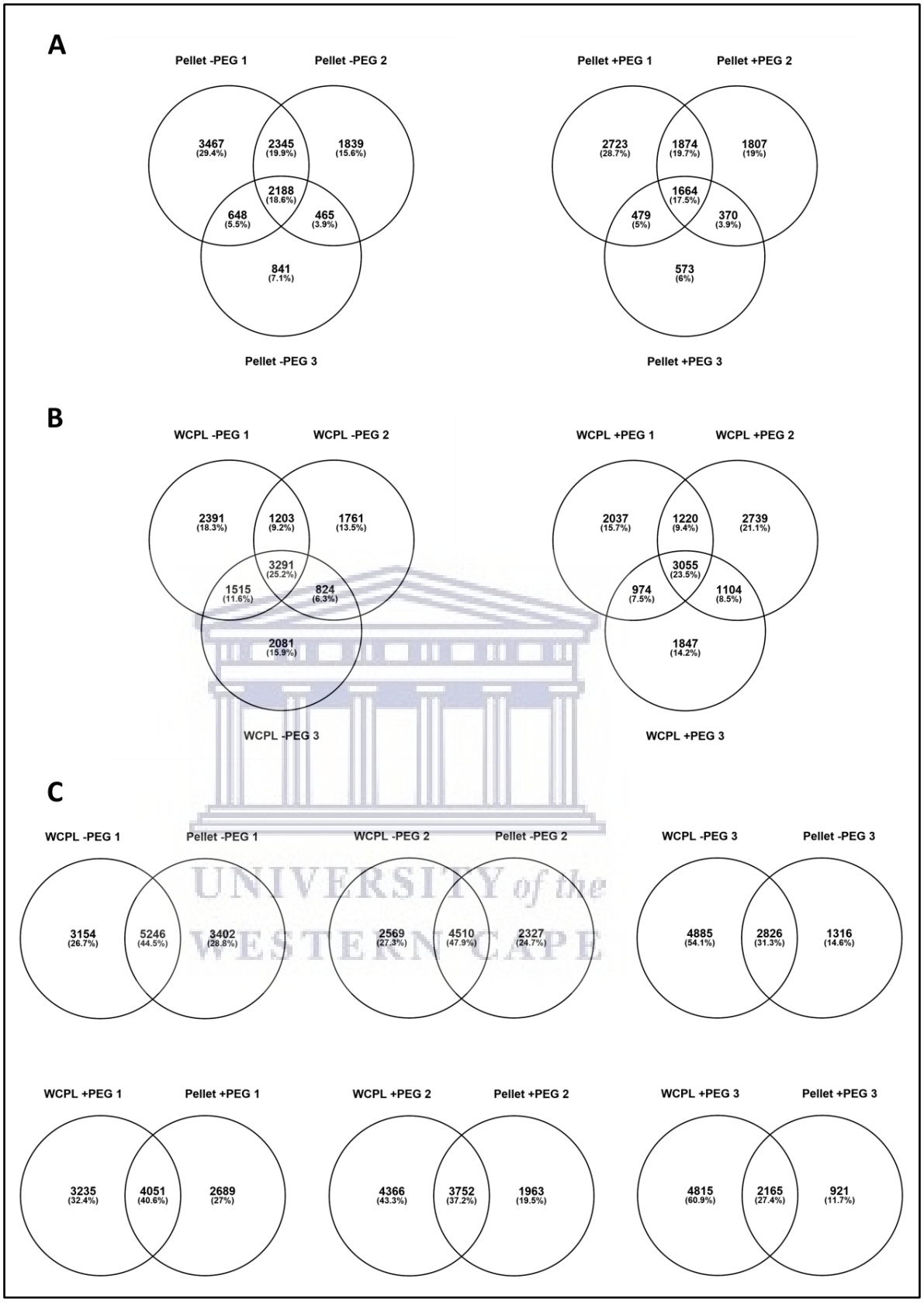

Supplementary figure S1. Comparison of the qualitative reproducibility of the experimental conditions in terms of peptide identification overlap. (A) Venn diagrams depicting the distribution of identified peptides for all three sample pellets, extracted with or without PEG (B) Venn diagrams depicting the distribution of identified peptides for all three WCPLs, extracted with or without PEG (C) Venn diagrams showing the overlap of identified peptides between sample pellets and their respective WCPLs for each sample set analysed (top panel – extracted without PEG; bottom panel – extracted with PEG). -PEG refers to protein extraction without PEG and +PEG refers to protein extraction with PEG.

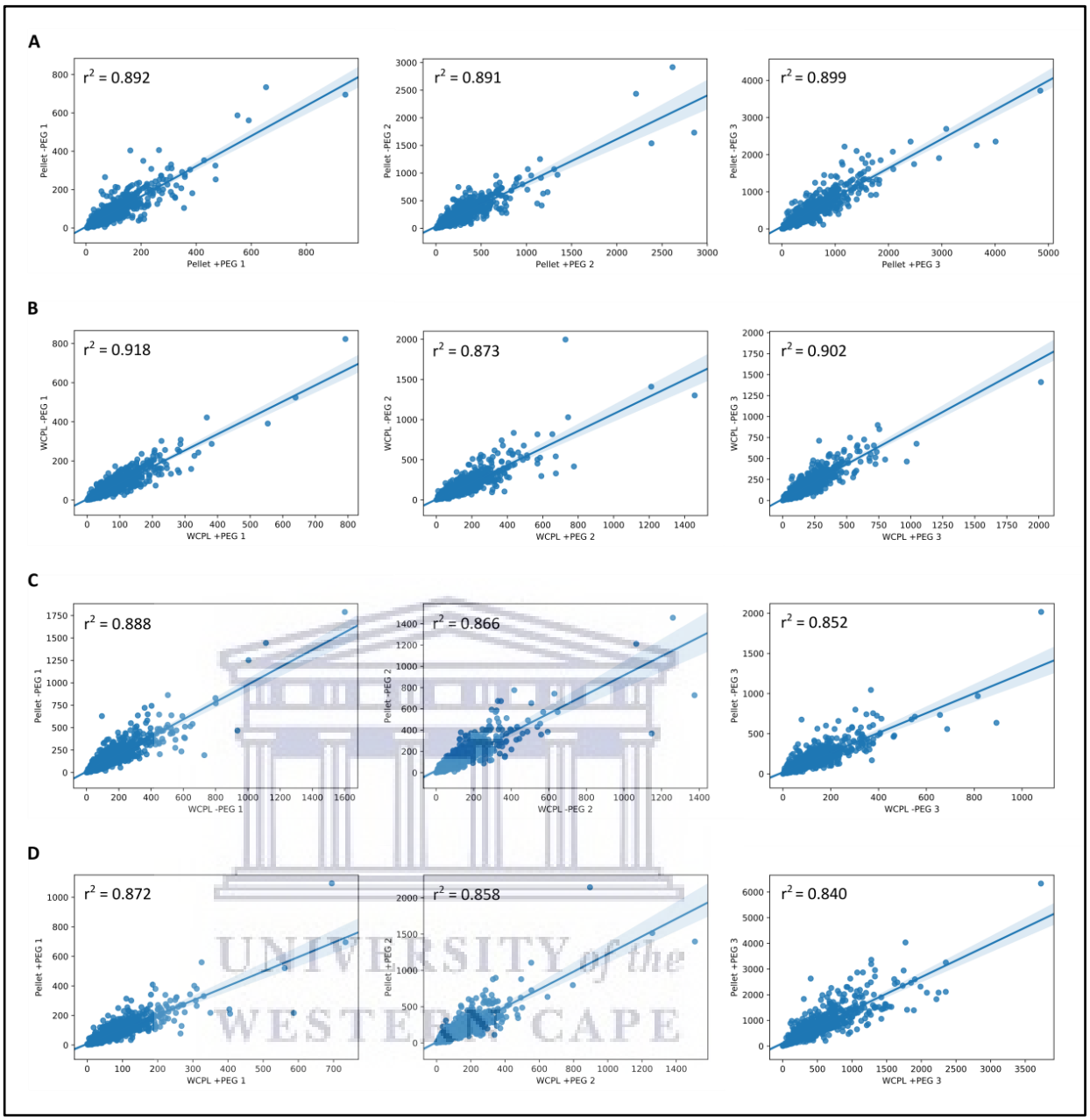

Supplementary figure S2. Correlation of protein abundance between all conditions for each patient. (A) Correlation of protein abundance for pellet samples (extracted with or without PEG and 4% SDS) for each patient sample 1 - 3 (B) Correlation of protein abundance for WCPL samples (extracted with or without PEG and 2% SDS) for each patient sample 1 - 3 (C) Correlation of protein abundance for samples extracted without PEG; pellet samples (extracted with 4% SDS) vs WCPLs (extracted with 2% SDS) for each patient sample 1 - 3 (D) Correlation of protein abundance for samples extracted with PEG; pellet samples (extracted with 4% SDS) vs WCPLs (extracted with 2% SDS) for each patient sample 1 – 3. The Pearson correlation coefficients (r^2) are indicated on each plot and plot axes values are the normalised NSAF values for proteins present in both condition compared per plot. (-PEG) refers to protein extracted without PEG and (+PEG) refers to protein extracted with PEG.

Appendix C: Supplementary table 1

Supplementary table 1. Average physicochemical properties of identified peptides for all conditions for each patient.

Sample:	Peptide feature:	WCPL:	Pellet:	Shared peptides:
Patient 1 (-PEG)	Hydropathicity:	-0.42	-0.24	-0.29
	MW (Da):	1423.31	1398.38	1458.93
	pI:	5.96	6.06	5.95
Patient 1 (+PEG)	Hydropathicity:	-0.49	-0.20	-0.29
	MW (Da):	1418.23	1376.74	1421.45
	pI:	5.88	6.09	5.98
Patient 2 (-PEG)	Hydropathicity:	-0.40	-0.20	-0.25
	MW (Da):	1440.36	1435.79	1451.00
	pI:	5.81	6.08	5.95
Patient 2 (+PEG)	Hydropathicity:	-0.38	-0.21	-0.24
	MW (Da):	1437.87	1403.03	1470.18
	pI:	5.97	5.97	5.97
Patient 3 (-PEG)	Hydropathicity:	-0.38	-0.14	-0.21
	MW (Da):	1427.47	1407.65	1457.32
	pI:	6.02	6.00	5.94
Patient 3 (+PEG)	Hydropathicity:	-0.35	-0.10	-0.15
	MW (Da):	1426.00	1405.48	1480.52
	pI:	6.02	5.97	6.01

Appendix D: Supplementary table 2

Supplementary table 2. Statistical tests for Chapter 3 and 4 data.

Data analysed:	**Statistical tests:**	**Conclusions:**
Figure 19 A: Comparison of the number of peptides identified using protein extraction buffer with or without addition of PEG.	1. Shapiro–Wilk test: W = 0.924, p = 0.533 2. One-way ANOVA: F(1,4) = 0.25, p = 0.65	1. p > 0.05 therefore the distribution is not significantly different from a normal distribution, i.e. it is normal. 2. With regards to the number of peptide identifications, there is no significant difference between WCPL extracted with or without addition of PEG.
Figure 19 C: Comparison of the number of proteins identified using protein extraction buffer with or without addition of PEG.	1. Shapiro–Wilk test: W = 0.965, p = 0.854 2. One-way ANOVA: F(1,4) = 0.04, p = 0.851	1. p > 0.05 therefore the distribution is not significantly different from a normal distribution, i.e. it is normal. 2. With regards to the number of protein identifications, there is no significant difference between WCPL extracted with or without addition of PEG.
Figure 25: BCA total protein quantitation assay	1. Shapiro–Wilk test: W = 0.921, p = 0.002 2. Kruskal–Wallis test: H(2) = 23.92, p < 0.0001 3. Dunn's post hoc test, α = 0.05	1. p < 0.05 therefore the distribution is significantly different from a normal distribution, i.e. it is non-normal. 2. Protein yield was significantly affected by block age, H(2) = 23.92, p < 0.05. 3. Protein yields from 1-year-old blocks vs 10-year-old blocks: there is evidence (at α = 0.05) to reject the null hypothesis (that the groups are equal/there is no significant difference). Therefore, there is significant location differences between groups. Protein yields from 1-year-old blocks vs 5-year-old blocks: there is evidence (at α = 0.05) to reject the null

		hypothesis. Therefore, there is significant location differences between groups. Protein yields from 5-year-old blocks vs 10-year-old blocks: there is evidence (at $\alpha = 0.05$) to accept the null hypothesis. Therefore, there is no significant location differences between groups.
Figure 26 A: Comparison of the number of peptides identified for different protein purification methods for 1-year-old blocks	1. Shapiro–Wilk test: $W = 0.979$, $p = 0.48$ 2. One-way ANOVA: $F(2,48) = 12.78$, $p < 0.0001$ 3. Bonferroni (Dunn) t Tests for validated peptides identified: $F(2) = 12.78$, $p < 0.0001$ ($\alpha = 0.05$)	1. $p > 0.05$ therefore the distribution is not significantly different from a normal distribution, i.e. it is normal. 2. With regards to peptide identifications, there is a significant difference ($p < 0.05$) between protein purification/sample preparation methods for 1-year old blocks. 3. Compared to the other protein purification methods, the DRP method differs significantly with regards to peptide identifications for 1-year-old-blocks. There is no significant difference between the APFAR and SP3/HILIC methods.
Figure 26 A: Comparison of the number of peptides identified for different protein purification methods for 5-year-old blocks	1. Shapiro–Wilk test: $W = 0.987$, $p = 0.83$ 2. One-way ANOVA: $F(2,48) = 1.51$, $p = 0.23$	1. $p > 0.05$ therefore the distribution is not significantly different from a normal distribution, i.e. it is normal. 2. With regards to peptide identifications, there is not a significant difference ($p > 0.05$) between protein purification/sample preparation methods for 5-year old blocks.
Figure 26 A: Comparison of the number of peptides	1. Shapiro–Wilk test: $W = 0.994$, $p = 0.99$ 2. One-way ANOVA:	1. $p > 0.05$ therefore the distribution is not significantly different from a normal distribution, i.e. it is normal.

identified for different protein purification methods for 10-year-old blocks	F(2,48) = 3.78, p = 0.03 3. Bonferroni (Dunn) t Tests for validated peptides identified: F(2) = 3.78, p = 0.0299 (α = 0.05)	2. With regards to peptide identifications, there is a significant difference (p < 0.05) between protein purification/sample preparation methods for 10-year old blocks. 3. The DRP and APFAR methods differ significantly with regards to peptide identifications for 10-year-old-blocks. There is no significant difference between the APFAR and SP3/HILIC and the DRP and SP3/HILIC methods.
Figure 26 A: Comparison of the number of peptides identified for different block ages for the APFAR method	1. Shapiro–Wilk test: W = 0.982, p = 0.65 2. One-way ANOVA: F(2,48) = 0.88, p = 0.42	1. p > 0.05 therefore the distribution is not significantly different from a normal distribution, i.e. it is normal. 2. With regards to peptide identifications, there is not a significant difference (p > 0.05) between block ages when processed with the APFAR method.
Figure 26 A: Comparison of the number of peptides identified for different block ages for the DRP method	1. Shapiro–Wilk test: W = 0.988, p = 0.90 2. One-way ANOVA: F(2,48) = 4.81, p = 0.01 3. Bonferroni (Dunn) t Tests for validated peptides identified: F(2) = 4.81, p = 0.0125 (α = 0.05)	1. p > 0.05 therefore the distribution is not significantly different from a normal distribution, i.e. it is normal. 2. With regards to peptide identifications, there is a significant difference (p < 0.05) between block ages when processed with the DRP method. 3. With regards to peptide identifications, there is a significant difference (p < 0.05) between 1-year-old blocks and 5-year-old blocks, as well as 1-year-old blocks and 10-year-old blocks processed via the DRP method. There is no significant difference between 5 and 10-year-old blocks.

Figure 26 A: Comparison of the number of peptides identified for different block ages for the HILIC method	1. Shapiro–Wilk test: W = 0.970, p = 0.22 2. One-way ANOVA: F(2,48) = 0.03, p = 0.97	1. p > 0.05 therefore the distribution is not significantly different from a normal distribution, i.e. it is normal. 2. With regards to peptide identifications, there is not a significant difference (p > 0.05) between block ages when processed with the HILIC method.
Figure 26 B: Comparison of the number of proteins identified for different protein purification methods for 1-year-old blocks	1. Shapiro–Wilk test: W = 0.924, p = 0.003 2. Kruskal–Wallis test: H(2) = 16.70, p = 0.0002 3. Dunn's post hoc test, α = 0.05	1. p < 0.05 therefore the distribution is significantly different from a normal distribution, i.e. it is non-normal. 2. With regards to protein identifications, there is a significant difference (p < 0.05) between protein purification/sample preparation methods for 1-year old blocks. 3. For 1-year old blocks, protein identifications from DRP vs APFAR processing: there is evidence (at α = 0.05) to reject the null hypothesis (that the groups are equal/there is no significant difference). Therefore, there is significant location differences between these groups. For DRP vs HILIC and APFAR vs HILIC: there is evidence (at α = 0.05) to accept the null hypothesis. Therefore, there is no significant location differences between these groups.
Figure 26 B: Comparison of the number of proteins identified for different protein purification methods for 5-year-	1. Shapiro–Wilk test: W = 0.950, p = 0.03 2. Kruskal–Wallis test: H(2) = 3.58, p = 0.17	1. p < 0.05 therefore the distribution is significantly different from a normal distribution, i.e. it is non-normal. 2. With regards to protein identifications, there is not a significant difference (p > 0.05) between protein purification/sample

old blocks		preparation methods for 5-year old blocks.
Figure 26 B: Comparison of the number of proteins identified for different protein purification methods for 10-year-old blocks	1. Shapiro–Wilk test: W = 0.991, p = 0.97 2. One-way ANOVA: F(2,48) = 2.44, p = 0.098	1. p > 0.05 therefore the distribution is not significantly different from a normal distribution, i.e. it is normal. 2. With regards to protein identifications, there is not a significant difference (p > 0.05) between protein purification/sample preparation methods for 10-year old blocks.
Figure 26 B: Comparison of the number of proteins identified for different block ages for the APFAR method	1. Shapiro–Wilk test: W = 0.951, p = 0.03 2. Kruskal–Wallis test: H(2) = 2.28, p = 0.32	1. p < 0.05 therefore the distribution is significantly different from a normal distribution, i.e. it is non-normal. 2. With regards to protein identifications, there is not a significant difference (p > 0.05) between block ages when processed with the APFAR method.
Figure 26 B: Comparison of the number of proteins identified for different block ages for the DRP method	1. Shapiro–Wilk test: W = 0.983, p = 0.69 2. One-way ANOVA: F(2,48) = 2.53, p = 0.09	1. p > 0.05 therefore the distribution is not significantly different from a normal distribution, i.e. it is normal. 2. With regards to protein identifications, there is no significant difference (p > 0.05) between block ages when processed with the DRP method.
Figure 26 B: Comparison of the number of proteins identified for different block ages for the HILIC method	1. Shapiro–Wilk test: W = 0.894, p = 0.0003 2. Kruskal–Wallis test: H(2) = 0.101, p = 0.95	1. p < 0.05 therefore the distribution is significantly different from a normal distribution, i.e. it is non-normal. 2. With regards to protein identifications, there is not a significant difference (p > 0.05) between block ages when processed with the HILIC method.
Figure 28 A: Comparison of the	1. Kolmogorov-Smirnov test: D = 0.013, p < 0.01	1. p < 0.05 therefore the distribution is significantly different from a normal

hydropathicity of identified peptides for different protein purification methods for 1-year-old blocks	2. Kruskal–Wallis test: H(2) = 124.67, p < 0.0001	distribution, i.e. it is non-normal. 2. There is a significant difference (p < 0.05) between the hydropathicity of peptides generated via the different protein purification/sample preparation methods for 1-year old blocks.
Figure 28 A: Comparison of the hydropathicity of identified peptides for different protein purification methods for 5-year-old blocks	1. Kolmogorov-Smirnov test: D = 0.012, p < 0.01 2. Kruskal–Wallis test: H(2) = 78.92, p < 0.0001	1. p < 0.05 therefore the distribution is significantly different from a normal distribution, i.e. it is non-normal. 2. There is a significant difference (p < 0.05) between the hydropathicity of peptides generated via the different protein purification/sample preparation methods for 5-year old blocks.
Figure 28 A: Comparison of the hydropathicity of identified peptides for different protein purification methods for 10-year-old blocks	1. Kolmogorov-Smirnov test: D = 0.012, p < 0.01 2. Kruskal–Wallis test: H(2) = 67.39, p < 0.0001	1. p < 0.05 therefore the distribution is significantly different from a normal distribution, i.e. it is non-normal. 2. There is a significant difference (p < 0.05) between the hydropathicity of peptides generated via the different protein purification/sample preparation methods for 10-year old blocks.
Figure 28 A: Comparison of the hydropathicity of identified peptides for different block ages for the APFAR method	1. Kolmogorov-Smirnov test: D = 0.013, p < 0.01 2. Kruskal–Wallis test: H(2) = 30.61, p < 0.0001	1. p < 0.05 therefore the distribution is significantly different from a normal distribution, i.e. it is non-normal. 2. There is a significant difference (p < 0.05) between the hydropathicity of peptides generated from 1, 5 and 10-year old blocks when using the APFAR method.
Figure 28 A: Comparison of the hydropathicity of	1. Kolmogorov-Smirnov test: D = 0.013, p < 0.01 2. Kruskal–Wallis test:	1. p < 0.05 therefore the distribution is significantly different from a normal distribution, i.e. it is non-normal.

identified peptides for different block ages for the DRP method	H(2) = 55.79, p < 0.0001	2. There is a significant difference (p < 0.05) between the hydropathicity of peptides generated from 1, 5 and 10-year old blocks when using the DRP method.
Figure 28 A: Comparison of the hydropathicity of identified peptides for different block ages for the HILIC method	1. Kolmogorov-Smirnov test: D = 0.013, p < 0.01 2. Kruskal–Wallis test: H(2) = 39.49, p < 0.0001	1. p < 0.05 therefore the distribution is significantly different from a normal distribution, i.e. it is non-normal. 2. There is a significant difference (p < 0.05) between the hydropathicity of peptides generated from 1, 5 and 10-year old blocks when using the HILIC method.
Figure 28 B: Comparison of the molecular weights of identified peptides for different protein purification methods for 1-year-old blocks	1. Kolmogorov-Smirnov test: D = 0.085, p < 0.01 2. Kruskal–Wallis test: H(2) = 94.28, p < 0.0001	1. p < 0.05 therefore the distribution is significantly different from a normal distribution, i.e. it is non-normal. 2. There is a significant difference (p < 0.05) between the molecular weights of peptides generated via the different protein purification/sample preparation methods for 1-year old blocks.
Figure 28 B: Comparison of the molecular weights of identified peptides for different protein purification methods for 5-year-old blocks	1. Kolmogorov-Smirnov test: D = 0.085, p < 0.01 2. Kruskal–Wallis test: H(2) = 138.67, p < 0.0001	1. p < 0.05 therefore the distribution is significantly different from a normal distribution, i.e. it is non-normal. 2. There is a significant difference (p < 0.05) between the molecular weights of peptides generated via the different protein purification/sample preparation methods for 5-year old blocks.
Figure 28 B: Comparison of the molecular weights of identified peptides for different protein	1. Kolmogorov-Smirnov test: D = 0.086, p < 0.01 2. Kruskal–Wallis test: H(2) = 488.53, p < 0.0001	1. p < 0.05 therefore the distribution is significantly different from a normal distribution, i.e. it is non-normal. 2. There is a significant difference (p < 0.05) between the molecular weights of

purification methods for 10-year-old blocks		peptides generated via the different protein purification/sample preparation methods for 10-year old blocks.
Figure 28 B: Comparison of the molecular weights of identified peptides for different block ages for the APFAR method	1. Kolmogorov-Smirnov test: D = 0.089, p < 0.01 2. Kruskal–Wallis test: H(2) = 208.75, p < 0.0001	1. p < 0.05 therefore the distribution is significantly different from a normal distribution, i.e. it is non-normal. 2. There is a significant difference (p < 0.05) between the molecular weights of peptides generated from 1, 5 and 10-year old blocks when using the APFAR method.
Figure 28 B: Comparison of the molecular weights of identified peptides for different block ages for the DRP method	1. Kolmogorov-Smirnov test: D = 0.084, p < 0.01 2. Kruskal–Wallis test: H(2) = 2.71, p = 0.26	1. p < 0.05 therefore the distribution is significantly different from a normal distribution, i.e. it is non-normal. 2. There is no significant difference (p < 0.05) between the molecular weights of peptides generated from 1, 5 and 10-year old blocks when using the DRP method.
Figure 28 B: Comparison of the molecular weights of identified peptides for different block ages for the HILIC method	1. Kolmogorov-Smirnov test: D = 0.085, p < 0.01 2. Kruskal–Wallis test: H(2) = 9.57, p = 0.0084	1. p < 0.05 therefore the distribution is significantly different from a normal distribution, i.e. it is non-normal. 2. There is a significant difference (p < 0.05) between the molecular weights of peptides generated from 1, 5 and 10-year old blocks when using the HILIC method.
Figure 28 C: Comparison of the isoelectric points of identified peptides for different protein purification methods for 1-year-old blocks	1. Kolmogorov-Smirnov test: D = 0.17, p < 0.01 2. Kruskal–Wallis test: H(2) = 338.16, p < 0.0001	1. p < 0.05 therefore the distribution is significantly different from a normal distribution, i.e. it is non-normal. 2. There is a significant difference (p < 0.05) between the isoelectric points of peptides generated via the different protein purification/sample preparation

		methods for 1-year old blocks.
Figure 28 C: Comparison of the isoelectric points of identified peptides for different protein purification methods for 5-year-old blocks	1. Kolmogorov-Smirnov test: $D = 0.17$, $p < 0.01$ 2. Kruskal–Wallis test: $H(2) = 774.40$, $p < 0.0001$	1. $p < 0.05$ therefore the distribution is significantly different from a normal distribution, i.e. it is non-normal. 2. There is a significant difference ($p < 0.05$) between the isoelectric points of peptides generated via the different protein purification/sample preparation methods for 5-year old blocks.
Figure 28 C: Comparison of the isoelectric points of identified peptides for different protein purification methods for 10-year-old blocks	1. Kolmogorov-Smirnov test: $D = 0.17$, $p < 0.01$ 2. Kruskal–Wallis test: $H(2) = 374.56$, $p < 0.0001$	1. $p < 0.05$ therefore the distribution is significantly different from a normal distribution, i.e. it is non-normal. 2. There is a significant difference ($p < 0.05$) between the isoelectric points of peptides generated via the different protein purification/sample preparation methods for 10-year old blocks.
Figure 28 C: Comparison of the isoelectric points of identified peptides for different block ages for the APFAR method	1. Kolmogorov-Smirnov test: $D = 0.17$, $p < 0.01$ 2. Kruskal–Wallis test: $H(2) = 81.01$, $p < 0.0001$	1. $p < 0.05$ therefore the distribution is significantly different from a normal distribution, i.e. it is non-normal. 2. There is a significant difference ($p < 0.05$) between the isoelectric points of peptides generated from 1, 5 and 10-year old blocks when using the APFAR method.
Figure 28 C: Comparison of the isoelectric points of identified peptides for different block ages for the DRP method	1. Kolmogorov-Smirnov test: $D = 0.17$, $p < 0.01$ 2. Kruskal–Wallis test: $H(2) = 19.10$, $p < 0.0001$	1. $p < 0.05$ therefore the distribution is significantly different from a normal distribution, i.e. it is non-normal. 2. There is a significant difference ($p < 0.05$) between the isoelectric points of peptides generated from 1, 5 and 10-year old blocks when using the DRP method.
Figure 28 C:	1. Kolmogorov-Smirnov	1. $p < 0.05$ therefore the distribution is

Comparison of the isoelectric points of identified peptides for different block ages for the HILIC method	test: D = 0.17, p < 0.01 2. Kruskal–Wallis test: H(2) = 40.55, p < 0.0001	significantly different from a normal distribution, i.e. it is non-normal. 2. There is a significant difference (p < 0.05) between the isoelectric points of peptides generated from 1, 5 and 10-year old blocks when using the HILIC method.
Figure 34 Percentage of peptides containing oxidised methionine for APFAR processed samples	1. Shapiro–Wilk test: W = 0.920, p = 0.002 2. Kruskal–Wallis test: H(2) = 1.23, p = 0.54	1. p < 0.05 therefore the distribution is significantly different from a normal distribution, i.e. it is non-normal. 2. There are no significant differences (p > 0.05) in levels of oxidised peptides between the different block ages processed via the APFAR method.
Figure 34 Percentage of peptides containing oxidised methionine for DRP processed samples	1. Shapiro–Wilk test: W = 0.944, p = 0.019 2. Kruskal–Wallis test: H(2) = 0.86, p = 0.65	1. p < 0.05 therefore the distribution is significantly different from a normal distribution, i.e. it is non-normal. 2. There are no significant differences (p > 0.05) in levels of oxidised peptides between the different block ages processed via the DRP method.
Figure 34 Percentage of peptides containing oxidised methionine for HILIC processed samples	1. Shapiro–Wilk test: W = 0.860, p = < 0.0001 2. Kruskal–Wallis test: H(2) = 3.38, p = 0.18	1. p < 0.05 therefore the distribution is significantly different from a normal distribution, i.e. it is non-normal. 2. There are no significant differences (p > 0.05) in levels of oxidised peptides between the different block ages processed via the HILIC method.